An Investigation on Harmonic Filtering Techniques in Power Systems

By

Xin Li

A thesis submitted in partial fulfillment of the requirements for the degree of

Doctor of Philosophy

in

Energy Systems

Department of Electrical and Computer Engineering
University of Alberta

Abstract

Harmonic filtering is an effective method to mitigate harmonic distortions in power systems. Over the last decades, a number of harmonic filtering techniques have been proposed to deal with the increasing proliferation of harmonic-producing loads. Among these techniques, passive harmonic filtering is still the primary choice of industry, especially in medium and high voltage systems. In spite of its widespread application, there are still a lot of filter design issues that need clarifications. There is also a need to develop new filtering schemes that can overcome the limitations of existing schemes.

This thesis first clarifies design issues for several common passive filters. An equivalent circuit model is introduced to define the filter design problem in industrial systems. Four passive filter topologies are investigated. Design factors such as parameter variations, quality factor selection and filter power loss etc. are analyzed. Improved design methods are then developed based on such analysis. Effectiveness of the improved design methods are demonstrated through comparative case studies.

The thesis then proposes a new filter to mitigate harmonic and interharmonic resonance associated with multi-pulse converter systems. The core idea behind this filter is a frequency-dependent damping block that is able to achieve a high damping performance for a wide frequency range. Application of this filter to multi-

pulse variable speed drives and HVDC links are demonstrated. Case study indicates that the proposed filter is a cost-effective solution for harmonic mitigation of multi-pulse converters.

Preface

This thesis is an original work by Xin Li. As detailed in the following, some chapters of this thesis have been published as intellectual properties and scholarly articles, in which Prof. Wilsun Xu is the primary supervisor and has contributed to concepts formations and manuscript composition, Tianyu Ding is the co-author and has assisted with mathematical analysis and case studies, Yang Wang is the co-author and has been involved in the discussion and manuscript composition.

Chapter 4 of this thesis has been published as:

W. Xu, X. Li, "Harmonic filter for multipulse converter systems," US Patent 966,706,3B1, May 30, 2017.

X. Li, W. Xu and T. Ding, "Damped high passive filter - a new filtering scheme for multipulse rectifier systems," in *IEEE Transactions on Power Delivery*, vol. 32, no. 1, pp. 117-124, June 2017.

X. Li, W. Xu, "A novel filter to mitigate interharmonic problems caused by variable frequency drives," in 2017 *IEEE International Conference on Power Electronics and Drive System*, pp. 887-892, Dec. 2017.

Chapter 5 of this thesis has been submitted as:

X. Li, Y. Wang and W. Xu, " A new filtering scheme for HVDC terminals based on damped high pass filter," in *IEEE Transactions on Power Delivery* (early access).

Acknowledgements

I would like to show my sincere gratitude to Dr. Wilsun Xu for his patient guidance, advice and encouragement throughout my research. It would not have been possible to complete this thesis without his supervisory. I will always be proud to say I had the privilege of being his student and I ever remain grateful to him.

I would also express my thanks to the other professors from my Ph.D. examining committee, Dr. Yunwei Li, Dr. Ali Khajehoddin, Dr. Venkata Dinavahi and Dr. Peter Lehn, for reviewing my thesis and providing invaluable comments.

Thanks also go to all my colleagues in the PDS Lab, for their kind help, inspiring advices and friendship. It is my honor to work with these talented and enthusiastic researchers. Special thanks go to Dr. Jing Yong for her selfless help during various stages of this project.

I would express my gratitude for my parents Jixian Li and Fengyan Wang. There are not enough words to describe how thankful I am to them. Their endless love and great support are what sustained me to the present.

Finally, I dedicate this thesis to my beloved wife, Rui Li, who accompanied me to Canada for pursuing the Ph.D. I would never make this far without her love, care, support and every little effort she is doing for me.

Contents

List of Tables

List of Figures

List of Abbreviations

VFD	Variable Frequency Drive
HVDC	High Voltage Direct Current Transmission
DG	Distributed Generation
PC	Personal Computer
PV	Photovoltaic
THD	Total Harmonic Distortion
TDD	Total Demand Distortion
IHD	Individual Harmonic Distortion
PCC	Point of Common Coupling
RMS	Root Mean Square
CSC	Current Source Converter
VSC	Voltage Source Converer
ST Filter	Single-tuned Filter
2nd HP Filter	Second-order High-pass Filter
3rd HP Filter	Third-order High-pass Filter
DHP Filter	Damped High-pass Filter
HAR	Harmonic Amplification Ratio
AMR	Automatic Meter Reader
LCC	Line Communited Converter
PLC	Power Line Communication
BIL	Basic Insulation Level

Chapter 1

Introduction

Harmonic distortion has always been one of the major power quality concerns in power systems. The presence of harmonics will lower system operational efficiency, damage power equipment and interfere with protection and control circuits [1]-[7]. In recent years, this issue has received increasing research attention due to the following two trends. First, the widespread proliferation of harmonic-producing devices significantly raises the distortion level in power systems. Second, there is a more stringent requirement for the power quality supplied by utility companies. An effective and reliable harmonic filtering technique is critical to control harmonic distortions and provide clean power to customers. Although a number of research efforts have been spent on harmonic filtering in the past decades, there are still many problems and challenges that need to be addressed. Therefore, this thesis will present a thorough investigation of the unsolved issues involved in the current harmonic filtering practice.

In this introduction, an overview of power system harmonics is presented in Section 1.1. Section 1.2 introduces the harmonic indexes that will be adopted to quantify the harmonic distortions in power systems. Section 1.3 and Section 1.4 review the current harmonic filtering techniques and highlight the remaining issues and challenges. Finally, the scope and outline of this thesis are summarized in Section 1.5.

1.1 Overview of Power System Harmonics

Harmonics are defined as the periodic waveform components whose frequencies are integer multiples of the fundamental frequency. These components are caused by the non-linear characteristics of customer devices. Currently, the major harmonic-producing loads are power-electronic based equipment, such as variable

frequency drives (VFDs), high voltage direct current transmission (HVDC), distributed generations (DGs) and modern home appliances [8]-[13]. These non-linear loads are widespread at different voltage levels of power systems, as illustrated in Figure 1.1.

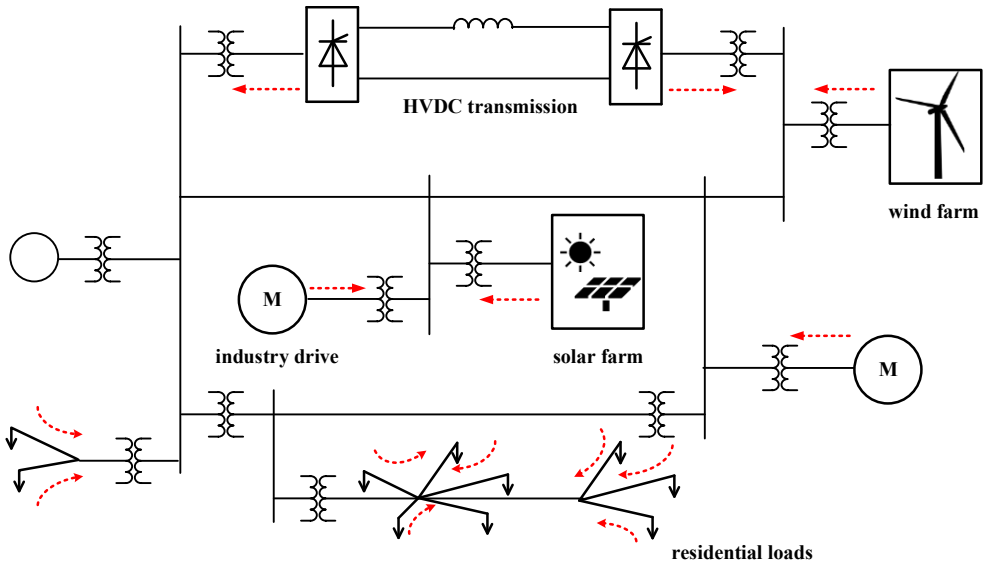

Figure 1.1 Harmonic sources in power systems

In transmission networks, HVDC transmission technology is globally used to transmit power over long distances or to interconnect two separate power grids. The large capacity and non-linear characteristics of HVDC transmission make it the primary harmonic source in high voltage systems [14]-[15]. Large industrial loads are also typical harmonic sources in transmission networks.

In primary distribution networks, the industrial facilities are the major harmonic sources. Examples are the pipeline stations, metal rolling plants, cement factories, and water pumping stations [16]-[21]. They are also the predominant harmonic producers in power systems. With the increasing integration of renewable energy, the distributed generation (DG) system has become a new type of harmonic source in medium-voltage systems [22]-[27].

In residential networks, there has been a dramatic penetration of modern home appliances in the last decade, such as PCs, LED-lights, PV panels, microwaves,

vacuums, etc. These power-electronic based appliances have a highly distorted current waveform. The previous studies [28]-[33] have shown that special attentions should be paid to the distortions caused by these massively distributed home appliances in low-voltage systems.

1.2 Harmonic Indexes

In view of the increasing harmonic-producing loads, several harmonic indexes have been defined to quantify the distortion level, and they will be introduced in the following sections.

1.2.1 Total Harmonic Distortion

The total harmonic distortion (*THD*) is an index to describe the overall effects of harmonics on power systems [34]. The total harmonic voltage distortion (THD_V) is defined as a total harmonic percentage of the system fundamental component; i.e.,

$$THD_V(\%) = \frac{\sqrt{V_2^2 + V_3^2 + \cdots + V_n^2}}{V_1} \times 100\%, \tag{1.1}$$

where V_1 is the fundamental voltage component, and V_2, V_3, …, V_n are the harmonic voltage components.

A similar method can also be used to define the total harmonic current distortion. However, this index sometimes is unable to properly reflect the actual distortion level, especially under light-load conditions. This is because the fundamental current at the light-load condition is very low; thus, a small amount of harmonic current can result in a large *THD* value. Hence, another index called total demand distortion (*TDD*) is defined in (1.2). This index uses the maximum load current as the reference and thereby provides a better evaluation for harmonic current.

$$TDD_I(\%) = \frac{\sqrt{I_2^2 + I_3^2 + \cdots + I_n^2}}{I_L} \times 100\%, \tag{1.2}$$

where I_L is the maximum load current.

1.2.2 Individual Harmonic Distortion

The individual harmonic distortion (*IHD*) is used to quantify the severity of harmonic distortion at a specific harmonic. The voltage and current individual harmonic distortions are defined as:

$$IHD_V(\%) = \frac{V_h}{V_1} \times 100\%, \tag{1.3}$$

$$IHD_I(\%) = \frac{I_h}{I_L} \times 100\%, \tag{1.4}$$

where V_h and I_h are the harmonic voltage and current components, respectively.

1.3 Harmonic Filtering Practice

The harmonic penetration has many adverse effects on the power system, which includes generator and motor overheating, transformer derating, overloading of shunt capacitors, telephone interference and extra losses in power transmission. To control harmonic distortions, significant efforts have been made, and two standards have been established [34]-[35]. These standards provide guidelines to identify the responsibility for harmonic mitigation and specify the permissible harmonic emissions that may be produced by each customer.

Harmonic filtering is the most effective method to prevent the harmonics from entering the distribution and transmission networks, and to reduce their adverse effects on the electrical equipment. The current filtering practice is mainly focused on the concentrated harmonic-producing loads in medium and high voltage systems. A variety of harmonic filtering techniques have been developed, as summarized in Figure 1.2.

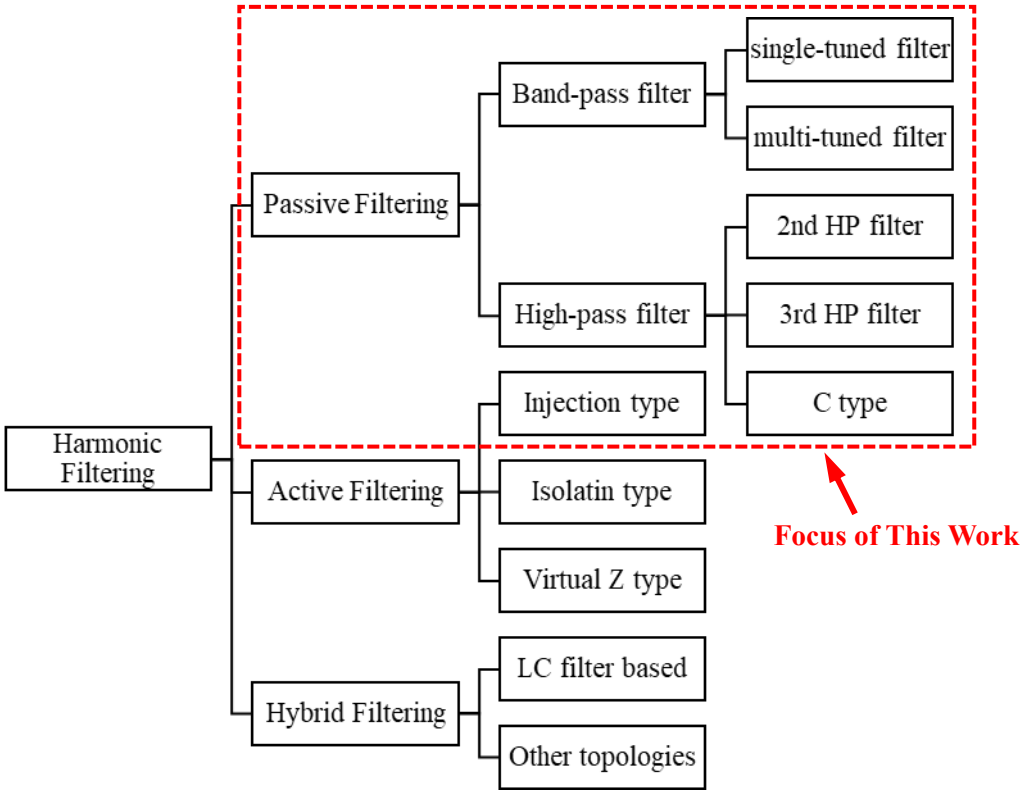

Figure 1.2 Summary of harmonic filtering technique

Passive harmonic filtering is the common harmonic mitigation method in power systems [36]-[46]. Its basic principle is to provide a low impedance path by the resonance between the filter capacitor and reactor, and thereby prevents harmonics penetrating into the network. To accommodate different applications, various filter topologies have been proposed, such as single-tuned filters, high-pass filters, double-tuned filters, etc. The researchers are still working on other promising topologies.

Active harmonic filtering is a new harmonic elimination technology, which can provide a more flexible performance than the passive filtering [47]-[53]. The most basic active filtering is to extract the undesired harmonics and inject an opposite signal back into the line for cancellation. Although the active harmonic filtering has been studied for years, the number of projects applying this new filtering technique is still limited. The main reason is due to its high cost, low reliability, and excessive switching loss.

Hybrid harmonic filtering is proposed as a combination of passive and active harmonic filters [54]-[59]. The intention is to minimize the capacity of the active filter and optimize the performance of the passive filter. In general, the passive part is designed to reduce the dominant harmonics and provides reactive power support. The active part addresses the non-characteristic harmonics and high-frequency harmonics that have a low content.

Among the above methods, passive harmonic filtering is still the preferable selection due to its simplicity, reliability and economic advantages, especially for the harmonic-producing loads above 1 MW. Therefore, the purpose of this thesis is to address the critical issues and constraints of passive harmonic filtering.

1.4 Issues of Passive Harmonic Filters

Although passive harmonic filters have been studied for decades, there are still many problems that need to be addressed. They can be categorized into the following two groups.

1.4.1 Design Issues for Common Passive Filters

An appropriate filter design is key to achieve the required harmonic filtering performance. A poorly designed filter may fail to complete its function or even result in operational problems. There are still many technical details that need to be clarified for passive filter design, and the following lists several examples.

- **How to deal with the impact of the parameter variations?**

For practical reasons, the filter parameters might deviate from their designed values due to factors such as manufacturing tolerance and system frequency deviation. These variations will affect the filter harmonic performance. The current practice is to roughly tune the filter to a lower frequency below the desired harmonic (normally 3%~9%). However, it is still unclear whether such a design is necessary and sufficient for different filter topologies.

- **What is the relationship between the quality factor and harmonic filtering performance, and how can a proper quality factor be selected for different filter topologies?**

The quality factor is introduced to quantify the filter resistance at its tuning frequency. Most previous studies use the bandwidth concept to explain the filter quality factor; i.e., a small quality factor indicates a wide filter bandwidth and a large one indicates a narrow filter bandwidth. However, it is difficult to use this concept to evaluate filter performance in power systems directly. Moreover, the impacts of the quality factor on different filter topologies are not the same. An analytical study to clarify these issues is needed.

- **How can the appropriate filter topology be selected to satisfy a particular harmonic filtering requirement?**

Various passive filter topologies are now available for harmonic mitigation. Generally speaking, a single-tuned filter is effective in filtering one harmonic, while a high-pass filter can mitigate several harmonics simultaneously. However, in practice, such a general principle cannot be easily used to choose the most appropriate filter topology for a given application. At present, it is common to see different filter topologies being used under similar conditions.

1.4.2 Limitations and Challenges for Current Filter Application

Despite its widespread application, passive harmonic filtering still has inherent critical limitations and challenges that need to be overcome [36]. Several examples are listed below.

- **How to avoid harmonic amplification caused by the resonance between the supply system and passive filters?**

It is known that each passive filter will introduce a parallel resonance point below its tuning frequency [60]. For example, a 7th harmonic filter may create a parallel resonance point at the 4.5th harmonic. Once this point coincides with a

harmonic frequency, the result will be a significant harmonic amplification. Thus, the current practice is to install filters starting from the lowest harmonic of concern. This practice significantly increases the complexity and cost of the current filtering scheme. An alternative solution is still desired to solve the harmonic amplification caused by passive filters.

- **How to use passive filters to mitigate interharmonic problems, such as light flicker or communication interference?**

Interharmonics are defined as spectral components of frequencies that are not integer multiples of the fundamental frequency. These components can cause severe problems like voltage fluctuations, light flicker, communication interference, etc. Traditional passive filters are not valid for these problems since the interharmonic frequencies may vary with different operating conditions [61]. How to mitigate interharmonics is still a challenging question that needs to be solved.

- **How to design a filter to ensure a satisfactory filtering performance under the condition of network impedance variation?**

Since passive filters are designed to provide a shunt path for harmonic currents, the network impedance is an important factor that affects the filter harmonic mitigation performance. In some cases, passive filters may experience a severe variation of network impedance. It is necessary to consider such effect in filter design for achieving a satisfactory filtering performance.

In summary, there are still many unsolved issues and challenges in passive harmonic filtering. Therefore, it is preferred to conduct further clarifications about the unclear issues and propose novel methods to overcome the challenges.

1.5 Thesis Scope and Outline

The scope of this thesis is to address the unsolved issues of passive harmonic filtering in medium and high voltage systems. To be more specific, two primary tasks are accomplished in this thesis:

1) The first task is to conduct a mathematical analysis for clarifying the design issues of common passive filters. Four filter topologies are studied: the single-tuned filter, second-order high-pass filter, third-order high-pass filter, and C-type filter.

2) The second task is to propose a novel filter topology that can eliminate the harmonic resonance concern of passive filters. The proposed filter provides an alternative solution for multi-pulse systems like industrial drives and HVDC links.

The following paragraphs summarize the organization of this thesis and describe the main topics and research discussed in each chapter.

Chapter 2 first defines the harmonic filtering problem in industrial systems. An equivalent circuit model is introduced to simplify the filtering analysis. This circuit model provides a general tool for filter design in any network. After this, an extensive study is conducted on the single-tuned filter since it is the basis for understanding other complex passive filters. Two unsolved design issues, the impact of quality factor and the selection of filter tuning frequency, are analytically investigated, and an improved design method is proposed accordingly.

Chapter 3 investigates three common high-pass filters, including second-order high-pass filters, third-order high-pass filters, and C-type filters. One focus is to clarify the issues about the design of these high-pass filters, including the selection of the filter tuning frequency and Q factor. An in-depth discussion is conducted to discuss the effect of selecting the Q factor on the filter component and operating costs respectively. Improved design methods are proposed, and their effectiveness is demonstrated through case studies. In addition, the performance of these high-pass filters is evaluated under various conditions. The advantages and constraints of each filter are summarized to guide the application in practice.

Chapter 4 presents an alternate harmonic solution to solve the non-characteristic harmonic problem in multi-pulse industrial systems. The basic concept is to provide sufficient damping at the non-characteristic harmonic frequencies. A novel filter

topology named the Damped High-Pass (DHP) filter makes the above concept feasible. This topology connects a frequency-dependent damping block in series with a single-tuned filter. The damping block uses the parallel resonance between the *LC* components to boost the filter resistance in the concerned frequency range. Its effectiveness is verified through a comparative case study. The proposed filter is also helpful to solve interharmonic problems such as voltage flicker and communication interference.

Chapter 5 applies the DHP filter at HVDC terminals. As a transmission-level application, HVDC terminals have several features that are quite different from those of the industrial systems. Examples are the severe network impedance variation and variable reactive power compensation. These features put a more stringent requirement on the performance of the DHP filter. Therefore, an improved design method is developed to accommodate this new situation. A real-life HVDC project is studied to demonstrate the feasibility of the proposed method. The sensitivity of the DHP filter to the parameter variation is also evaluated.

Finally, Chapter 6 summarizes the main contributions of this thesis and provides suggestions for future research.

Chapter 2

Single-tuned Filter Design

The single-tuned filter is the simplest and most widely used passive filter topology in industry. An in-depth understanding of this filter is the basis for the further study of more complex topologies. In this chapter, the harmonic filtering problem in industrial systems is first defined. An equivalent circuit model is also introduced to simplify the filter design in the rest of this thesis. Then, extensive analysis is conducted to clarify two technical issues regarding the design of the single-tuned filter. An improved design method is proposed correspondingly.

This chapter is organized as follows: Section 2.1 defines the harmonic filtering problem in industrial systems. Section 2.2 introduces the IEEE-13 bus industrial system, and this system will be used as an example case in the following study. Section 2.3 discusses two design issues of the single-tuned filter, and then an improved design method is proposed in Section 2.4. Finally, an example case is studied to verify the effectiveness of the proposed method in Section 2.5.

2.1 Problem Definition

This section defines the harmonic filtering problem in industrial systems. The configuration of a typical industrial system is used as an example for illustration. An equivalent circuit model is then developed, and this circuit model provides a general tool for filter design in any complex industrial systems.

2.1.1 Harmonic Filtering in Industrial Systems

Figure 2.1 presents the configuration of a typical industrial system. This system has both linear and non-linear loads. Example linear loads are motors. The nonlinear loads shown in the figure are marked as the CSC- and VSC- type of harmonic loads. The CSC-type harmonic load represents rectifier-feed loads such

as current source converter (CSC) based variable frequency drives. The VSC-type harmonic load represents the industrial loads based on voltage source converter (VSC). According to various research results [8]-[13], the CSC-type harmonic load behaves close to a harmonic current source while the VSC-type harmonic load behaves approximately as a harmonic voltage source. For harmonic studies, they can be modeled approximately as harmonic current and voltage sources respectively. The supply system can be modeled as an equivalent circuit in harmonic domain. Thus, the network of Figure 2.1 can be considered as a linear network that contains voltage and current sources at various harmonic frequencies.

For this research, the network and its loads are assumed to be approximately balanced so the single-phase analysis can be performed. The assumption of balanced network and loads are valid for most industrial facilities that require harmonic mitigation studies.

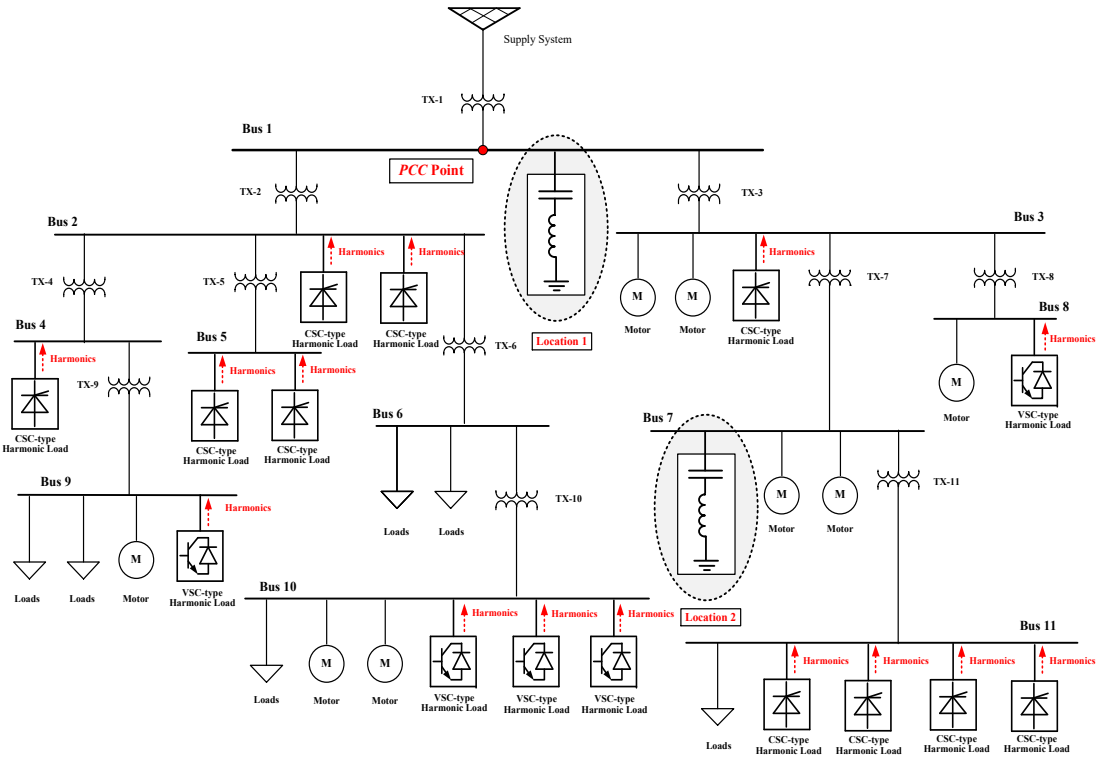

Figure 2.1 Example of an industrial system

It is understandable that some of the harmonic currents can flow into the supply system. Utility companies have established harmonic limits at the point of common

coupling (PCC) to limit the harmonic currents that can flow into the system. The customer must fulfill these limits to get connected. Installing harmonic filters is a common method to meet the harmonic limits. The filters shunt the harmonic currents produced by various loads and thus limit their flow into the system. The filters are normally installed at one location in a facility. Figure 2.1 shows two potential locations at Bus 1 and Bus 7.

2.1.2 Equivalent Circuit Model for Harmonic Filter Design

Since the customer's objective is to meet the harmonic limits at the PCC bus, the filter design should focus on the relationship between the voltage and current at the PCC bus with those at the filter bus. Figure 2.2 presents a general circuit to describe the harmonic filtering problem in industrial systems. In this figure, $V_s(\omega_h)$, $V_f(\omega_h)$, $I_s(\omega_h)$ and $I_f(\omega_h)$ are vol ges and currents at the PCC bus and filter bus.

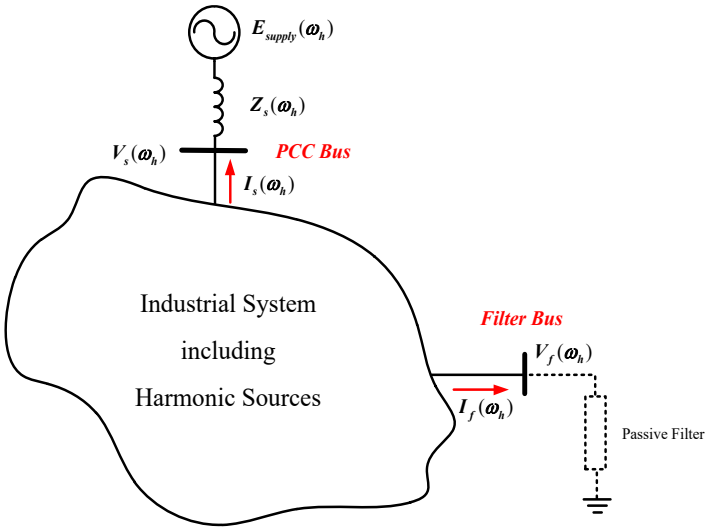

Figure 2.2 Harmonic filtering problem in industrial systems

The supply system normally has background harmonic voltages. So it is modeled as a Thevenin circuit in Figure 2.2 with $E_{supply}(\omega_h)$ representing the background harmonics, and $Z_s(\omega_h)$ representing the impedance of the supply system. According to interconnection guides, a customer is only responsible for filtering the harmonics produced by itself. Therefore, it is reasonable to assume the supply system $E_{supply}(\omega_h)$=0 when designing a filter and checking if harmonic limits are

met. This leads to a compact circuit model, as shown in Figure 2.3.

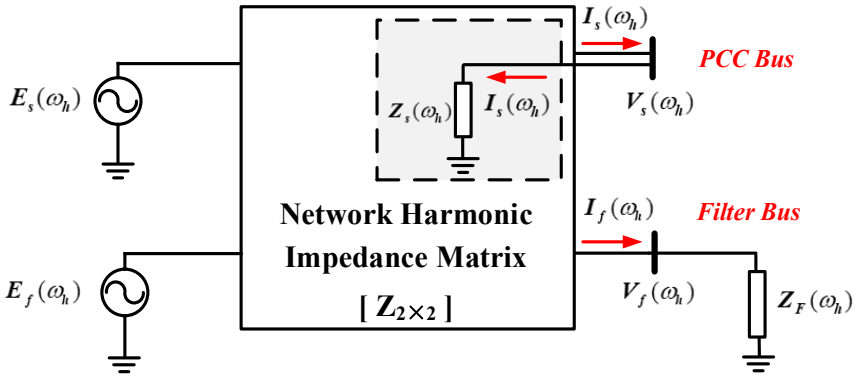

Figure 2.3 Simplified equivalent circuit model for filter design

In this circuit model, the system impedance has been included into the network impedance matrix. The circuit can be modeled as the following equivalent circuit:

$$\begin{bmatrix} V_s(\omega_h) \\ V_f(\omega_h) \end{bmatrix} = \begin{bmatrix} E_s(\omega_h) \\ E_f(\omega_h) \end{bmatrix} - \begin{bmatrix} Z_{ss}(\omega_h) & Z_{sf}(\omega_h) \\ Z_{fs}(\omega_h) & Z_{ff}(\omega_h) \end{bmatrix} \begin{bmatrix} 0 \\ I_f(\omega_h) \end{bmatrix} \tag{2.1}$$

$$I_f(\omega_h) = \frac{V_f(\omega_h)}{Z_F(\omega_h)}. \tag{2.2}$$

In the above equations, $Z_{ss}(\omega_h)$, $Z_{sf}(\omega_h)$, $Z_{fs}(\omega_h)$ and $Z_{ff}(\omega_h)$ are the coupling impedance among the ports. $E_s(\omega_h)$ and $E_f(\omega_h)$ are the open circuit voltages at the PCC bus and filter bus before filter connection. These voltages are the results of equivalent harmonic sources caused by the customer harmonic loads. $Z_F(\omega_h)$ is the filter impedance. A method to obtain the parameters of Equation (2.1) is explained in Appendix A.

Based on the above circuit model, one can calculate the harmonic voltage $V_s(\omega_h)$ at the PCC bus; i.e.,

$$V_s(\omega_h) = E_s(\omega_h) - \frac{Z_{sf}(\omega_h) E_f(\omega_h)}{Z_{ff}(\omega_h) + Z_F(\omega_h)} \tag{2.3}$$

Accordingly, the harmonic current $I_s(\omega_h)$ entering the supply system can be obtained as:

$$I_s(\omega_h) = \frac{E_s(\omega_h)}{Z_s(\omega_h)} - \frac{Z_{sf}(\omega_h)E_f(\omega_h)}{Z_s(\omega_h)(Z_{ff}(\omega_h) + Z_F(\omega_h))}. \quad (2.4)$$

As can be seen, the system harmonic current $I_s(\omega_h)$ becomes a function of the filter impedance $Z_F(\omega_h)$. Before filter connection, the filter bus is an open circuit, i.e., $Z_F(\omega_h)=inf$. The harmonic current $I_s(\omega_h)$ only contains the first item in (2.4). After filter connection, the second item in (2.4) is introduced. If the filters are properly designed, this term can reduce the first term at harmonic frequencies, leading to reduced harmonic currents flowing into the system.

Although the background harmonic distortion is set to zero for constructing the above equivalent circuit, the distortion shall be considered when assessing the loading condition of the filter components. The loading condition is defined as the Root Mean Square (RMS) voltage and current that are experienced by each *R*, *L* and *C* component of a filter. The physical size (not the impedance value) of a component is determined according to its loading condition. The loading condition is determined by computing the RMS voltage and current of a filter component when both background harmonics and facility harmonic loads are modeled.

2.1.3 Evaluation of Harmonic Filtering Performance

For performance evaluation, an index is introduced to quantify the harmonic mitigation performance of a filter, as shown below. This index can be used to evaluate the degree of harmonic reduction. For example, α%=70% indicates that the filter can reduce 70% of the harmonic currents entering the system.

$$\left| \frac{I_{s.post}(\omega_h)}{I_{s.pre}(\omega_h)} \right| = 1 - \alpha\%, \quad (2.5)$$

where $I_{s.pre}(\omega_h)$ and $I_{s.post}(\omega_h)$ are the harmonic currents before and after filter connection.

It is worthwhile to mention that this study mainly focuses on the reduction of harmonic current because customers are responsible for limiting their harmonic current emissions. Since the supply system's background harmonics are set to zero for filter design, the harmonic voltages at the PCC bus can be obtained by simply multiplying the harmonic currents by the impedance of the supply system. Therefore, the reduction ratio of harmonic voltage that are solely due to customer loads can be obtained in (2.6).

$$\left|\frac{V_{s.post}(\omega_h)}{V_{s.pre}(\omega_h)}\right| = \left|\frac{I_{s.post}(\omega_h)}{I_{s.pre}(\omega_h)}\right| = 1-\alpha\% \tag{2.6}$$

where $V_{s.pre}(\omega_h)$ and $V_{s.post}(\omega_h)$ are the harmonic voltages before and after filter connection.

The above equation reveals that the reduction ratio of harmonic voltage is the same as that of harmonic current. This finding can link the two performance indexes together. For a single customer, a α% harmonic current reduction is equivalent to attenuating α% of harmonic voltage.

2.1.4 Determination of Harmonic Filtering Requirements

In North America, IEEE Std. 519 is widely accepted to guide the customer connection. Table 2.1 lists the harmonic limits for systems below 69 kV [34].

Table 2.1 IEEE 519 harmonic distortion limits for systems below 69 kV

Maximum individual harmonic distortion (*IHD*) in percentage %					
$I_{sc}(\omega_1)^a / I_L(\omega_1)^b$	3≤h<11	11≤h<17	17≤h<23	23≤h<35	35≤h≤50
<20	4.0	2.0	1.5	0.6	0.3
20<50	7.0	3.5	2.5	1.0	0.5
50<100	10.0	4.5	4.0	1.5	0.7
100<1000	12.0	5.5	5.0	2.0	1.0
>1000	15.0	7.0	6.0	2.5	1.4

a. $I_{sc}(\omega_1)$ is the maximum short circuit current at *PCC*

b. $I_L(\omega_1)$ is the maximum demand current at *PCC* under normal conditions

To meet the harmonic limits, industrial customers should determine the required harmonic filtering performance based on the distortion level, as illustrated in (2.7):

$$(1-\alpha\%)\times IHD_h\% \le IHD_{limit}\%, \tag{2.7}$$

where $IHD_h\%$ is the individual harmonic distortion prior to the filter connection, and $IHD_{limit}\%$ is the corresponding harmonic limit.

As a result, the required harmonic reduction ratio $\alpha\%$ can be obtained in the following equation.

$$\alpha\% = (1-\frac{IHD_{limit}\%}{IHD_h\%})\times 100\% \tag{2.8}$$

The above equation can be used to determine the harmonic reduction ratio that needs to be achieved. For example, if the customer has a 20% *IHD* at the 5th harmonic, the filter needs to reduce at least 80% of the 5th harmonic for complying with the 4% harmonic limit; i.e., $\alpha\% \ge (1-4\%/20\%)\times 100\% = 80\%$.

2.2 Study System

This thesis (Section 2.3-3.5) uses the IEEE 13-bus industrial system as the main study case for verifying the proposed design methods of common passive filters. Figure 2.4 depicts the system configuration [62].

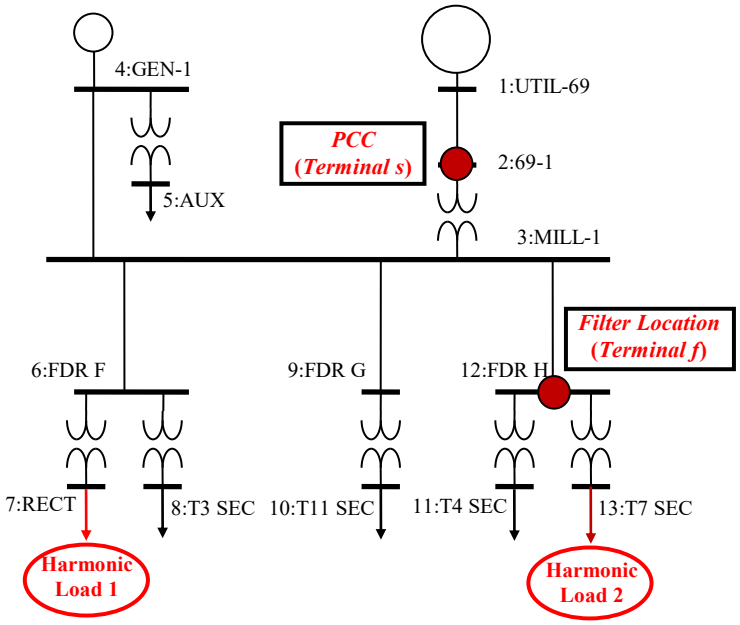

Figure 2.4 IEEE 13-bus industrial system

This system represents a medium-sized industrial customer. It is fed by a 69 kV supply system from Bus 2 (69-1). This plant also has a small local generator at Bus 4 (GEN-1). Two harmonic-producing loads connect at Bus 7 (RECT) and Bus 13 (SEC) respectively. The ideal filter location is assumed to be at Bus 12 (FDR H), as marked in Figure 2.4. The detailed parameters of this system can be found in Appendix B.

Parameters of the equivalent circuit model has been determined using the method described in Appendix A. Table 2.2 illustrates the Z matrix at harmonic frequencies.

Table 2.2 Z matrix parameters of equivalent circuit model

Harmonic	$Z_{ss}(\omega_h)$ (pu[a])	$Z_{sf}(\omega_h)/Z_{fs}(\omega_h)$ (pu)	$Z_{ff}(\omega_h)$ (pu)
3	0.003+j0.115	0.002+j0.084	0.006 + j0.179
5	0.003+j0.192	0.002+j0.139	0.006 + j0.298
7	0.003+j0.267	0.002+j0.195	0.006 + j0.417
11	0.003+j0.422	0.002+j0.306	0.006 + j0.655
13	0.003+j0.499	0.002+j0.361	0.006 + j0.774
17	0.003+j0.653	0.002+j0.472	0.006 + j1.011
19	0.003+j0.729	0.002+j0.528	0.006 + j1.130
23	0.003+j0.883	0.002+j0.583	0.006 + j1.249
25	0.003+j0.960	0.002+j0.639	0.006 + j1.368

a. the base capacity is 10,000 kVA and the base voltage are selected as 13.8 kV.

2.3 Single-tuned Harmonic Filter

A single-tuned filter is configured by connecting a reactor in series with a shunt capacitor, as shown in Figure 2.5(a). At the fundamental frequency, the single-tuned filter behaves as a capacitor to provide reactive power support, as shown in Figure 2.5(b). At the harmonic frequency, the reactance of the capacitor is canceled out by the reactor, resulting in a low impedance path for harmonics, as shown in Figure 2.5(c).

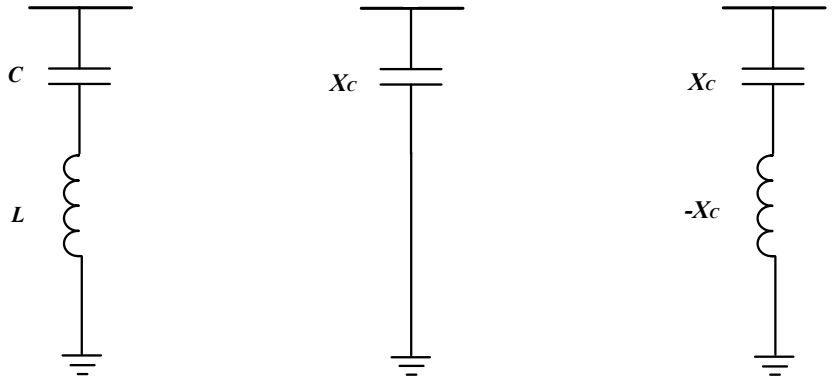

(a) single-tuned filter (b) fundamental frequency circuit (c) harmonic frequency circuit

Figure 2.5 Single-tuned filter and its equivalent circuit at different frequencies

2.3.1 Review of Single-tuned Filter

The earliest recorded application of the single-tuned filter was in 1941 [63]. A large amount of 5th harmonic voltage was found in a 33 kV Edison transmission system. Many capacitors were tripped due to overheating and fuse blowing. To solve this problem, the utility company installed a shunt capacitor tuning with a series reactor at 5th harmonic at the 33 kV bus. After this installation, the harmonic voltage was well controlled within an acceptable level. The success of this project makes the single-tuned filter become a general tool for harmonic mitigation. In 1960s and 1970s, the rapid development of HVDC technology stimulated the wide use of single-tuned filters in transmission systems [64]-[67]. To avoid telephone interference, multiple single-tuned filters are normally installed at HVDC terminals to suppress converter harmonics. With the penetration of solid-state converters into industrial processes, single-tuned filters started to gain acceptance in industrial power systems [68]-[70]. In the early 90s, two international standards were established to restrict the harmonic emissions of industrial customers [34]-[35]. To meet the harmonic limits, the single-tuned filter becomes an essential part of large industrial systems. At present, it is still the primary filtering choice in power systems.

Many research efforts have been spent on the design and application of single-tuned filters. The classic design method was proposed by Kimbark [64]. In this

work, he first evaluated the deviation of the filter tuning frequency caused by parameter variations. Then, the filter design was discussed under different supply impedance conditions: 1) infinite impedance, 2) purely inductive impedance and 3) impedance with a limited angle. A graphic approach was used to choose a proper quality factor (Q factor) to minimize the harmonic voltage. Based on this work, D.E. Steeper discussed the design of the single-tuned filter in industrial systems [68]. He noted that the filter tuning at the harmonic frequency could easily get overloaded by background harmonics. Therefore, it was suggested to tune the filter slightly away from harmonic frequency. For example, a 5th filter can be tuned at the 4.7th or 5.2th harmonic. However, D.A. Gonzalez noted that selecting a higher tuning frequency may result in an undesired harmonic resonance since the filter presents a capacitive impedance at the harmonic frequency, and therefore he recommended to select the tuning frequency below the harmonic [69]. In addition, he also concerned that the optimum Q factor of Kimbark may significantly increase the filter loss. As a summary of the previous works, Reference [36] provided an iterative design method in which a trial-and-error process was adopted to choose the filter tuning frequency until the filtering requirement is met. Today, this method is still widely accepted in practice.

Despite the above activity, the available design method still has two issues that need to be addressed. The first issue is related to the Q factor that plays a key role in Kimbark's design method. In practice, the Q factor is used to quantify the reactor winding resistance, and the normal manufacturing range is from 30 to 100. For a single-tuned filter, a high Q factor indicates a small filter resistance and a low Q factor indicates a large filter resistance. In [64], Kimbark tried to optimize the filter harmonic performance by selecting a proper Q factor. This concept is still accepted by many textbooks [1], [71]. However, the optimum Q value is obtained based on a pessimistic assumption that the filter resonates with the supply system. This assumption may lead to a very low Q factor, i.e., a large filter resistance and losses, since it provides the needed damping for the extreme condition. For example, the optimum Q is only 14 for Φ_m=75° (system impedance angle) and δ_m=4.5% (filter equivalent frequency deviation). Such a low Q factor is far below the normal range

and may result in an excessive filter loss in operation. Hence, the optimum Q factor is barely considered in the practical design. These facts reveal that there is a need to clarify the role of Q in the design of single-tuned filter and the necessity to insert a (costly) resistor.

The second issue is related to the filter tuning frequency. As explained, the tuning frequency of the single-tuned filter is commonly selected below the harmonic frequency. For example, a 5th single-tuned filter may be tuned to the 4.85th harmonic. This design is based on the following two considerations:

- **Economic Consideration:** A single-tuned filter tuned exactly at the harmonic frequency will attract nearly all the harmonics at this frequency. Selecting a low tuning frequency can avoid too many unnecessary harmonics flowing into the filter, which leads to a reduced filter component loading. Therefore, it is economical to select the filter tuning frequency based on the required filtering performance.
- **Performance Consideration:** The parameter variation may deviate the filter away from its designed tuning frequency. If the filter is directly tuned at the harmonic, a small variation may shift the tuning frequency to a higher frequency and place the resonance point close to this harmonic, resulting in a significant harmonic amplification.

Although it is widely accepted that the tuning frequency should be selected below the desired harmonic, there is still no available guideline on how to select it properly in practice. In current design methods, the filter tuning frequency is determined based on the experience of engineers. Such a design adds uncertainties to the filter harmonic performance, especially accounting for the parameter variations. The designed filter may either attract more harmonics than necessary or fail to achieve the required filtering performance. There is a need to develop a technically sound approach to determine the filter tuning frequency.

2.3.2 Analysis of Filter Characteristics

According to Figure 2.5(a), the impedance of the single-tuned filter can be derived as:

$$Z_F(\omega_h) = \frac{1}{j\omega_h C} + j\omega_h L \,. \tag{2.9}$$

The filter tuning frequency ω_t is defined as the frequency where the capacitor has the same reactance value but an opposite sign as the reactor; i.e.,

$$\omega_t = \frac{1}{\sqrt{LC}} \,. \tag{2.10}$$

By substituting (2.10) into (2.9), the filter impedance can be simplified as:

$$Z_F(\omega_h) = j\frac{(\omega_h^2/\omega_t^2 - 1)}{\omega_h C} \,. \tag{2.11}$$

The single-tuned filter is configured from shunt capacitors, so it should be designed to provide certain reactive power support at the fundamental frequency. This condition decides the capacitor C in (2.11). Therefore, the harmonic filtering performance of the single-tuned filter is mainly controlled by the filter tuning frequency ω_t.

Hence, in theory, the filter design just needs to select a tuning frequency to achieve the required filtering performance. However, two practical factors, including the Q factor and the parameter variation, add to the complexity of the design. Therefore, the following study will further examine on these two factors separately, and then an improved design method will be proposed accordingly.

2.3.3 Design Issue related to Quality Factor

In the prior study, the Q factor was selected to optimize the filter performance at the harmonic frequency [64]. Such a design normally results in a small Q factor, i.e., a large filter resistance. Although the optimum Q value can provide damping

at the extreme condition, it also leads to an excessive filter loss. There is still concern about whether it is necessary to select the optimum Q value. In view of this concern, an in-depth analysis is conducted to clarify the role of the Q factor in single-tuned filter design.

The reactor of the single-tuned filter is not purely inductive in practice, and power dissipation occurs when the current flows through it. Such an effect can be physically modeled by a resistance R_L, as illustrated in Figure 2.6.

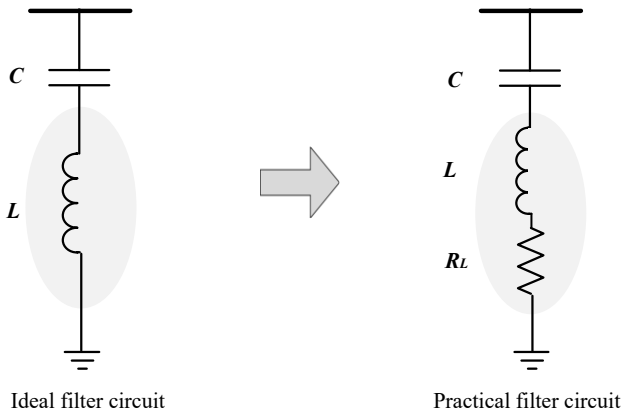

Figure 2.6 Topology of a practical single-tuned filter

The Q factor is defined to quantify this resistance, as shown in the following equation.

$$Q = \frac{\omega_t L}{R_L} = \frac{X_0}{R_L}, \tag{2.12}$$

where $X_0=\sqrt{L/C}$ is the filter characteristic impedance at the tuning frequency.

The impedance of the single-tuned filter can then be rewritten as:

$$Z_F(\omega_h) = R_F(\omega_h) + jX_F(\omega_h) = \frac{X_0}{Q} + j2\delta X_0 , \tag{2.13}$$

where $\delta=(\omega_h-\omega_t)/\omega_t$ is the frequency deviation from the filter tuning frequency.

Figure 2.7 presents a general filter circuit to facilitate the following analysis. In this circuit, $I_h(\omega_h)$ represents the harmonic source, and $Z_s(\omega_h)=R_s(\omega_h)+jX_s(\omega_h)$ and

$Z_F(\omega_h)=R_F(\omega_h)+jX_F(\omega_h)$ are the system impedance and filter impedance at the harmonic frequency.

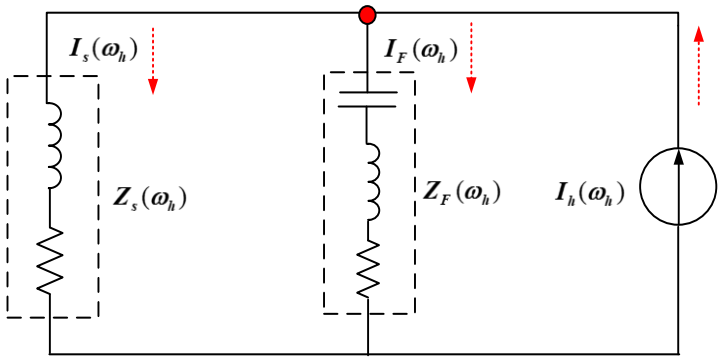

Figure 2.7 General harmonic filter circuit

In this circuit, the system harmonic current $I_s(\omega_h)$ can be solved as:

$$I_s(\omega_h)=\frac{I_h(\omega_h)}{Y_{total}(\omega_h)Z_s(\omega_h)}, \tag{2.14}$$

where $Y_{total}(\omega_h)$ is the total admittance between the filter and supply system; i.e.,

$$Y_{total}(\omega_h)=\frac{Z_s(\omega_h)+Z_F(\omega_h)}{Z_s(\omega_h)Z_F(\omega_h)}. \tag{2.15}$$

Since a large $Y_{total}(\omega_h)$ implies a good harmonic filtering performance, one can directly use $Y_{total}(\omega_h)$ to evaluate the Q factor effect on the filter harmonic performance. An extensive analysis has been conducted in Appendix C. The results show that a small Q factor only improves the harmonic filtering performance when the condition in (2.16) is satisfied.

$$\delta Q > \frac{X_s(\omega_h)}{R_s(\omega_h)} \tag{2.16}$$

In this equation, the typical range of δQ is limited from 1 to 10, where Q is from 30 to 100 and δ is within 0.1 [60]. For industrial systems, the $X_s(\omega_h)/R_s(\omega_h)$ ratio should be higher than 10. Therefore, it is hard to satisfy the condition in (2.16). This result indicates that, in most cases, the filter with a large Q factor provides a good

harmonic filtering performance. In an extreme case, the filter has an infinity Q factor, i.e., no filter resistance. Assuming (2.16) is satisfied in some special cases, a further study is also conducted in Appendix C for assessing the performance improvement by selecting the Q factor. According to the results, the performance improvement is only 3% to 4%, and such a minor effect is ignorable in practice.

In conclusion, the Q factor selection is not effective in improving the filter harmonic performance. Therefore, there is no need to pay special attention to select the optimum Q value. As a small Q value increases the filter operating loss, the practical design should choose a large Q factor within the manufacturing range.

2.3.4 Design Issue related to Tuning Frequency Selection

The filter harmonic performance depends on its tuning frequency. As explained, it should be selected below the harmonic based on the filtering requirement [60]. For the selection of the tuning frequency, the primary challenge is the parameter variations, including the manufacturing tolerance and system frequency deviation. The parameter variations have a random feature and can significantly affect the filter harmonic performance. However, there is still no scientific way to select the tuning frequency with the consideration of the parameter variations. Motivated by this fact, a technically sound approach will be proposed to guide the tuning frequency selection in filter design.

The manufacturing tolerance and frequency deviation make the actual parameter of the filter components deviate from their preferred values. Therefore, each filter parameter should be expressed as its preferred value plus a random variable, as shown in (2.17)−(2.18). Note that $\Delta\omega_1$, ΔL, and ΔC are the variations of the frequency, inductance and capacitance in per unit, respectively.

$$\omega_1^{'} = \omega_1 \times (1 + \Delta\omega_1) \tag{2.17}$$

$$L^{'} = L \times (1 + \Delta L) \tag{2.18}$$

$$C^{'} = C \times (1 + \Delta C) \tag{2.19}$$

It can be expected that these variations may affect the filter performance at the harmonic frequency. The following study intends to quantify such effect by analyzing the filter impedance change at the harmonic frequency, as defined in (2.20). The harmonic order h is used to replace ω_h since the actual harmonic frequency also changes with $\Delta\omega_1$. For example, if $\Delta\omega_1 = -0.1$, the 5th harmonic frequency will change from 300 Hz to 270 Hz.

$$\Delta Z_F(h) = \frac{Z_F'(h) - Z_F(h)}{Z_F(h)} = f(h, h_t, Q, \Delta\omega_1, \Delta L, \Delta C) \tag{2.20}$$

where $Z_F'(h)$ and $Z_F(h)$ are the filter harmonic impedance with and without the parameter variations.

A Monte-Carlo simulation is used to obtain the statistical characteristics of $\Delta Z_F(h)$. The results show that $\Delta Z_F(h)$ can be as high as 1.5 in some cases. Such a large variation can have a considerable impact on the filter harmonic performance. It is therefore necessary to compensate for the parameter variation in filter design. Since the parameter variations are statistical in nature, it is reasonable to use a statistical-based approach to correct their impacts. If $Z_{F.\alpha\%}(\mathrm{h})$ is the preferred filter impedance satisfying the α% harmonic filtering requirement, one should guarantee a high probability (95%) that the actual filter impedance is smaller than this value; i.e.,

$$PDF(Z_F(\mathrm{h})(1 + \Delta Z_F(\mathrm{h})) \le Z_{F.\alpha\%}(\mathrm{h})) \ge 95\% . \tag{2.21}$$

This condition indicates that, even with parameter variations, the designed filter still has a 95% chance of achieving the required harmonic performance. If $\Delta Z_F(h)$ has a normalized probability density function (*PDF*), one can easily adjust the filter impedance based on (2.21). For example, if the 95% confidence interval of $\Delta Z_F(h)$ is from −0.2 to 0.8, the filter needs to be designed as $Z_F(h) = Z_{F.\alpha\%}(\mathrm{h})/1.8$. However, $\Delta Z_F(h)$ is also a function of h and h_t, referring to (2.20). This fact makes it a case-dependent variable and hard to be normalized. Fortunately, the analysis in Appendix D reveals that $\Delta Z_F(h)$ shares a nearly linear relationship with $\Delta h_t(h)$ as defined in (2.22). Δh_t is only a function of the parameter variations, which makes

it easy to be normalized. This desired feature can be used to help correct the impact of the parameter variation, as illustrated in Figure 2.8.

$$\Delta h_t = \frac{h_t^{'} - h_t}{h_t} = \frac{1}{(1+\Delta\omega_1)\sqrt{(1+\Delta L)(1+\Delta C)}} \tag{2.22}$$

where h_t' and h_t are the filter tuning point with or without the parameter variations.

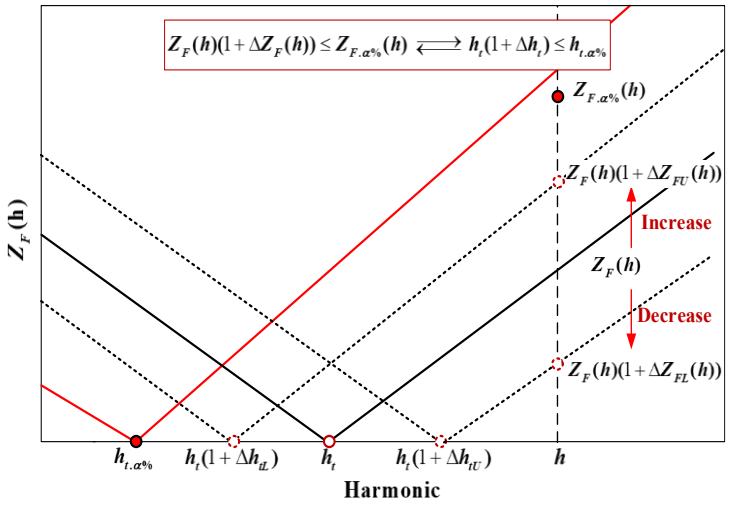

Figure 2.8 Illustration of the proposed compensation method

In the above figure, $h_{t.\alpha\%}$ is the ideal tuning point satisfying the $\alpha\%$ harmonic filtering requirement without any parameter variations. As shown in Figure 2.8, the design should slightly move the tuning point close to the harmonic, i.e., from $h_{t.\alpha\%}$ to h_t, to guarantee its actual value $h_t(1+\Delta h_{tL})$ with the parameter variation still above the desired point $h_{t.\alpha\%}$. Consequently, the condition in (2.21) can be replaced by the following equation.

$$PDF(h_t(1+\Delta h_t) \le h_{t.\alpha\%}) \ge 95\%, \tag{2.23}$$

where $h_{t.\alpha\%}$ is the filter tuning point corresponding to $Z_{F.\alpha\%}(h)$ that satisfies the $\alpha\%$ filtering requirement at the harmonic frequency.

Table 2.3 lists the typical range of parameter variations [60]. To facilitate the analysis, this study assumes: (1) all the parameter variations follow Gaussian distribution, and (2) the variation ranges in the table below are 99% confidence

intervals.

Table 2.3 Typical range of the parameter variation

	$\Delta\omega_1$	ΔL	ΔC	ΔR
variation in p.u.	−0.01 ~ 0.01	−0.03 ~ 0.03	0 ~ 0.04	−0.03 ~ 0.03

A Monte-Carlo simulation is used to obtain the normalized Δh_t range, as shown in Figure 2.9. It shows that Δh_t is approaching a Gaussian distribution with an average value μ=-0.010 and a standard deviation σ=0.007.

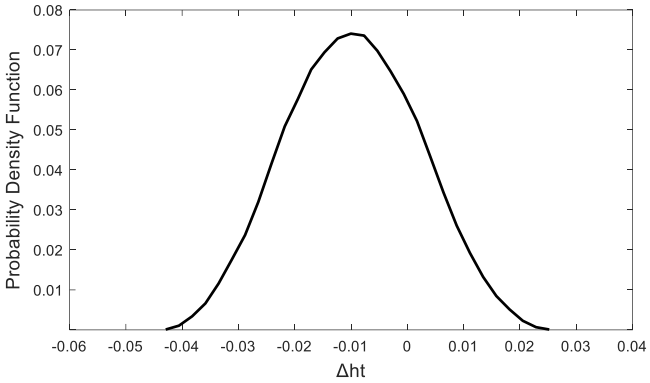

Figure 2.9 Probability density function of Δh_t

Therefore, the lower end of the 95% confidence interval can be calculated as:

$$\Delta h_{tL} = -\mu - Z_{95\%} \times \sigma = -0.022 \,, \tag{2.24}$$

where $Z_{95\%}$=1.65 is selected based on the Z-list of Gaussian distribution.

Finally, the filter tuning point satisfying (2.23) can be calculated by the following equation. Note that Δh_{tL} is regarded as the compensation factor, and it is a case-independent variable.

$$h_t = \frac{h_{t.\alpha\%}}{1 + \Delta h_{tL}} \tag{2.25}$$

The above equation can be used to statistically compensate for the parameter variation impact. The main advantage of this method is to guarantee a satisfactory filtering performance without over attracting unnecessary harmonics. In practical

design, $h_{t.\alpha\%}$ should be obtained first based on the required filtering performance, and then (2.25) can be used to determine the final tuning point h_t.

2.4 Proposed Design Method

Based on the above analysis, the design of a single-tuned filter needs to consider three factors. The first factor is the reactive power required by the supply system. The second one is the selection of the tuning frequency. The last factor is to compensate for the parameter variation. As explained, the filter tuning frequency should be shifted to a frequency close to the harmonic.

- **Design Equation 1: Reactive Power Requirement**

The first design equation is specified by supporting the capacitive reactive power required by the system. This condition can be used to solve the capacitor C as:

$$C = \frac{Q_F}{\omega_1 V_s^2(\omega_1)}, \tag{2.26}$$

where ω_1 is the fundamental frequency, Q_F is the reactive power required by the system, and $V_s(\omega_1)$ is the system rated voltage.

- **Design Equation 2: Selection of Filter Tuning Frequency**

The second equation is to select the tuning frequency that satisfies the filtering requirements in (2.27). This condition determines the ideal filter tuning point $h_{t.\alpha\%}$.

$$\left|\frac{I_{s.post}(\omega_h)}{I_{s.pre}(\omega_h)}\right| = 1-\alpha\% \tag{2.27}$$

- **Design Equation 3: Compensation for Parameter Variation**

Based on the obtained $h_{t.\alpha\%}$, the final tuning frequency can be calculated by the following equation.

$$h_t = \frac{h_{t.\alpha\%}}{1+\Delta h_{tL}} \approx 1.02 h_{t.\alpha\%}, \tag{2.28}$$

where Δh_{tL}=-0.022 is the lower end of 95% confidence interval, referring to (2.24).

2.5 Example Case Study

An example case is studied to evaluate the proposed design method, and this case involves the IEEE 13-bus industrial system in Section 2.2. It is assumed that 18.24% of the 5th harmonics are produced by the two harmonic-producing loads. The two-terminal equivalent circuit is developed. Table 2.4 illustrates the circuit parameters.

Table 2.4 Parameters of the equivalent circuit

H	Equivalent Source (pu)		Network Z Matrix (pu)		
	$E_s(\omega_h)$	$E_f(\omega_h)$	$Z_{ss}(\omega_h)$	$Z_{sf}(\omega_h)/Z_{fs}(\omega_h)$	$Z_{ff}(\omega_h)$
5th	0.020+j0.016	0.041+j0.034	0.003+j0.192	0.002+j0.139	0.006+j0.298

As the first step, the harmonic distortions at the PCC point are computed. The result shows that the industrial system has an 11% *IHD* at the 5th harmonic. To meet the harmonic limits specified by IEEE, the required filtering performance can be determined as:

$$\alpha\% = (1 - \frac{4\%}{11\%}) \times 100\% = 64\% . \tag{2.29}$$

The above result indicates that the filter should be designed to mitigate 64% of the 5th harmonics. The following presents the detailed process for filter design.

- ***Step 1: Reactive Power Requirement***

It is assumed that the supply system requires a 2000 kvar reactive power support. The filter capacitor can then be determined as:

$$C = \frac{2000\ kVar}{(13.8\ kV)^2 \times (2 \times \pi \times 60)} = 27.86\ \mu F . \tag{2.30}$$

- ***Step 2: Selection of Filter Tuning Frequency***

To meet the 64% harmonic filtering requirement, the filter tuning point should be selected by the following equation. This equation decides the ideal tuning point

$h_{t.\alpha\%}$. If the Q factor is selected at 50, $h_{t.\alpha\%}$ can be calculated as 4.63.

$$\left|\frac{I_{s.post}(\omega_h)}{I_{s.pre}(\omega_h)}\right| = 1 - 64\% \tag{2.31}$$

- ***Step 3: Compensation for Parameter Variation***

The last step is to compensate for the parameter variation, and the final tuning frequency can be computed as:

$$h_{t\alpha} = \frac{h_{t.\alpha\%}}{1 + \Delta h_{tL}} = 4.72\,. \tag{2.32}$$

The above design leads to a single-tuned filter with Q_C=2000 kvar, h_t=4.72. This filter can mitigate 72% of the 5th harmonic if no parameter variation is considered. The extra 8% harmonic reduction is for the compensation of the parameter variation. The designed filter is also compared to a filter that selects its tuning frequency 3% below the harmonic. Table 2.5 lists the component loadings of the two filters. A 2% background 5th harmonic voltage is considered at the filter bus.

Table 2.5 Comparison results of component loading

Option		Comparative	Proposed	Relative Value
h_t		4.85	4.72	----
α%		82%	72%	----
C	C (uF)	27.86	27.86	1.00
	Voltage /kV	11.34	10.07	1.13
	Capacity /Mvar	1.35	1.07	1.26
L	L (mH)	10.7	11.3	0.95
	Current /A	204.88	145.43	1.41
	Capacity /kvar	169.92	90.40	1.88

Compared to the comparative case, the proposed method leads to a much lower component loading. This is because it can effectively compensate for the parameter variation without attracting too many harmonics. Although it has a slight increase on the reactor value, such a small variation has a minor impact on the reactor cost and is ignorable in practice.

The costs of the two filters are listed in Table 2.6. As shown, the proposed design saves 20% in filter cost. This result verifies the economic advantage of the proposed method. The details of the cost calculation are discussed in Appendix E.

Table 2.6 Comparison results of filter cost

Option	Comparative	Proposed	Saving Ratio
Capacitor cost ($)	32,670	24,096	26%
Reactor cost ($)	17,465	14,979	15%
Total cost ($)	50,135	39,075	22%

2.6 Summary

Based on the above analysis, the main findings and contributions of this chapter can be summarized as follows:

- This chapter introduced an equivalent circuit model to define the harmonic filtering problem in industrial systems. By replacing the rest of the system with their equivalent circuit, the proposed model can only focus on the relationship between the PCC bus and the filter bus. This approach provides a general tool to simplify the filter design in any complex network.

- An investigation was conducted to clarify the effect of selecting the Q factor on the filter harmonic performance. The analysis revealed that the Q factor selection is ineffective in optimizing the filter performance. Since a small Q factor leads to an excessive filter operating loss, it is preferred to choose a large Q value for filter design.

- The selection of the filter tuning frequency was also discussed considering the impact of parameter variations. To compensate for this effect, a statistical-based method was proposed. This design can provide a satisfactory filtering performance without attracting too many unnecessary harmonics. Its effectiveness was verified through an example case study.

Chapter 3

High-pass Passive Filter Design

High-pass harmonic filters are another type of passive filters in power systems. These filters have a wide-band harmonic filtering characteristic, and thereby can suppress several harmonic components simultaneously. To provide the desired filtering performance, the design of high-pass filters is more sophisticated than that of single-tuned filters. Despite their wide acceptance in industry, a consensus on the design of high-pass filters has still not been achieved. In view of this fact, this chapter presents a thorough study of three common high-pass filters, including the second-order high-pass filter, C-type filter, and third-order high-pass filter. One objective of this chapter is to clarify the unsolved issues involved in the design of these filters. Improved design methods will be proposed and verified through case studies. Another objective is to assess the performance of these high-pass filters under different conditions and provide guidance to help choose the right topology for a given application.

This chapter is organized as follows: Section 3.1 provides an overview of high-pass filters. The design issues for three high-pass filters are discussed separately in Section 3.2-3.4. In Section 3.5, further analysis is conducted to compare these filters under various conditions. Finally, Section 3.6 summarizes the main findings and contributions.

3.1 Overview of High-pass Filters

A single-tuned filter is effective in mitigating the harmonic it is tuned to. However, after the tuning frequency, its impedance is dominated by the reactor and increases dramatically. As a result, it has limited filtering capabilities at the other harmonics. Multiple single-tuned filters are required to cover the harmonics in a wide range. In view of this fact, [72] proposed a new topology (second-order high-

pass filter) by connecting a shunt resistor in parallel with the reactor of the single-tuned filter, as shown in Figure 3.1(a). This filter presents a low impedance over a wide frequency range, and thereby can mitigate several harmonics simultaneously. Compared with the solution of multiple single-tuned filters, it is a more economical option for the conditions where a broad range of harmonics needs to be filtered. As a compromise, the resistor will cause the filter loss in operation. Due to its unique filtering characteristic, the second-order high-pass filter (2nd HP filter) has been widely used to solve the high-order harmonic problems, such as the telephone interference at HVDC terminals [65]-[67],[73].

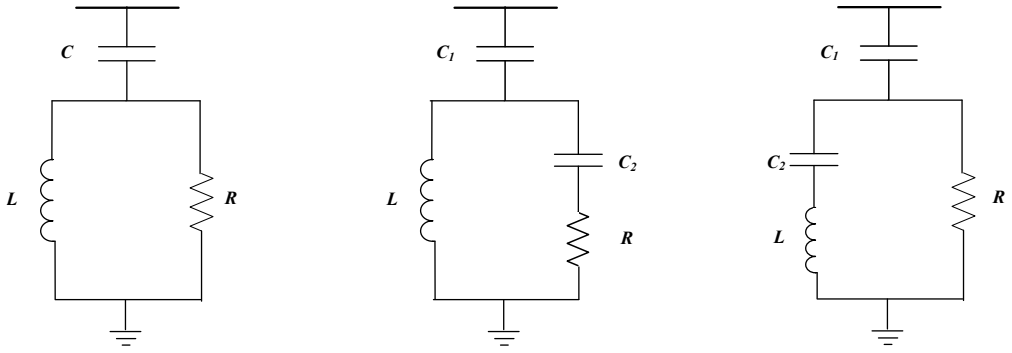

(a) 2nd HP Filter (b) 3rd HP Filter (c) C-type Filter

Figure 3.1 Common high-pass filter topologies

However, the filter resistor causes a large amount of fundamental frequency loss, especially when the filter is used at low-order harmonics. For the purpose of reducing the fundamental frequency loss, Reference [72] also proposed another high-pass filter topology, third-order high-pass filter (3rd HP filter), by connecting a capacitor in series with the resistor (Figure 3.1(b)). This capacitor increases the impedance of the resistor branch at low frequencies so more current will flow to the reactor branch. This results in reduced resistor loss. The third-order high-pass filter was first employed in New Zealand HVDC link (1965), and then in Vancouver Island HVDC (1968) and Cross-Channel HVDC (1982). Reference [74] proposed a different way to reduce the filter loss by connecting the second capacitor in series with the filter reactor (C-type filter), as in Figure 3.1(c). The capacitor was tuned to resonate with the reactor at the fundamental frequency so that there is little current flowing to the resistor. As a result, the fundamental frequency loss is

reduced. Now it is common to see the application of the C-type filter at HVDC terminals and industrial systems [75]-[76]. Another potential application of the C-type filter is to prevent the harmonic resonance of shunt capacitors in transmission systems [77]-[78].

The increasing proliferation of high-pass filters has attracted research interests in filter design. For the design of the 2nd HP filter, two important works were conducted by Ainsworth [73] and Kimbark [64]. This filter has three components, R, L and C. So three equations are required to determine the component parameters. Since a passive filter is required to provide certain amount of reactive power support at the fundamental frequency, the first design equation can be developed based on this requirement. This leaves two equations to be established for completing the design of the 2nd HP filter.

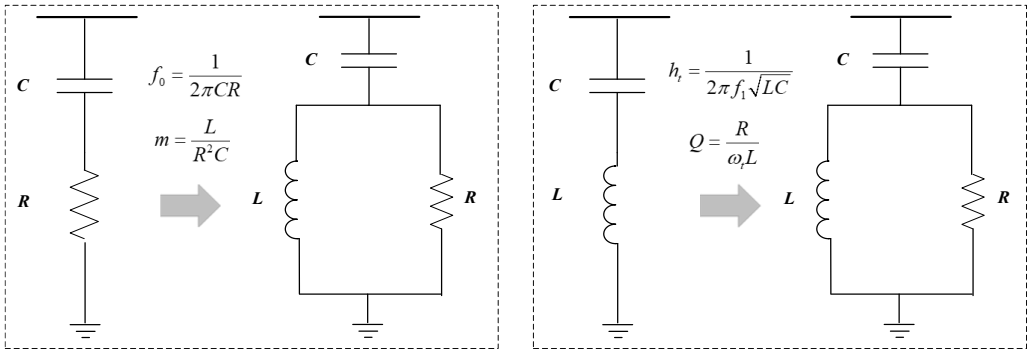

(a) Anisworth (b) Kimbark

Figure 3.2 Illustration of design theory in [64] and [73]

Ainsworth approached the design problem from the perspective of the *RC* high-pass filter, as illustrated in Figure 3.2(a) [73]. The *RC* filter is the simplest high-pass filter topology, and its characteristic frequency f_0 is defined as the boundary where the harmonic begins to be filtered. Ainsworth considered the *RC* filter as the basis of the other high-pass filters. The characteristic frequency f_0 was still used for the analysis of the 2nd HP filter. Another parameter m named the damping ratio was introduced for determining the filter response. Similar to the quality factor, the damping ratio can also quantify the filter sharpness. These two parameters (f_0 and m) were used to analyze the 2nd HP filter. However, since f_0 is unable to reflect the

filter tuning frequency, it is impracticable to obtain a design equation through it. This fact makes the filter resistor and reactor being coupled by m and hard to be determined. Therefore, Ainsworth only provided a recommended range for m (0.5 to 2), but the two design equations were still not established.

Kimbark approached the design problem from the perspective of single-tuned filter, as illustrated in Figure 3.2(b) [64]. From this view, the two critical parameters of the single-tuned filter, the tuning point h_t and Q factor, were used to discuss the characteristics of the 2nd HP filter. The analysis showed that the filter behavior can be described by these two parameters. The tuning point h_t represents the harmonic where the filter has the lowest impedance, and the Q factor determines the filter characteristics in the harmonic range. Unfortunately, no criterion was provided to specify the rest two equations for determining the filter reactor and resistor.

As a continuous work of Kimbark, Reference [69] showed that it is common to select the tuning frequency of the 2nd HP filter at the lowest harmonic of concern. Such a design can guarantee a satisfactory harmonic filtering performance in most cases. This condition can be used to establish the second equation to solve for the reactor. Nevertheless, there are still different options on the selection of the filter tuning frequency. In several studies, the tuning frequency is selected slightly below the harmonic, but there are also designs selecting it directly at the harmonic frequency [37],[79]-[81]. How to choose a proper tuning frequency is still an issue that needs to be clarified. Finally, the third equation needs to determine the filter resistor or Q factor. A consensus is that it should be specified to satisfy the harmonic filtering requirement. The work in [69] pointed out that the filter loss is also an important factor for determining this equation. The cost of the filter loss could be significant for a lossy design. However, the third equation has not been explicitly specified. In practical design, the Q factor is normally determined based on the engineering experience [79]-[81].

Compared to the 2nd HP filter, the C-type filter and 3rd HP filter have a second capacitor C_2. A fourth equation is therefore required to determine this capacitor. Since the capacitor C_2 aims to reduce the filter loss at the fundamental frequency,

this condition can be used to establish the fourth design equation. For the C-type filter, the fourth equation is to cause a zero impedance for the L and C_2 branch at the fundamental frequency [83]-[87]. For the 3rd HP filter, this equation is specified by [88] to minimize the filter fundamental frequency loss.

The third equation is also an issue for the C-type filter and 3rd HP filter. In previous studies, various design conditions have been proposed for the C-type filter. Reference [84] specified the third equation based on the filtering requirement at the lowest harmonic, and as a result, a small Q factor could be selected for a good high-pass performance. Reference [85] proposed to minimize the total harmonic voltage distortion to reduce the negative effects of harmonics on the supply system. There are also studies employing the C-type filter as anti-resonance capacitors, and the third equation was specified to limit the harmonic amplification caused by the filter [77]-[78], [87]. However, all of the above designs only focus on the filter harmonic performance but ignore the importance of filter economics. The research on the 3rd HP filter is similar but even more limited. The required filtering performance at the lowest harmonic was used as the condition for specifying the third equation in [88]. Reference [89] proposed to minimize a cost function that considers the component cost and the cost of filter loss, but the 3rd HP filter was designed to address the capacitor resonance instead of filtering harmonics.

It can be seen that a consensus on high-pass filter design is still elusive. The following summarized the main issues in the current design methods.

1). The design of the 2nd HP filter has at least two unsolved issues. The first issue is that there is still a need to define the third design equation. The second issue is about the second design equation that is related to the tuning frequency h_t. There is confusion on the selection of h_t; i.e., whether the filter should be tuned at or slightly below the harmonic frequency.

2). Similar design issues also exist for the C-type filter and 3rd HP filter. Although various design conditions have been proposed, there is still no consensus on what is the best way to establish the third design equation. The

current design methods still need to be improved.

3). Although three high-pass filter topologies are available now, limited attention has been spent to the selection of a particular topology for a given application. Currently, it is common to see different topologies being used under similar conditions. It is worthwhile to develop a guideline for determining the most appropriate high-pass filter topology for a design project.

In summary, there are still unsolved issues in the design of high-pass filters. It is therefore desirable to conduct a further research to clarify them.

3.2 Second-order High-pass Filter

Figure 3.3(b) shows the topology of the second-order high-pass filter (2nd HP filter). It can be seen as a single-tuned filter with a resistor *R* connected in parallel with the filter reactor *L*.

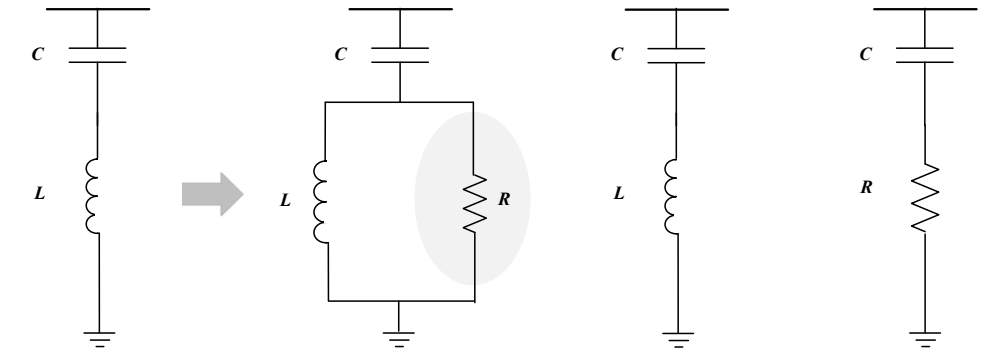

(a) Single-tuned Filter (b) 2nd HP Filter (c) Low frequency equivalent circuit (d) High frequency equivalent circuit

Figure 3.3 2nd HP filter and its equivalent circuit at different frequencies

At low frequencies, the reactor *L* presents a smaller impedance than the resistor *R*, so the entire filter behaves as a single-tuned filter, as shown in Figure 3.3(c). At high frequencies, the impedance of reactor *L* grows and gets bypassed by the resistor *R*, and the filter becomes a *RC* high-pass filter, as shown in Figure 3.3(d).

3.2.1 Analysis of the Filter Characteristics

The 2nd HP filter can also be characterized by the tuning frequency and quality factor. These two parameters are defined in the following equations. Note that a large Q factor indicates a large resistor value, which is the opposite of the definition for the single-tuned filter.

$$\omega_t = \frac{1}{\sqrt{LC}}, \tag{3.1}$$

$$Q = \frac{R}{\omega_t L}. \tag{3.2}$$

Based on the above definitions, the impedance of the 2nd HP filter can be written as in (3.3). Note that ω is expressed in per-unit form.

$$Z_F(\omega) = R_F(\omega) + jX_F(\omega) = Z_F(\omega_{pu})\frac{1}{\omega_t C} \tag{3.3}$$

where

$$Z_F(\omega_{pu}) = \frac{\omega_{pu}^2 Q}{(Q^2 + \omega_{pu}^2)} + j\frac{Q^2\omega_{pu}^2 - Q^2 - \omega_{pu}^2}{\omega_{pu}(Q^2 + \omega_{pu}^2)} \tag{3.4}$$

$$\omega_{pu} = \frac{\omega}{\omega_t} \quad \text{(per-unit value of } \omega_t\text{)}. \tag{3.5}$$

Similar to the single-tuned filter, the capacitor of the 2nd HP filter is also determined by the system reactive power requirement. As a result, the filter impedance in (3.3) can be evaluated by the per-unit impedance $Z_F(\omega_{pu})$. Figure 3.4 shows the frequency responses of $Z_F(\omega_{pu})$ for different Q factors. In this figure, the x-axis is the per-unit frequency referring to the tuning frequency; i.e., ω_{pu}=1 indicates the filter tuning frequency.

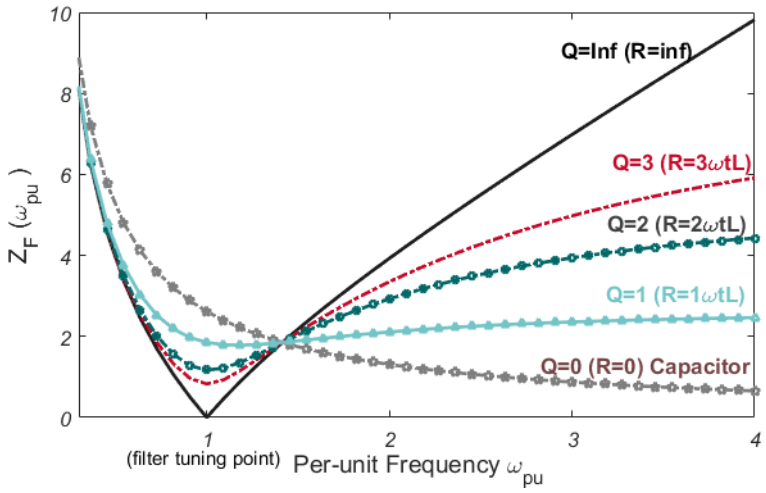

Figure 3.4 2nd HP filter frequency response for different Q values

According to Figure 3.4, all of the filter impedance curves have a common intersection at $\omega_{pu}=\sqrt{2}$. For the frequency range $1\leq\omega_{pu}\leq\sqrt{2}$, the filter impedance is decreasing on the Q factor. A large Q factor provides a good filtering performance near the tuning frequency. In an extreme case ($Q=inf$), the filter becomes a single-tuned filter. For the frequency range $\omega_{pu}>\sqrt{2}$, the filter impedance is increasing on the Q factor. A small Q factor provides a good high-pass performance. In an extreme case ($Q=0$), the filter becomes a pure capacitor. Therefore, the Q factor should be selected to strike a balance between the filtering performance around the tuning frequency and at high frequencies.

It can also be noticed that the filter impedance has the smallest value close to $\omega_{pu}=1$. For the frequency range $\omega_{pu}>1$, the filter provides a certain high-pass filtering performance. In practice, when a range of harmonics needs to be filtered, the lowest harmonic is normally the worst. The lowest harmonic is therefore selected as the filter tuning frequency. The high-pass characteristic of the filter, which can be adjusted by Q, is then used to mitigate the other high-frequency harmonics.

3.2.2 Filter Design Equations

The 2nd HP filter has three components, so the filter design requires three equations to determine the component parameters. The passive filter needs to provide capacitive reactive power at the fundamental frequency, and this condition can be used to determine the filter capacitor, as illustrated in (3.6):

$$C = \frac{Q_F}{\omega_1 V_s^2(\omega_1)}, \tag{3.6}$$

where $V_s(\omega_1)$ is the system rated voltage at the fundamental frequency, Q_F is the filter size determined by the system reactive power requirement.

Two other equations are still needed to solve the filter reactor and resistor. The previous overview shows that the current design methods still have issues on the rest two equations. Therefore, the following studies are intended to clarify these issues and provide an improved method to specify these equations.

3.2.3 Filter Tuning Frequency based Design Equation

It is widely accepted that the second equation should be specified by selecting the filter tuning frequency. Although the common practice is to choose it at the lowest harmonic of concern, there is still disagreement on whether it should be select at or below this harmonic. In single-tuned filter design, the tuning frequency is selected below the harmonic since the filter is quite sensitive to the parameter variation. For the same reason, this design method was directly extended to the 2nd HP filter in several previous studies.

However, such a design has several drawbacks. As explained, the 2nd HP filter needs to strike a balance of filtering performance around the tuning frequency and at high frequencies. If one selects a tuning frequency below the harmonic, the lowest impedance of the filter will deviate from the concerned harmonic range. As a result, the filter design may fail to achieve the required performance balance. Furthermore, selecting a low tuning frequency also increases the filter loss at both

the fundamental frequency and harmonic frequencies. A detailed analysis about this will be done in the next section.

Therefore, it is necessary to evaluate the sensitivity of the 2nd HP filter to the parameter variations. Since a tuned filter is more susceptible at its tuning frequency, the filter impedance change at this frequency is used to quantify its sensitivity, as defined in (3.7). Note that the actual harmonic frequency changes with $\Delta\omega_1$ so the harmonic order h_t is used to replace ω_t.

$$\Delta Z_F(h_t) = \frac{Z_F'(h_t) - Z_F(h_t)}{Z_F(h_t)} = f(Q, \Delta\omega_1, \Delta L, \Delta C) \tag{3.7}$$

This equation shows that $\Delta Z_F(h_t)$ not only depends on the parameter variations $\Delta\omega_1$, ΔC and ΔL but also is a function of the Q factor. Therefore, the Monte-Carlo simulation has been conducted for different Q factors, and the results are shown in Figure 3.5. Note that the parameter variation in Table 2.3 is used for the study.

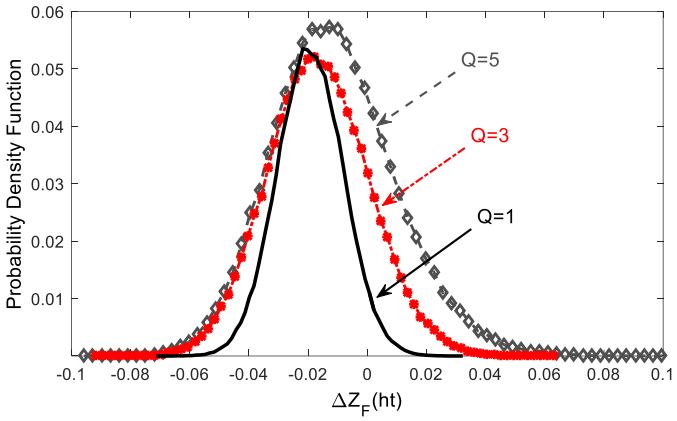

Figure 3.5 Probability density function of $\Delta Z_F(h_t)$ for different Q factors

As can be observed, due to its high-pass filtering characteristic, the 2nd HP filter is not sensitive to the impact of the parameter variations. The impedance change is limited in a very narrow range, only -5% to 3% for the 95% confidence interval. Such a small change is ignorable in practice. Note that a larger Q value leads to a wider variation range since it makes the filter behave more like a single-tuned filter.

Based on the above analysis, the parameter variations should not be a concern for filter design, so there is no need to tune the 2nd HP filter below the harmonic frequency. As a result, the second equation is specified by selecting the tuning frequency directly at the lowest harmonic, as shown in (3.8).

$$\omega_t = \min(\omega_h), \tag{3.8}$$

The above equation can be used to solve for the filter reactor L. As explained, this design can achieve the best performance balance within the filtering range. Then, the harmonic current entering the filter can be controlled by choosing the filter resistor or Q factor.

3.2.4 Filter Loss and Performance based Design Equation

The first two equations have determined the filter capacitor and reactor. To complete the filter design, it is necessary to specify a third equation to determine the filter resistor. Since the resistor value can be quantified by Q factor, the objective of the third equation is to select an appropriate Q value for the 2nd HP filter. As mentioned earlier, this equation has still not been explicitly specified. The only consensus is that it should be established under the condition of meeting the harmonic filtering requirement.

It is common to have more than one Q factor satisfying the required harmonic performance. In such cases, an economical filter should be preferred, especially for industrial customers. The cost of the 2nd HP filter includes the component cost and the operating cost related to filter loss. As will be shown later, the filter component cost is not sensitive to the selection of Q factor, but a proper Q factor is helpful to save the filter loss or operating cost. Therefore, an economical design should specify the third equation by minimizing filter loss, as illustrated in (3.9).

$$\min\left(\sum_{h=1}^{N} P_{\text{loss}}(\omega_h)\right) \qquad s.t. \quad \left|\frac{I_{s.post}(\omega_h)}{I_{s.pre}(\omega_h)}\right| \le 1-\alpha_h\%, \tag{3.9}$$

where ω_h is the harmonic frequency, and $\alpha_h\%$ is the required harmonic filtering requirement at ω_h.

3.2.4.1 Analysis of Filter Component Cost

It has been mentioned that the component cost of the 2nd HP filter is insensitive to the Q factor selection. This section will conduct a detailed justification for this point. In the following study, the cost-related index of each filter component will be introduced first, and then an evaluation will be performed to discuss the Q factor effect on them.

- **Loading Index for Component Cost**

The cost of the filter capacitor is determined by its total capacity Q_{total}, where $Q_{total}=V_c^2\omega_1 C$. Since the capacitor value has been determined in (3.6), the total capacity only depends on the capacitor rated voltage. This fact makes the voltage become the capacitor primary cost index. For accounting the harmonic impacts, this voltage is the arithmetic sum of the voltage at each frequency, as illustrated in (3.10). This equation reveals that the capacitor cost is decided by the total current entering the filter.

$$V_C=I_F(\omega_1)\frac{1}{\omega_1 C}+\sum_{h=2}^{N} I_F(\omega_h)\frac{1}{\omega_h C} \tag{3.10}$$

The cost of the filter reactor contains two parts, a constant part and a variable part. The variable part depends on the reactor value and the current flowing through it. In the previous section, the tuning frequency has fixed the reactor value. As a result, the cost of the filter reactor is mainly determined by its RMS current specified in (3.11). It can expect that the reactor cost also depends on the total filter current.

$$I_{L.RMS}=\sqrt{I_L^2(\omega_1)+\sum_{h=1}^{N} I_L^2(\omega_h)} \tag{3.11}$$

The resistor cost is only a small portion of the entire filter. In general, the resistor cost is relatively stable since it highly depends on the resistor insulation level. However, if the resistor loss causes heating problem, the extra cooling system may be needed, which increases the resistor cost. The filter loss will be discussed in the next section.

- **Impact of the *Q* Factor on Filter Harmonic Current**

All the above analysis reveals that the component cost of the 2nd HP filter highly depends on the total filter current. The filter fundamental frequency current is determined by the filter size (reactive power support). Thus, the *Q* factor selection only affects the filter current at harmonic frequencies. For evaluating such an effect, Figure 3.6 illustrates a general filter circuit.

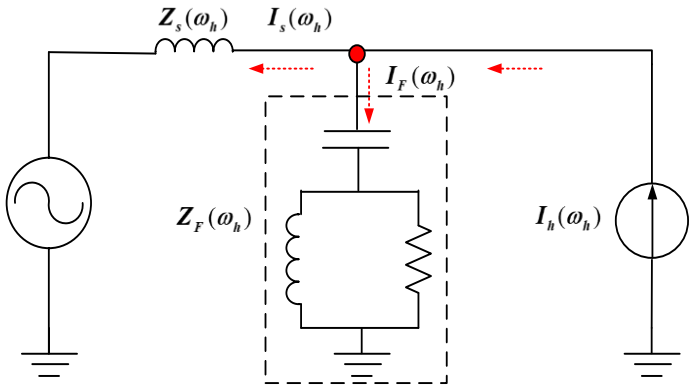

Figure 3.6 General circuit for harmonic analysis

In this circuit, the system impedance $Z_s(\omega)$ is pure inductive, and the non-linear load $I_h(\omega)$ has a typical $1/h$ harmonic characteristic. They can be expressed in the following equations:

$$Z_s(\omega_h) = \frac{V_s^2(\omega_1)}{S_s} \times \frac{1}{SCR} \times h\,, \tag{3.12}$$

$$I_h(\omega_h) = I_h(\omega_1) \times \frac{1}{h} = \frac{S_s}{V_s(\omega_1)} \times \frac{1}{h}\,. \tag{3.13}$$

After the filter connection, the harmonic reduction ratio $\alpha_h\%$ can be calculated by (3.14).

$$\alpha_h\%=\frac{Z_s(\omega_h)}{Z_F(\omega_h)+Z_s(\omega_h)}, \tag{3.14}$$

where $Z_F(\omega_h)$ is the filter impedance, and it can be rewritten as a function of the filter size Q_F, i.e.,

$$Z_F(\omega_h)=Z_F(\omega_{hpu})\frac{1}{\omega_t C}=Z_F(\omega_{hpu})\frac{V_s^2(\omega_1)}{h_t Q_F}. \tag{3.15}$$

Accordingly, the harmonic current flowing into the filter can be obtained by the equation below:

$$I_F(\omega_h)=I_h(\omega_h)\times\alpha_h\%=\frac{S_s}{V_s(\omega_1)}\times\frac{1}{h}\times\alpha_h\%. \tag{3.16}$$

In practice, the Q factor selection affects the harmonic reduction ratio $\alpha_h\%$, which in turn changes the filter harmonic current in (3.16). The following equation is used to quantify the variation of the filter harmonic current with respect to its fundamental frequency component.

$$\frac{\Delta I_F(\omega_h)}{I_F(\omega_1)}=\frac{I_F(\omega_h)-I_F^{'}(\omega_h)}{I_F(\omega_1)}=\frac{S_s(\alpha_h\%-\alpha_h^{'}\%)}{Q_F h}, \tag{3.17}$$

where $I_F(\omega_h)$ and $I_F^{'}(\omega_h)$ are the filter harmonic currents with different Q factors, and $\alpha_h\%$, $\alpha^{'}_h\%$ are their corresponding harmonic reduction ratios, $I_F(\omega_1)$ is the filter fundamental frequency current, and it can be written as:

$$I_F(\omega_1)=\frac{Q_F}{V_s(\omega_1)}. \tag{3.18}$$

It can be observed that the ratio in (3.17) is a function of the system capacity S_s and filter size Q_F. For further analysis, the relation between these two variables is required. This relationship can be obtained by the harmonic filtering requirement at a given harmonic h_a, as illustrated in (3.19). It indicates that the filter should have a $\alpha_{ha}\%$ mitigation ratio at harmonic h_a.

$$\alpha_{ha}\% = \frac{Z_s(\omega_{ha})}{Z_F(\omega_{ha}) + Z_s(\omega_{ha})}. \tag{3.19}$$

Based on the above equation, the relationship between S_s and Q_F can be derived as:

$$Q_F = \frac{\alpha_{ha}\% Z_F(\omega_{hapu}) SCR}{(1-\alpha_{ha}\%) h h_t} S_s. \tag{3.20}$$

where $Z_F(\omega_{hapu})$ is the per-unit filter impedance at harmonic h_a.

By substituting (3.20) back into (3.17), the variation ratio of the filter harmonic current can be rewritten below.

$$\frac{\Delta I_F(\omega_h)}{I_F(\omega_1)} = \frac{(1-\alpha_{ha}\%)(\alpha_h\% - \alpha_h^{'}\%) h_t}{\alpha_{ha}\% Z_F(\omega_{hapu}) SCR} < 0.2. \tag{3.21}$$

In the above equation, $(\alpha_h\% - \alpha^{'}_h\%)$ varies with the Q factor selection but should be below 0.5. $\alpha_{ha}\%$ is from 0.5 to 1, and the system short circuit ratio (SCR) is between 20 and 50. For a good high-pass performance, $Z_F(\omega_{hapu})$ is commonly around 2. Thus, the variation ratio in (3.21) should be within 0.2 even for a conservative estimation. This result indicates that, although the selection of the Q factor affects the filter performance at harmonic frequencies, the variation of the filter harmonic current is insignificant compared to its fundamental frequency component. Since the filter component cost is related to the total filter current, it can expect that such a small variation should have limited impact on the component cost. As a result, selecting the Q factor is not helpful to save the filter component cost.

3.2.4.2 Analysis of Filter Operating Cost

This section discusses the effect of the Q factor selection on the filter operating cost. The operating cost is related to the filter loss caused by the resistor. Since a filter commonly operates for years, the operating cost will be significant for a lossy design. Although the previous works have pointed out the importance of Q factor

to the filter loss, limited research efforts have been spent on clarifying the relationships between them. In [37], the author concerned that a large Q factor or filter resistor might cause a high filter loss, but he only considered the resistor value but ignored the current sharing between the filter reactor and resistor.

Compared with the single-tuned filter, the power loss analysis of high-pass filters is more complicated due to the following reasons. First, a large Q factor indicates a small resistor for the single-tuned filter, but it indicates a large resistor for high-pass filters. Second, the single-tuned filter resistor is connected serially in the circuit, and thereby a large resistor indicates high losses at all frequencies. In contrast, the resistor of high-pass filters is in parallel with the reactor, so the filter loss depends on the current sharing between them. Furthermore, the high-pass filter normally covers a broader harmonic range than the single-tuned filter, which makes it susceptible to the harmonic losses other than its tuning frequency.

As a result, it is necessary to discuss the Q factor impact on the filter losses at different frequencies separately. The filter losses mainly include the fundamental frequency loss and the losses at the filtered harmonics. For a given frequency ω, the filter power loss can be calculated as:

$$P_{loss}(\omega) = I_F^2(\omega) \times R_F(\omega), \tag{3.22}$$

where $I_F(\omega)$ is the filter current at frequency ω and $R_F(\omega)$ is the filter equivalent resistance at frequency ω.

- **Fundamental Frequency Loss**

By substituting $\omega=\omega_1$ into (3.22), the filter fundamental frequency loss can be written as:

$$P_{loss}(\omega_1) = I_F^2(\omega_1) \times R_F(\omega_1). \tag{3.23}$$

Since $I_F(\omega_1)$ is pre-determined by the filter size, $P_{loss}(\omega_1)$ becomes proportional to $R_F(\omega_1)$. Based on (3.4), the expression of $R_F(\omega_1)$ can be illustrated below.

$$R_F(\omega_1) = \frac{1}{\omega_t C} \times \frac{{\omega_{1.pu}}^2 Q}{(Q^2 + {\omega_{1.pu}}^2)} \approx \frac{{\omega_1}^2}{\omega_t^3 C Q} \tag{3.24}$$

where $\omega_{1.pu}=\omega_1/\omega_t$ is the per-unit frequency at the fundamental frequency, and it is ignorable in the denominator because the Q value is way larger than $\omega_{1.pu}$.

This equation reveals that $R_F(\omega_1)$ decreases linearly with the increase of Q factor. Therefore, a large Q factor is effective in reducing the filter fundamental frequency loss. Another finding is that the filter equivalent resistance shares an inversely exponential relationship with its tuning frequency, and thereby a high tuning frequency can significantly reduce the filter fundamental frequency loss. This feature makes the 2nd HP filter more suitable for high frequency applications such as the 11th harmonic or above. The details about this will be further discussed in Section 3.5.

- **Harmonic Frequency Loss**

Similarly, the filter loss at the harmonic frequency ω_h is calculated as:

$$P_{loss}(\omega_h) = I_F^2(\omega_h) \times R_F(\omega_h). \tag{3.25}$$

where $I_F(\omega_h)$ is the filter harmonic current, it can be expressed by the following equation.

$$I_F(\omega_h) = \frac{R_s(\omega_h) + jX_s(\omega_h)}{[R_s(\omega_h) + R_F(\omega_h)] + j[X_s(\omega_h) + X_F(\omega_h)]} I_h(\omega_h). \tag{3.26}$$

By substituting (3.26) back into (3.25), the filter loss at the harmonic frequency can be rewritten as:

$$P_{loss}(\omega_h) = \frac{[R_s^2(\omega_h) + X_s^2(\omega_h)]R_F(\omega_h)}{[R_s(\omega_h) + R_f(\omega_h)]^2 + [X_s(\omega_h) + X_F(\omega_h)]^2} I_h^2(\omega_h). \tag{3.27}$$

For further analysis, one can differentiate $P_{loss}(\omega_h)$ with respect to $R_F(\omega_h)$. Consequently, the critical $R_F(\omega_h)$ value resulting in $\partial P_{loss}(\omega_h)/\partial R_F(\omega_h)=0$ can be obtained as:

$$R_{F.cp}(\omega_h) = \sqrt{R_s^2(\omega_h) + [X_s(\omega_h) + X_F(\omega_h)]^2} \ . \tag{3.28}$$

The study shows that $P_{loss}(\omega_h)$ is increasing on $R_F(\omega_h)$ for $R_F(\omega_h)<R_{F.cp}(\omega_h)$ and is decreasing on $R_F(\omega_h)$ for $R_F(\omega_h)>R_{F.cp}(\omega_h)$. In fact, $R_F(\omega_h)<R_{F.cp}(\omega_h)$ is always true at harmonic frequencies. The reason is that $R_F(\omega_h)$ should be smaller than the system impedance $Z_s(\omega_h)$ for filtering purposes, and $X_s(\omega_h)$ and $X_F(\omega_h)$ normally have positive values. As a result, a large $R_F(\omega_h)$ indicates a high $P_{loss}(\omega_h)$. The analysis can use $R_F(\omega_h)$ to quantify $P_{loss}(\omega_h)$. Note that this finding is also applicable to the other filters in the following sections.

The expression of the filter equivalent resistance $R_F(\omega_h)$ is shown in (3.29), where $\omega_{h.pu}=\omega_h/\omega_t$ is the per-unit frequency at harmonic frequency.

$$R_F(\omega_h) = \frac{{\omega_{h.pu}}^2 Q}{\omega_t C(Q^2 + {\omega_{h.pu}}^2)} \tag{3.29}$$

The analysis of the above equation reveals that, under the condition of $Q>\omega_{h.pu}$, a large Q factor can reduce $R_F(\omega_h)$ and $P_{loss}(\omega_h)$. The $\omega_{h.pu}$ value is approximately 1 for the harmonics around the tuning frequency. Since the filter Q factor is usually higher than 1, a large Q value is effective in reducing the harmonic losses around the filter tuning frequency. As aforementioned, these harmonics are the dominant ones in the filtering range. It is therefore reasonable to assume the total harmonic loss decreases with a large Q factor.

Two findings can be obtained from the above analysis. The first one is that the selection of Q factor is helpful to save the filter operating cost. Since the filter component cost is insensitive to Q factor, it is reasonable to specify the third design equation to minimize the filter loss, as shown in (3.9). The second finding is that the filter loss is decreasing on the Q factor. To minimize the filter loss, the design only needs to select the largest Q value satisfying the required filtering performance. This finding can significantly simplify the filter design process.

3.2.5 Proposed Design Method

According to the previous study, the three equations proposed for the 2nd HP filter design can be summarized as follows.

- **Design Equation 1: Reactive Power Requirement**

The first equation is established by the system reactive power requirement. This condition can be used to solve for the filter capacitor *C*, as illustrated below:

$$C = \frac{Q_F}{\omega_1 V_s^2(\omega_1)}, \tag{3.30}$$

- **Design Equation 2: Selection of Filter Tuning Frequency**

The second equation is related to the selection of the filter tuning frequency. As explained, the 2nd HP filter is not sensitive to the parameter variations, so the tuning frequency is selected directly at the lowest harmonic of concern.

$$\omega_t = \min(\omega_h), \tag{3.31}$$

where ω_h is all the harmonics of concern.

- **Design Equation 3: Filtering Loss and Performance Consideration**

For an economical design, the last equation is to minimize the filter loss under the condition of satisfying the required harmonic performance.

$$\min\left(\sum_{h=1}^{N} P_{\text{loss}}(\omega_h)\right) \qquad s.t. \quad \left|\frac{I_{s.post}(\omega_h)}{I_{s.pre}(\omega_h)}\right| \le 1-\alpha_h\% \ , \tag{3.32}$$

- ***Design Process***

The filter capacitor and reactor can be calculated by (3.30) and (3.31) directly. As a result, the filter design becomes an optimization problem with *Q* as the only variable. The simplest way to solve this problem is to scan all the possible *Q* values to find the one satisfying (3.32). Since a large *Q* factor leads to a low filter loss, the design process can be simplified by searching the maximum *Q* value that meets all

the filtering requirements. Figure 3.7 illustrates the flow-chart for the 2nd HP filter design.

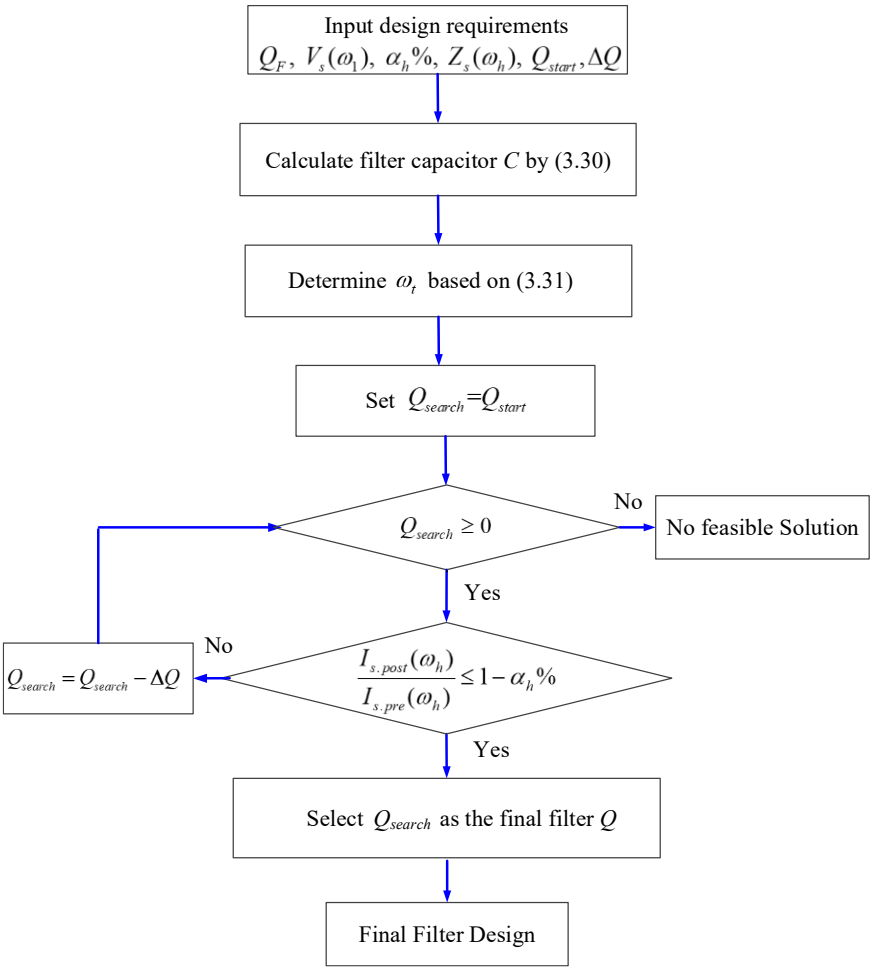

Figure 3.7 Flow-chart for the 2nd HP filter design

Note that there might be no feasible solutions if the above conditions are too stringent. In such cases, the above design conditions should be relaxed, such as reducing the filtering requirements or increasing the filter reactive power support.

3.2.6 Example Case Study

For evaluating the proposed design method, a case study is conducted based on the typical industrial system in Chapter 2. Figure 3.8 depicts the configuration of this industrial system. The spectrums of the two harmonic-producing loads are listed in Table 3.1.

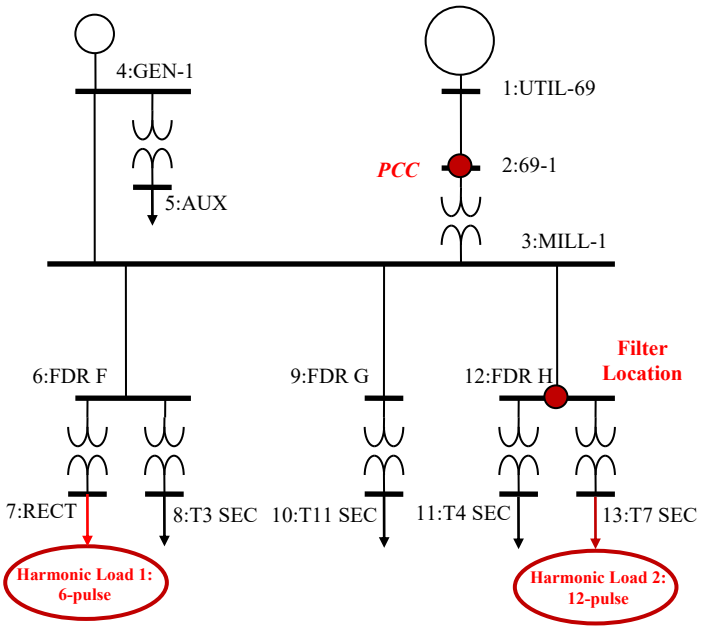

Figure 3.8 Configuration of the studied industrial system

Table 3.1 Harmonic-producing load spectrum

Harmonic	6-pulse harmonic load 1		12-pulse harmonic load 2	
	Percent (%)	Relative Angle (°)	Percent (%)	Relative Angle (°)
1st	100.00	0.00	100.00	0.00
5th	18.24	-55.68	----	----
7th	11.30	-84.11	----	----
11th	6.67	-143.56	6.67	-143.56
13th	5.72	-175.58	5.72	-175.58
17th	4.80	111.39	----	----
19th	4.79	68.30	----	----
23th	3.90	-24.61	3.90	-24.61
25th	3.83	-67.64	3.83	-67.64
29th	0.71	-145.46	----	----
31th	0.62	176.83	----	----
35th	0.44	97.40	0.44	97.40
37th	0.38	54.36	0.38	54.36

The harmonic analysis is conducted, and the results are given in Table 3.2. As shown, there are excessive distortions at the 11th, 13th, 23th and 25th harmonics. In order to meet the harmonic limits, the required harmonic mitigation performance is also calculated in the following table.

Table 3.2 Harmonic analysis results

Harmonic #	Individual harmonic distortion (*IHD*) in percentage %							
	11th	13th	17th	19th	23th	25th	35th	37th
Harmonic Distortions	4.00	3.43	0.80	0.80	2.33	2.28	0.26	0.23
IEEE Harmonic Limits	2.00	2.00	1.50	1.50	0.60	0.60	0.30	0.30
Filtering requirement	50%	42%	----	----	74%	73%	----	----

- ***Performance Evaluation***

Based on the proposed design method, a three-phase 3000 kvar 2nd HP filter is designed. The filter is tuned at the 11th harmonic, and its parameters are illustrated in Table 3.3.

Table 3.3 Parameters of designed 2nd HP filters

Topology	$C\,(uF)$	$L\,(mH)$	$R\,(\Omega)$	h_t (th)	Q
2nd HP Filter	41.8	1.4	26.5	11	4.60

Figure 3.9 presents the harmonic performance of filters with different Q factors. In this figure, the bar-charts above the solid red line indicates that the harmonic filtering requirements are satisfied.

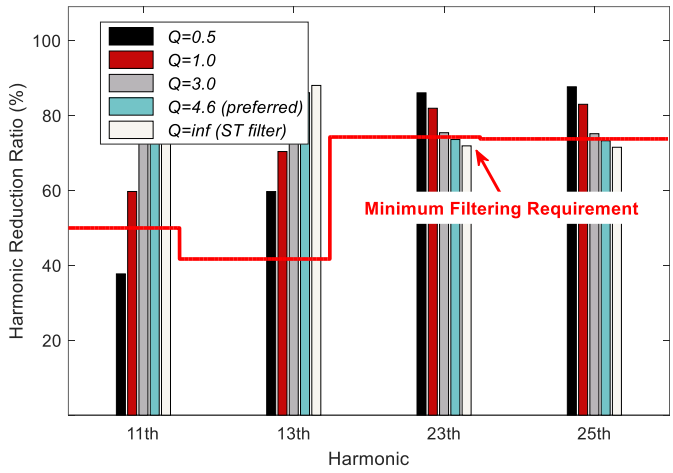

Figure 3.9 Harmonic mitigation performance of the 2nd HP filter

As can be seen, the filter with Q=*inf* (a single-tuned filter) cannot provide enough harmonic mitigation at high frequencies like 23rd and 25th harmonic. The reason is that the single-tuned filter is primarily designed to target only one

harmonic component. As the Q factor decreases, the 2nd HP filter has a poor harmonic filtering performance near the tuning frequency but presents a good performance at high frequencies. The filter with Q values from 0.74 to 4.6 can satisfy all the filtering requirements. For the Q value less than 0.74, the filter fails to meet the harmonic limit at the 11th harmonic. The proposed design selects Q=4.6 for loss minimization.

Table 3.4 lists the filter component loading. Consistent with the previous analysis, the loadings of the filter capacitor and reactor are insensitive to Q factor. There are some variations on the loading of the filter resistor, which is due to the Q factor impact on the filter loss.

Table 3.4 Comparison results of component loading

Q factor		0.74	2.00	3.00	4.60
Capacitor	Voltage /kV	8.45	8.36	8.34	8.33
	Capacity /Mvar	1.13	1.10	1.10	1.09
Reactor	Current /A	127.75	130.51	130.96	131.21
	Capacity /kvar	8.56	8.94	9.00	9.03
Resistor	Voltage /kV	0.20	0.28	0.29	0.30
	Current /A	47.74	24.02	16.94	11.40

Table 3.5 compares the filter loss for different Q factors. It indicates that a large Q leads to a reduced filter loss. Compared to the filter with Q=0.74, the proposed design saves about 70% in filter loss. Note that all the filters have a low fundamental frequency loss since their tuning frequencies are relatively high in this case. As discussed in Section 3.2.4, there will be a significant increase on the fundamental frequency loss if the 2nd HP filter is applied to a low-frequency application.

Table 3.5 Comparison results of filter loss

Q factor	Power loss at different frequencies (kW for each phase)							
	1st	11th	13th	17th	19th	23th	25th	Total
Q=0.74	1.00	3.87	2.51	0.12	0.12	1.07	1.03	9.73
Q=2.00	0.38	2.04	1.57	0.10	0.11	1.20	1.25	6.66
Q=3.00	0.25	1.42	1.11	0.08	0.09	0.97	1.05	4.97
Q=4.60	0.16	0.94	0.75	0.05	0.06	0.71	0.77	3.45

The costs of these filters are also analyzed, as given in Table 3.6. Since the component costs are relatively stable, the filter economics are mainly determined by the operating costs. As can be seen, the operating cost of a poorly designed filter is almost comparable to the filter component cost. It is therefore reasonable to select the Q factor for minimizing operating cost. The details of the cost calculation are available in Appendix E.

Table 3.6 Comparison results of filter cost

Q factor	0.74	2.00	3.00	4.60
Component Cost ($)	43,847	42,709	42,304	41,982
Operating Cost ($)	44,762	30,625	22,844	15,854
Total Cost ($)	88,608	73,334	65,148	57,837

- ***Additional Studies***

If the filtering requirement at the 25th harmonic is increased by 10%, it will result in a 2nd HP filter with Q=1.02. Figure 3.10 presents the frequency responses for Q=4.6 and Q=1.02 respectively.

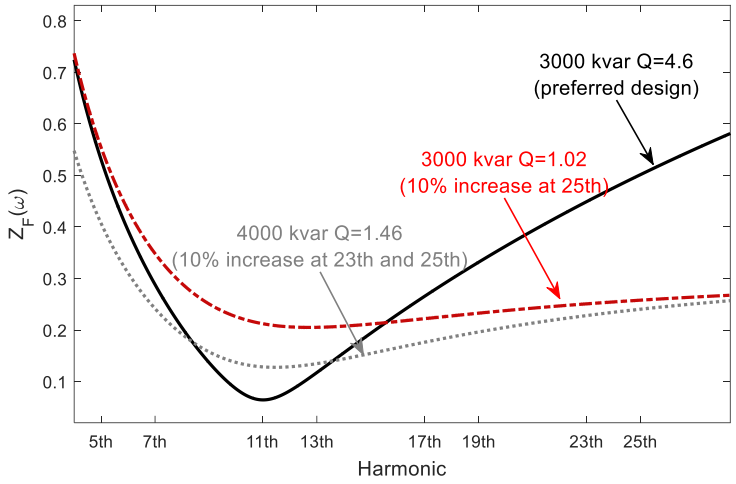

Figure 3.10 Filter frequency responses for different conditions

The proposed design method has no feasible solution if the filtering requirement at the 23rd harmonic is also increased by 10%. To address this problem, the filter size should be increased to 4000 kvar, resulting in a filter with Q=1.46. The reason is that a large filter size leads to a low filter impedance, as shown in Figure 3.10.

In conclusion, a comparative case study has been conducted to evaluate the performance of the proposed design method. The results revealed that the proposed design can provide an economical filter option to achieve the required filtering performance.

3.3 C-type Filter

It has been mentioned that the 2nd HP filter may have an excessive filter loss, especially at low-order harmonics. To address this concern, a topology named the C-type filter is configured by connecting a capacitor C_2 in series with the filter reactor L, as shown in Figure 3.11(b). The L-C_2 branch is designed to resonate at the fundamental frequency so that there is little current flowing to the resistor R. As a result, the fundamental frequency loss is reduced.

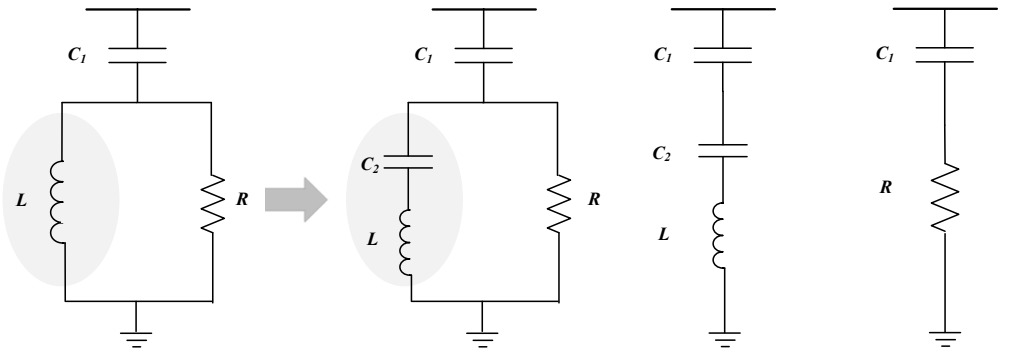

(a) 2nd HP Filter (b) C Type Filter (c) Low frequency equivalent circuit (d) High frequency equivalent circuit

Figure 3.11 C-type filter and its equivalent circuits at different frequencies

At low frequencies, the impedance of the L-C_2 branch is smaller than the resistor, so the C-type filter behaves as a single-tuned filter, as shown in Figure 3.11(c). As the frequency increases, the L-C_2 branch impedance becomes larger than the resistor. Therefore, the filter behaves as a series C_1+R circuit at high frequencies, as shown in Figure 3.11(d).

3.3.1 Analysis of Filter Characteristics

To reduce the filter loss, the capacitor C_2 is tuned to resonate with the reactor L at the fundamental frequency; i.e.,

$$C_2 = \frac{1}{\omega_1^2 L}. \tag{3.33}$$

Based on this condition, the impedance of the C-type filter can be expressed in (3.34). Note that ω_t and Q factor are defined in the same way as the 2nd HP filter.

$$Z_F(\omega) = R_F(\omega) + jX_F(\omega) = Z_F(\omega_{pu})\frac{1}{\omega_t C_1} \tag{3.34}$$

where

$$Z_F(\omega_{pu}) = \frac{K^2 Q}{K^2 + Q^2\omega_{pu}^2} + j\frac{Q^2\omega_{pu}^2 K - Q^2\omega_{pu}^2 - K^2}{\omega_{pu}[K^2 + Q^2\omega_{pu}^2]} \tag{3.35}$$

$$K = (\omega_{pu}^2 - \omega_{1.pu}^2). \tag{3.36}$$

Figure 3.12 compares the frequency responses of the C-type filter and the 2nd HP filter. Excepting for the capacitor C_2, all the other filter parameters are the same. As shown, the C-type filter presents a similar filter response as the 2nd HP filter. This can be explained by the analysis of the L-C_2 branch. According to (3.33), C_2 and L have the same reactance value at the fundamental frequency but opposite signs. As the frequency increases, the L reactance value continues to increase but the reactance value of C_2 decreases, which makes the reactor L dominate the L-C_2 branch at harmonic frequencies. Therefore, the C-type filter has a similar harmonic performance as the 2nd HP filter.

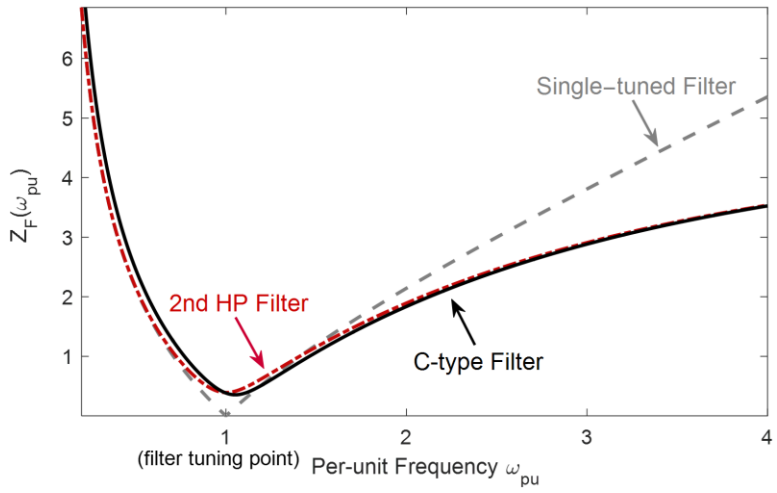

Figure 3.12 Frequency response of the C-type filter

3.3.2 Filter Design Equations

Since the C-type filter has four components, four equations are required to determine the component parameters. The first equation is still specified to provide the reactive power required by the supply system, and the capacitor C_1 can be solved accordingly, as shown below.

$$C_1 = \frac{Q_F}{\omega_1 V_s^2(\omega_1)}, \tag{3.37}$$

where $V_s(\omega_1)$ is the system rated voltage at the fundamental frequency.

The capacitor C_2 is used to reduce the filter loss at the fundamental frequency. To achieve this, the second design equation is established by tuning the L-C_2 branch resonate at this frequency, i.e.,

$$C_2 = \frac{1}{\omega_1^2 L}, \tag{3.38}$$

This leaves two other equations for determining the filter reactor and resistor. There are still issues with these two design equations, and a consensus on how to properly establish them has not been reached. Therefore, the following study will conduct a discussion on them separately.

3.3.3 Filter Tuning Frequency based Design Equation

The selection of the filter tuning frequency can be used to specify the one design equation. Similar to the 2nd HP filter, it is still controversial whether it is necessary to select it below the harmonic for concerning the parameter variations. To clarify this issue, the following study evaluates the impact of the parameter variations on the C-type filter. It is quantified by the change of the filter impedance at the tuning frequency, as shown in (3.39). The harmonic order h_t is used to replace ω_t to account for the harmonic frequency change due to $\Delta\omega_1$.

$$\Delta Z_F(h_t) = \frac{Z_F'(h_t) - Z_F(h_t)}{Z_F(h_t)} = f(h, Q, \Delta\omega_1, \Delta L, \Delta C) \tag{3.39}$$

The change of the filter impedance is evaluated by the Monte-Carlo simulation, and the results are shown in Figure 3.13. This analysis is still based on the typical variation range in Table 2.3. In this figure, the tuning frequency is selected at the 3rd harmonic, which is the common case in practice. Note that increasing the filter tuning frequency will narrow the variation range below.

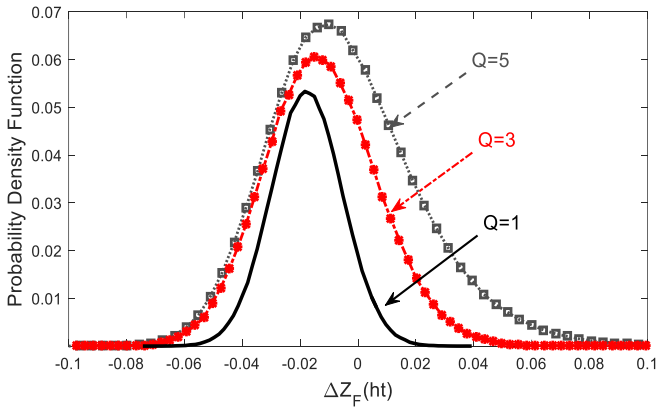

Figure 3.13 Probability density function of $\Delta Z_F(h_t)$ for typical Q values

The above results reveal that the parameter varations have very limited impact on the C-type filter. There is no need to select a low tuning frequency for such concern. As a result, it is suggested to select the tuning frequency directly at the lowest harmonic, as shown in (3.40). This equation can be used to solve for the filer reactor.

$$\omega_t = \min(\omega_h) \tag{3.40}$$

3.3.4 Filter Loss and Performance based Design Equation

Finally, one more equation is still needed to determine the filter resistor. Since the resistor can be quantified by the Q factor, the objective of this equation becomes to choose a proper Q factor. The previous works have proposed various design methods to establish this equation. Unfortunately, these design methods mainly focused on the filter harmonic performance but ignored the economics of the filter. In this work, this equation is specified by minimizing the filter loss, as shown in (3.41). As will be explained later, this design can guarantee an economical design satisfying the required harmonic filtering performance.

$$\min\left(\sum_{h=1}^{N} P_{\text{loss}}(\omega_h)\right) \qquad s.t. \quad \left|\frac{I_{s.post}(\omega_h)}{I_{s.pre}(\omega_h)}\right| \le 1-\alpha_h\%, \tag{3.41}$$

3.3.4.1 Analysis of Filter Component Cost

The filter cost is known to include the component cost and operating cost. In this section, an assessment is conducted on the Q factor impact on the filter component cost. As explained in Section 3.2.4.1, the filter component cost highly depends on the total current entering the filter, and the Q factor only affects the currents at the harmonic frequencies. Therefore, the filter component cost can be evaluated by the variation of the harmonic current.

The previous equation in (3.21) can still be used to evaluate such effects, as rewritten below.

$$\frac{\Delta I_F(\omega_h)}{I_F(\omega_1)} = \frac{(1-\alpha_{ha}\%)(\alpha_h\% - \alpha_h^{'}\%)h_t}{\alpha_{ha}\% Z_F(\omega_{hapu}) SCR} < 0.05 \tag{3.42}$$

The tuning point h_t shares a linear relationship with the variation ratio. Compared to the 2nd HP filter, the C-type filter typically has a lower h_t. This fact leads to a reduced ratio in the equation below. The per-unit impedance of the C-

type filter needs to be replaced by (3.35), but this does not affect the result significantly since the per-unit impedance of the C-type filter is almost the same as the 2nd HP filter. Consequently, the component cost of the C-type filter is also insensitive to the Q factor selection.

3.3.4.2 Analysis of Filter Operating Cost

This section will assess the effect of selecting the Q factor on the filter operating cost. Since the operating cost is related to the filter loss, the focus becomes to discuss the relationship between the Q factor and the filter loss. It has been shown in Section 3.2.3.2 that a small equivalent resistance indicates a low filter loss. This finding is directly used to simplify the following analysis. (3.43) presents the equivalent resistance of the C-type filter.

$$R_F(\omega) = \frac{(\omega_{pu}^2 - \omega_{1.pu}^2)^2 Q}{\omega_t C\,[(\omega_{pu}^2 - \omega_{1.pu}^2)^2 + Q^2 \omega_{pu}^2]}. \tag{3.43}$$

- **Fundamental Frequency Loss**

At the fundamental frequency, the resistor R is short-circuited by the L-C_2 branch, so the filter equivalent resistance equals to zero; i.e., $R_F(\omega_1) = 0$. Therefore, the C-type filter theoretically has no loss at this frequency. In fact, it is the most desirable feature of the C-type filter, making this filter an ideal choice for the applications at low frequencies.

However, the parameter variations may tune the L-C_2 branch away from the fundamental frequency. There exists the concern that it may lead to a significant increase in the filter loss [1]. A Monte-Carlo simulation has been conducted to assess the filter fundamental frequency loss under this condition, and the results are shown in Figure 3.14. Note that the power loss is expressed in the percentage of the filter size.

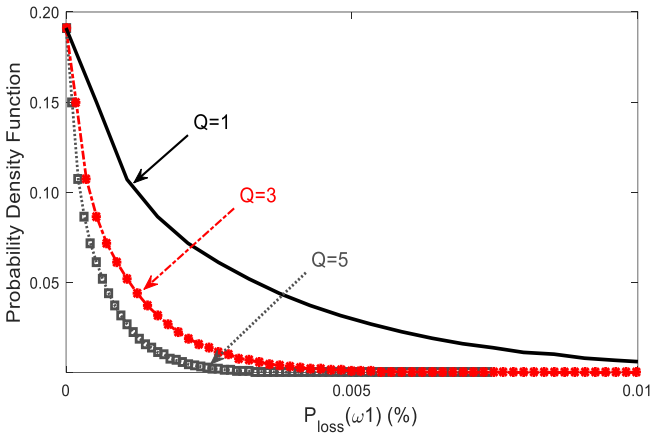

Figure 3.14 Probability density function of filter power frequency loss

According to Figure 3.14, the following results can be obtained: 1) the filter loss at the fundamental frequency is still well controlled even with parameter variations, 2) a large Q factor is also effective in reducing the filter fundamental frequency loss caused by the parameter variations.

- **Harmonic Frequency Loss**

The filter equivalent resistance at the harmonic frequency can be written as:

$$R_F(\omega_h) = \frac{(\omega_{h.pu}^2 - \omega_{1.pu}^2)^2 Q}{\omega_t C_1 \left[(\omega_{h.pu}^2 - \omega_{1.pu}^2)^2 + Q^2 \omega_{h.pu}^2\right]}. \tag{3.44}$$

In this equation, $\omega_{1.pu}^2$ is normally very small and ignorable comparing to $\omega_{h.pu}^2$. For example, if the C-type filter is tuned at the 3rd harmonic, $\omega_{h.pu}^2$ is approximately 10 times larger than $\omega_{1.pu}^2$. Therefore, the above equation can be further simplified as below.

$$R_F(\omega_h) = \frac{\omega_{h.pu}^2 Q}{\omega_t C_1 \left(\omega_{h.pu}^2 + Q^2\right)}. \tag{3.45}$$

The simplified equation in (3.45) is the same as (3.29) for the 2nd HP filter. As a result, it can be expected that a large Q factor also reduces the filter loss at harmonic frequencies.

The above analysis reveals that the Q factor selection is helpful to save filter loss and operating cost. Since the filter component cost is insensitive to the Q factor, it is logical to use the last equation to minimize the filter loss for an economical design. A large Q factor leads to a low filter loss, so the design can be simplified by selecting the maximum Q value that satisfies the required filtering performance in the harmonic range.

3.3.5 Proposed Design Method

As a summary of the previous sections, the four design equations of the C-type filter can be listed as follows.

- **Design Equation 1: Reactive Power Requirement**

The first equation is established based on the system reactive power requirement at the fundamental frequency, as shown in (3.46):

$$C_1 = \frac{Q_F}{\omega_1 V_s^2(\omega_1)}. \tag{3.46}$$

- **Design Equation 2: Fundamental Frequency Loss Minimization**

The second equation aims to reduce the filter loss at the fundamental frequency. This condition can be used to determine the capacitor C_2, i.e.

$$C_2 = \frac{1}{\omega_1^2 L}. \tag{3.47}$$

- **Design Equation 3: Selection of Filter Tuning Frequency**

The third equation is specified by selecting the filter tuning frequency. Since the C-type filter is not sensitive to the parameter variation, the tuning frequency is selected at the lowest harmonic of concern for achieving the best performance balance in the harmonic range.

$$\omega_t = \min(\omega_h), \tag{3.48}$$

where ω_h is all the harmonics of concern.

- **Design Condition 4: Filter Loss and Performance Consideration**

The last equation is to minimize the filter total loss under the constraints of the harmonic filtering requirements, as illustrated below.

$$\min\left(\sum_{h=1}^{N} P_{\text{loss}}(\omega_h)\right) \qquad s.t. \quad \left|\frac{I_{s.post}(\omega_h)}{I_{s.pre}(\omega_h)}\right| \le 1-\alpha_h\%, \tag{3.49}$$

- **Design Process**

Figure 3.15 illustrates the design process of the C-type filter. According to the above analysis, a large Q factor leads to a reduced filter loss. Therefore, the design is simplified by selecting the maximum Q value that satisfies the desired harmonic filtering performance.

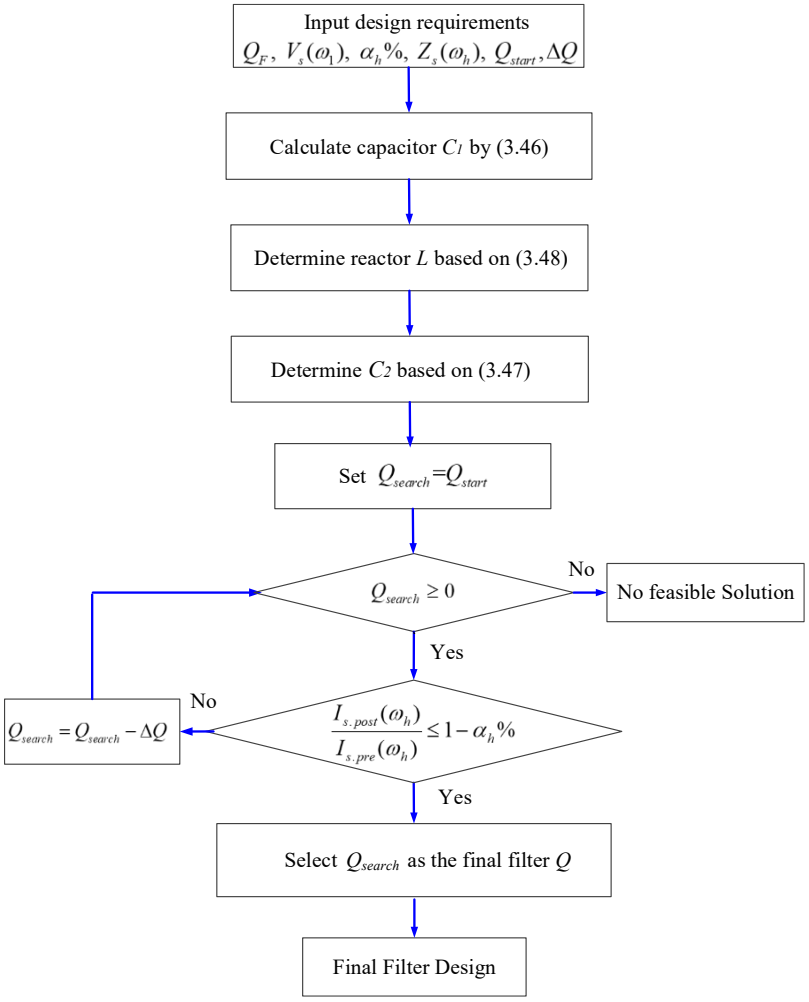

Figure 3.15 Flow-chart for the C-type filter design

3.3.6 Example Case Study

For performance evaluation, a C-type filter is designed to replace the 2nd HP filter in Section 3.2.6. Table 3.7 lists the parameters of the C-type filter.

Table 3.7 Parameters of designed C-type filters

Topology	$C_1\,(uF)$	$C_2\,(uF)$	$L\,(mH)$	$R\,(\Omega)$	h_t (th)	Q
C-type Filter	41.8	5056.1	1.4	27.0	11	4.68

Figure 3.16 compares the harmonic filtering performance of C-type filters with different Q factors, where Q=0.74 is based on the design in [84] to optimize the filter high-pass performance, and Q=3.35 is based on the design in [85] to minimize the total voltage harmonic distortion (VTHD). It can be observed that, although their performance is slightly different at specific harmonics, all the filters can meet the filtering requirements in the harmonic range.

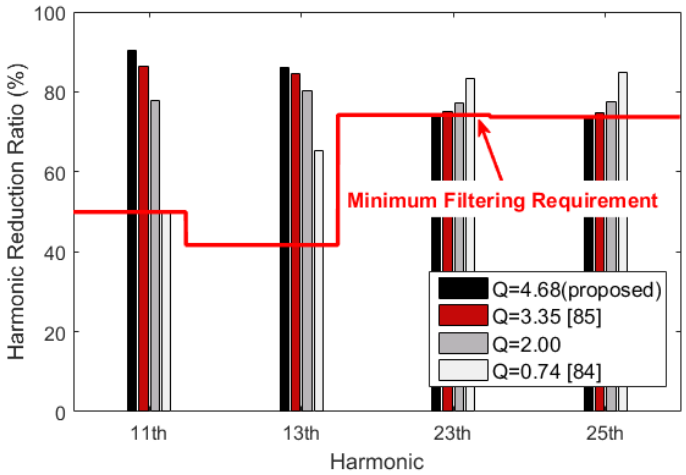

Figure 3.16 Harmonic mitigation performance of the C-type filter

The filter component loading and loss are also analyzed, as listed in Table 3.8 and Table 3.9. Consistent with the previous analysis, the filter component loading is relatively stable, but the filter loss decreases with the increase of the Q factor. This result justifies the proposed design equation in (3.49) for the minimization of filter loss.

Table 3.8 Comparison results of component loading

Q factor		4.68 (proposed)	3.35 (min VTHD)	2.00	0.74 (optimize HP)
C_1	Voltage /kV	8.27	8.27	8.30	8.39
	Capacity /Mvar	1.08	1.08	1.08	1.11
C_2	Voltage /kV	1.20	1.20	1.20	1.20
	Capacity /Mvar	2.74	2.74	2.74	2.74
L	Current /A	130.28	130.13	129.68	127.69
	Capacity /kvar	8.90	8.88	8.82	8.55
R	Voltage /kV	0.29	0.29	0.27	0.19
	Current /A	10.91	14.90	23.28	45.13

Table 3.9 Comparison results of filter loss

Q factor	Power loss at different frequencies (kW for each phase)							
	1st	11th	13th	17th	19th	23th	25th	Total
4.68	0.00	0.92	0.73	0.05	0.06	0.69	0.76	3.22
3.35	0.00	1.27	1.00	0.07	0.08	0.90	0.97	4.29
2.00	0.00	2.03	1.56	0.10	0.11	1.20	1.25	6.25
0.74	0.00	3.84	2.51	0.12	0.12	1.07	1.03	8.70

Table 3.10 lists the cost of each filter. As can be seen, the major difference is the filter operating cost that is related to power loss. Compared with the other options, the proposed method can provide a more economical solution.

Table 3.10 Comparison results of filter cost

Q	4.68	3.35	2.00	0.74
component cost ($)	102,152	102,384	102,886	104,089
operating cost ($)	14,794	19,479	28,757	40,008
total cost ($)	116.946	122,133	131,623	144,097

3.4 Third-order High-pass Filter

Another way to reduce the filter loss is to add the second capacitor in series with the filter resistor, as shown in Figure 3.17(b). This topology is named the third-order high-pass filter (3rd HP filter). The second capacitor has a large reactance at the fundamental frequency, reducing the current flowing through the resistor.

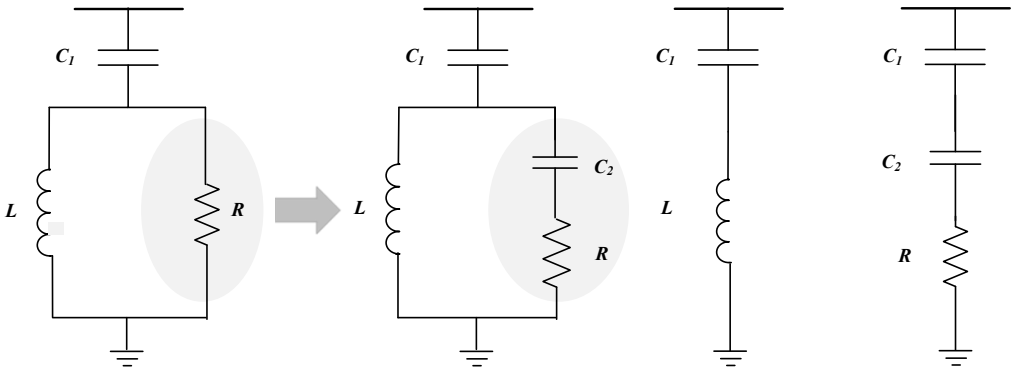

(a) 2nd HP Filter (b) 3rd HP Filter (c) Low frequency equivalent circuit (d) High frequency equivalent circuit

Figure 3.17 3rd HP filter and its equivalent circuits at different frequencies

The impedance of the reactor L is much smaller than the R-C_2 branch at low frequencies, so most of the currents flow through the reactor branch. The filter behaves as a single-tuned filter, as shown in Figure 3.17(c). As the frequency increases, the reactor L impedance becomes larger than the R-C_2 branch. Therefore, the filter behaves as a series C-R circuit at high frequencies, as shown in Figure 3.17(d).

3.4.1 Analysis of the Filter Characteristics

The capacitor C_2 is used to reduce the filter loss at the fundamental frequency. In [88], mathematical analysis was conducted to obtain the C_2 value for minimizing filter fundamental frequency loss. It revealed that the capacitor C_2 should satisfy the following condition.

$$C_2 = \frac{C_1 L}{R^2 C_1 - L} = \frac{C_1}{Q^2 - 1} \tag{3.50}$$

Based on the above equation, the impedance of the 3rd HP filter can be written in (3.51), where ω_t and Q are defined the same way as the 2nd HP filter.

$$Z_F(\omega) = R_F(\omega) + jX_F(\omega) = Z_F(\omega_{pu})\frac{1}{\omega_t C_1} \tag{3.51}$$

where

$$Z_F(\omega_{pu}) = \frac{\omega_{pu}^4 Q}{M} + j\frac{\omega_{pu}^2(Q^4 - Q^2 - 1) - (Q^2 - 1)^2}{\omega_{pu} M} \tag{3.52}$$

$$M = (\omega_{pu}^2 - Q^2 + 1)^2 + Q^2\omega_{pu}^2 . \tag{3.53}$$

Figure 3.18 compares the frequency response of the 3rd HP filter with the other high-pass filters. All the filters have the same reactive power support and Q factor. As shown, the harmonic performance of the 3rd HP filter is between the single-tuned filter and 2nd HP filter. The 3rd HP filter presents a lower impedance than the single-tuned filter at high frequencies, implying a better high-pass performance. Since a small C_2 value is required for loss reduction, the small C_2 value will increase the impedance of the resistor branch at harmonic frequencies. It presents a higher filter impedance than the other high-pass filters with the same Q factor. As a result, it is common to have a small Q factor for the 3rd HP filter, normally below 2.

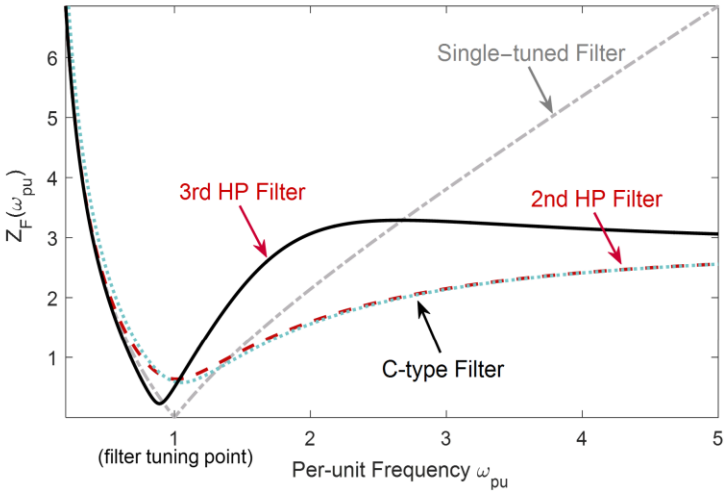

Figure 3.18 Frequency response of the 3rd HP Filter

Figure 3.19 illustrates the filter frequency responses with various Q factors. One can notice that a large Q factor provides a good filtering performance around tuning frequency, and a small Q factor leads to a good high-pass performance. As a result, the Q factor should be selected to strike a filtering performance balance in the harmonic range.

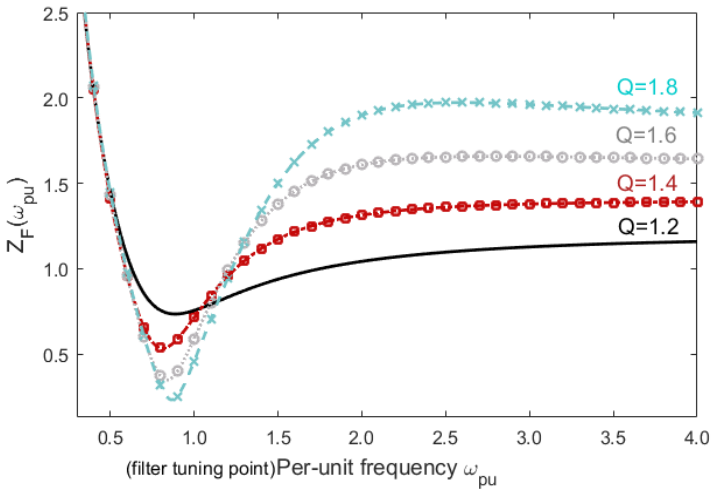

Figure 3.19 Filter frequency response for different Q values

3.4.2 Filter Design Equations

The 3rd HP filter also has four components, so four design equations are required to determine all the component parameters. The previous studies have already specified two of the design equations. The first equation is to determine the filter capacitance based on the system reactive power requirement at the fundamental frequency. It can be used to solve for the capacitor C_1, as illustrated in (3.54):

$$C_1 = \frac{Q_c}{\omega_1 V_s^2(\omega_1)}. \tag{3.54}$$

The second equation is to minimize filter loss at the fundamental frequency. To achieve this, the capacitor C_2 needs to satisfy the following equation [88].

$$C_2 = \frac{C_1}{Q^2 - 1}. \tag{3.55}$$

3.4.3 Filter Tuning Frequency based Design Equation

The selection of the filter tuning frequency can be used to establish the third design equation. As with the other high-pass filters, the analysis is also conducted to evaluate the sensitivity of the 3rd HP filter to the parameter variation. It is quantified by the change of the filter impedance at the tuning frequency, as shown

in (3.56). Note that h_t is used to replace ω_t to consider the harmonic frequency change caused by $\Delta\omega_1$.

$$\Delta Z_F(h_t) = \frac{Z_F'(h_t) - Z_F(h_t)}{Z_F(h_t)} = f(Q, \Delta\omega_1, \Delta L, \Delta C) \tag{3.56}$$

The above equation is evaluated by a Monte-Carlo simulation, and the results are shown in Figure 3.20. It reveals that the parameter variation also has ignorable impact on the 3rd HP filter. Therefore, the third equation is specified in (3.57) by selecting the tuning frequency at the lowest harmonic of concern, and this condition determines the filter reactor.

$$\omega_t = \min(\omega_h) \tag{3.57}$$

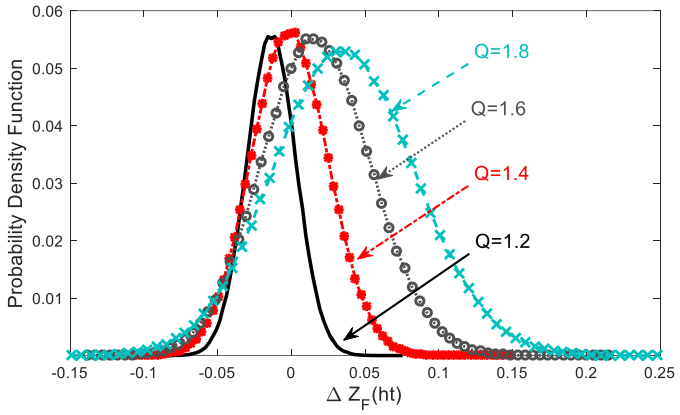

Figure 3.20 Probability density of $\Delta Z_F(h_t)$ for different Q factors

3.4.4 Filter Loss and Performance based Design Equation

Finally, one more equation is required to determine the filter resistor, i.e., the Q factor. Under the constraints of the required filtering performance, this equation should be established by considering the filter cost. As will be shown later, the Q factor selection also has a minor impact on the component cost of the 3rd HP filter. Therefore, an economical design is specified by minimizing filter loss, as illustrated in (3.58).

$$\min\left(\sum_{h=1}^{N} P_{\text{loss}}(\omega_h)\right) \qquad s.t. \quad \left|\frac{I_{s.post}(\omega_h)}{I_{s.pre}(\omega_h)}\right| \le 1-\alpha_h\%, \tag{3.58}$$

3.4.4.1 Analysis of Filter Component Cost

As with the other filters, this section discusses the relationship between the filter component cost and Q factor. The equation in (3.21) can still be used to evaluate the effect of the Q factor on the filter current. It is rewritten below for ease of analysis. Note that $Z_F(\omega_{hapu})$ needs to be replaced by (3.52).

$$\frac{\Delta I_F(\omega_h)}{I_F(\omega_1)} = \frac{(1-\alpha_{ha}\%)(\alpha_h\% - \alpha_h^{'}\%)h_t}{\alpha_{ha}\% Z_F(\omega_{hapu}) SCR} < 0.1 \tag{3.59}$$

The analysis indicates that the variation ratio in (3.59) is also very small. As a result, the component cost of the 3rd HP filter is not sensitive to the selection of the Q factor.

3.4.4.2 Analysis of Filter Operating Cost

This section evaluates the Q factor effect on the filter operating cost, i.e., the filter loss. As explained in 3.2.3.2, the filter equivalent resistance can be used to quantify the filter loss. Thus, the focus of the following study is to discuss the relationship between the Q factor and the equivalent resistance. The equivalent resistance of the 3rd HP filter can be derived as below:

$$R_F(\omega) = \frac{\omega_{pu}^4 Q}{\omega_t C_1[(\omega_{pu}^2 - Q^2 + 1)^2 + Q^2\omega_{pu}^2]}. \tag{3.60}$$

By differentiating $R_F(\omega)$ with respect to the Q factor. The critical Q factor that makes $\partial R_f(\omega_h)/\partial Q$=0 can be obtained as:

$$Q_{cp}(\omega_{pu}) = \sqrt{\frac{(13\omega_{pu}^4 + 28\omega_{pu}^2 + 16)^{1/2} + \omega_{pu}^2 + 2}{6}}. \tag{3.61}$$

The study shows that, under the condition of $Q>Q_{cp}(\omega)$, a large Q factor leads to a reduced $R_F(\omega)$. It is therefore possible to save the operating cost by selecting the

Q factor. Since the critical Q factor is also a function of frequency, the following study will discuss the critical Q factor at different frequencies.

- **Fundamental Frequency Loss**

The critical Q factor at the fundamental frequency can be derived in (3.62). In this equation, $\omega_{1.\text{pu}}$ can be neglected since $\omega_1 << \omega_t$. For a positive C_2 value, the Q factor is always greater than 1, referring to (3.55). This fact makes the filter always satisfy the condition $Q > Q_{cp}(\omega_1)$. Thus, a large Q factor is helpful for reducing the fundamental frequency loss.

$$Q_{cp}(\omega_{1.pu}) = \sqrt{\frac{(13\omega_{1.pu}^4 + 28\omega_{1.pu}^2 + 16)^{1/2} + \omega_{1.pu}^2 + 2}{6}} \approx 1 \tag{3.62}$$

- **Harmonic Frequency Loss**

The dominant harmonics to be filtered are close to the tuning frequency; i.e., $\omega_{h.pu} \approx 1$. Therefore, the critical Q factor at these frequencies can be simplified in (3.63). In most cases, a large Q factor also saves the filter loss at these harmonic frequencies.

$$Q_{cp}(\omega_{h.pu}) = \sqrt{\frac{(13\omega_{h.pu}^4 + 28\omega_{h.pu}^2 + 16)^{1/2} + \omega_{h.pu}^2 + 2}{6}} \approx 1.3\,. \tag{3.63}$$

The above analysis has shown that the filter loss or operating cost can be saved by selecting the Q factor. Therefore, for an economical design, it is reasonable to specify the fourth equation by minimizing the filter loss, as shown in (3.58). To achieve this, the maximum Q value that satisfies the filtering requirements should be preferred in practice.

3.4.5 Proposed Design Method

The proposed four design equations for the 3rd HP filter can be summarized as follows.

- **Design Equation 1: Reactive Power Requirement**

The system reactive power requirement determines the filter capacitance at the fundamental frequency:

$$C_1 = \frac{Q_F}{\omega_1 V_s^2(\omega_1)}. \tag{3.64}$$

- **Design Equation 2: Fundamental Frequency Loss Minimization**

The second equation is specified by minimizing the filter loss at the fundamental frequency. It can be achieved by the following equation, i.e.,

$$C_2 = \frac{C_1}{Q^2 - 1}. \tag{3.65}$$

- **Design Equation 3: Selection of Filter Tuning Frequency**

The third equation is to select the lowest harmonic in the filtering range as the filter tuning frequency:

$$\omega_t = \min(\omega_h), \tag{3.66}$$

- **Design Condition 4: Filter Loss and Performance Consideration**

Under the constraint of the harmonic filtering requirements, the fourth equation should minimize the filter loss, as specified in (3.67).

$$\min\left(\sum_{h=1}^{N} P_{\text{loss}}(\omega_h)\right) \qquad s.t. \quad \left|\frac{I_{s.post}(\omega_h)}{I_{s.pre}(\omega_h)}\right| \le 1 - \alpha_h\%, \tag{3.67}$$

- **Design Process**

Figure 3.21 illustrates the design flow-chart of the 3rd HP filter. As can be seen, this process is similar to the C-type filter, and the only difference is the design equation for determining the capacitor C_2.

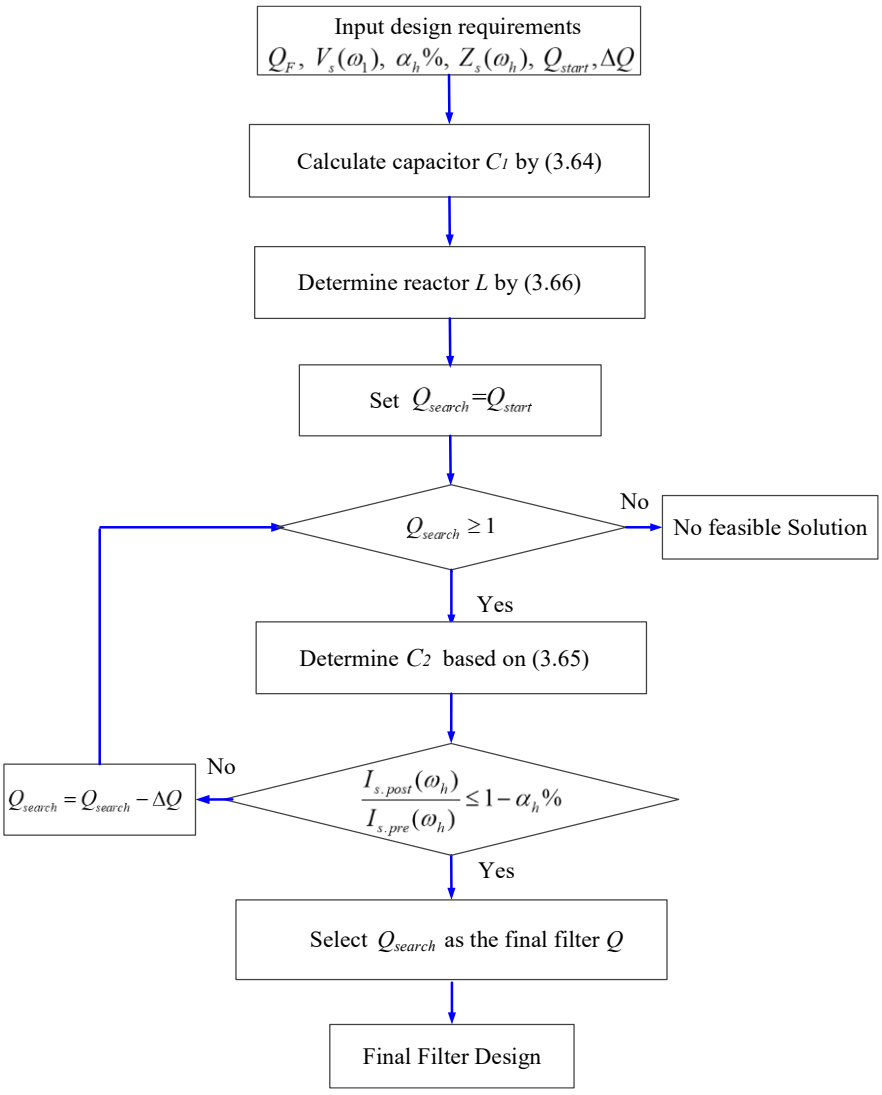

Figure 3.21 Flow-chart for the 3rd HP filter design

3.4.6 Example Case Study

For performance evaluation, a 3rd HP filter is designed to replace the 2nd HP filter in Section 3.2.6. The parameters of the 3rd HP filter are listed in Table 3.11.

Table 3.11 Parameters of designed 3rd HP filters

Topology	C_1 (uF)	C_2 (uF)	L (mH)	R (Ω)	h_t (th)	Q
3rd HP Filter	41.8	24.3	1.4	9.52	11	1.65

Figure 3.22 compares the harmonic filtering performance of 3rd HP filters with different Q factors, where Q=1.84 is designed by the proposed method, and Q=1.41 is designed by the method in [88]. It can be observed that the 3rd HP filter can also provide a satisfactory high-pass performance. All the designs meet the harmonic filtering requirements.

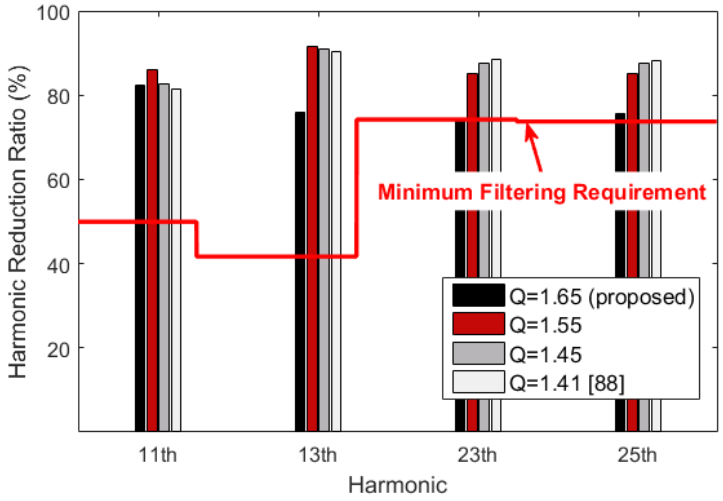

Figure 3.22 Harmonic mitigation performance of the 3rd HP filters

Table 3.12 and Table 3.13 lists the filter component loading and loss respectively. As can be expected, the filter component loading is relatively stable, but the filter loss decreases with the increase of the Q factor. Compared with the method in [88], the proposed design method can save about 30% in filter loss. Note that all the filters have a low loss at the fundamental frequency due to the introduction of the second capacitor C_2.

Table 3.12 Comparison results of component loading

Q factor		1.65	1.55	1.45	1.41
C_1	Voltage /kV	8.31	8.32	8.33	8.34
	Capacity /Mvar	1.09	1.09	1.09	1.10
C_2	Voltage /kV	1.20	1.20	1.20	1.20
	Capacity /kvar	13.17	16.17	20.58	22.68
L	Current /A	133.93	133.88	133.75	133.69
	Capacity /kvar	9.41	9.40	9.39	9.38
R	Voltage /kV	0.27	0.27	0.27	0.27
	Current /A	28.50	30.55	32.70	33.47

Table 3.13 Comparison results of filter loss

Q factor	Power loss at different frequencies (kW for each phase)							
	1st	11th	13th	17th	19th	23th	25th	Total
1.65	0.00	1.75	1.76	0.15	0.18	1.92	1.97	7.73
1.55	0.00	2.15	2.06	0.16	0.18	1.88	1.90	8.35
1.45	0.01	2.61	2.36	0.17	0.19	1.81	1.81	8.95
1.41	0.01	2.78	2.45	0.17	0.18	1.78	1.77	9.14

The costs of the above filters are given in Table 3.14. The following results verify that minimizing the filter operating cost is effective to reduce the filter total cost. The proposed design can offer a more economical filter option.

Table 3.14 Comparison results of filter cost

Q factor	1.65	1.55	1.45	1.41
Component Cost ($)	41,425	41,548	41,677	41,723
Operating Cost ($)	35,567	38,397	41,151	42,050
Total Cost ($)	76,992	79,945	82,828	83,773

3.5 High-pass Filters Selection

The previous sections have studied three common high-pass filters and proposed their design methods. As shown, all these filters can provide a satisfactory high-pass performance. However, there still lacks a guideline on how to choose the right topology for a given application. At present, it is common to see different filter topologies being used under similar conditions. Therefore, this section will further compare the performance of these high-pass filters, and the results will provide guidance for the selection of high-pass filter in the future.

3.5.1 Example Case Analysis

The results of the previous example are compiled for comparison purposes. Table 3.15 lists the parameters of the three high-pass filters.

Table 3.15 Comparison of filter parameter

Topology		2nd HP	C-type	3rd HP
Components	$C_1\,(uF)$	41.8	41.8	41.8
	$C_2\,(uF)$	----	5056.1	24.3
	$L\,(mH)$	1.4	1.4	1.4
	$R\,(\Omega)$	26.5	27.0	9.52
	h_t	11	11	11
	Q	4.60	4.68	1.65

As shown, the capacitor C_2 is the major difference of three high-pass filters. The 2nd HP filter has no capacitor C_2, which makes it save one filter component. To reduce the filter loss, the C_2/C_1 ratio of the C-type filter increases exponentially with the tuning frequency; i.e., $C_2/C_1=h_t^2$. In this case, a very large C_2 value is required due to the high tuning frequency. To increase the impedance of the resistor branch at low frequencies, the 3rd HP filter needs a small C_2 value.

Figure 3.23 compares the filter harmonic performance. All the filters can provide the desired high-pass filtering performance. The C-type filter and 2nd HP filter have a similar harmonic performance because the capacitor C_2 of the C-type filter is neglectable at harmonic frequencies. The 3rd HP filter has a slight compromise on the harmonic performance at low frequencies. This is due to the small C_2 required for filter loss reduction.

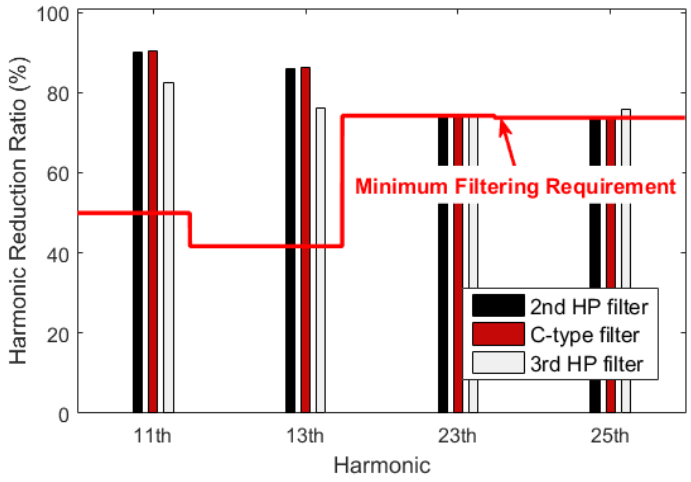

Figure 3.23 Harmonic mitigation performance comparison

A further comparison is also conducted on the filter component loading and loss, as listed in Table 3.16-Table 3.17. Due to the large C_2 value, the C-type filter requires a high capacity for the second capacitor. In contrast, the second capacitor of the 3rd HP filter has a much lower capacity.

Table 3.16 Comparison results of component loading

Topology		2nd HP	C-type	3rd HP
C_1	Voltage /kV	8.33	8.27	8.31
	Capacity /Mvar	1.09	1.08	1.09
C_2	Voltage /kV	----	1.20	1.20
	Capacity /Mvar	----	2.74	0.01
L	Current /A	131.21	130.13	133.93
	Capacity /kvar	9.03	8.88	9.41
R	Voltage /kV	0.30	0.29	0.27
	Current /A	11.40	10.91	28.50

Table 3.17 Comparison results of filter loss

Topology	Power loss at different frequencies (kW for each phase)							
	1st	11th	13th	17th	19th	23th	25th	Total
2nd HP	0.16	0.94	0.75	0.05	0.06	0.71	0.77	3.45
C-type	0.00	0.92	0.73	0.05	0.06	0.69	0.76	3.22
3rd HP	0.00	1.75	1.76	0.15	0.18	1.92	1.97	7.73

Both the C-type filter and 3rd HP filter can effectively reduce the filter loss at the fundamental frequency. However, the reduction effect on the total loss is not significant due to the high tuning frequency. One can notice that the 3rd HP filter has an even higher total loss than the 2nd HP filter. This is because its small resistor value increases its loss at harmonic frequencies.

Table 3.18 compares the costs of these high-pass filters. The C-type filter has the highest component cost among the three filters. This is because of its oversized capacitor C_2. The 3rd HP filter has the highest operating cost due to its excessive harmonic loss. As a result, the 2nd HP filter is the most economical option in this case.

Table 3.18 Comparison results of filter cost

Topology	2nd HP	C-type	3rd HP
Component Cost ($)	41,982	102,152	41,425
Operating Cost ($)	15,854	14,794	35,567
Total Cost ($)	57,837	116.946	76,992

3.5.2 Additional Case Studies

Additional cases have also been studied to determine the appropriate application for these high-pass filters. Figure 3.24 presents the harmonics of concern in each case. As shown, the harmonic contents at h1, h2 and h3 are kept the same, but their frequencies vary for different cases.

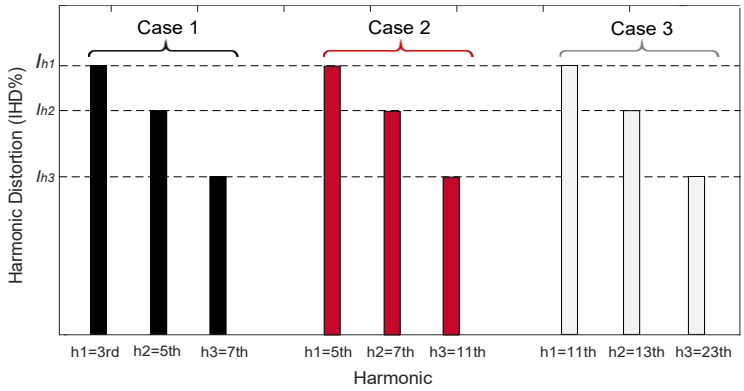

Figure 3.24 Harmonic spectrum for each study case

In this study, the filtering requirements at h1, h2 and h3 are fixed at 60%, 50% and 50%. The two-terminal equivalent circuit introduced in Section 2.1.2 is used for harmonic analysis. Table 3.19 lists the circuit parameters. To meet the filtering requirements, the filter size needs to be adjusted for different cases, and a large size is generally required as the decrease of the harmonic frequency.

Table 3.19 Parameters of the two-terminal equivalent circuit

#	$E_s(\omega_h)$ (pu[a])	$E_f(\omega_h)$ (pu)	$Z_{ss}(\omega_h)$ (pu)	$Z_{sf}(\omega_h)$ (pu)	$Z_{ff}(\omega_h)$ (pu)
h1	0.011+j0.001	0.024+j0.001	0.003+j0.624	0.002+j0.361	0.006+j0.774
h2	-0.010+j0.002	-0.020+j0.017	0.003+j1.103	0.002+j0.639	0.006+j1.368
h3	0.006+j0.008	0.012+0.017	0.003+j1.199	0.002+j0.512	0.006+j1.487

a. the base capacity is 10,000 kVA and the base voltage are selected as 13.8 kV.

- **Case 1：Low-frequency Application**

The first case is intended to compare these high-pass filters for low-frequency application. Three high-pass filters are designed with a three-phase size of 7000 kvar. Table 3.20 illustrates the parameters of these filters.

Table 3.20 Parameters of designed filters

Topology		2nd HP Filter	C-type Filter	3rd HP Filter
Components	C_1 (uF)	97.5	97.5	97.5
	C_2 (uF)	----	877.5	74.4
	L (mH)	8.0	8.0	8.0
	R (Ω)	25.2	26.4	13.8
	h_t	3	3	3
	Q	2.78	2.91	1.52

It can be noticed that the 2nd HP filter has no capacitor C_2. For loss reduction, the C_2 value of the C-type filter is about ten times (h_t^2=9) of the capacitor C_1. In comparison, the 3rd HP filter requires a much smaller C_2 value. As will be shown later, this feature can save the filter component cost.

Table 3.21 lists the harmonic filtering performance of these high-pass filters. All the filters present a satisfactory harmonic performance. Compared with the other two filters, the 3rd HP filter has a low harmonic reduction near the tuning frequency. This is due to its small capacitor C_2 value.

Table 3.21 Harmonic mitigation performance of the high-pass filters

Topology		2nd HP Filter	C-type Filter	3rd HP Filter
Harmonic mitigation performance	3rd	78%	79%	65%
	5th	73%	74%	60%
	7th	50%	50%	50%

The filter losses are also analyzed, as given in Table 3.22. The 2nd HP filter has an excessive loss at the fundamental frequency. This is due to the following reasons: (1) a large filter size is required at low frequency to satisfy the harmonic filtering requirements, and (2) for the same Q factor, a low tuning frequency leads to a large filter equivalent resistance at the fundamental frequency. In comparison, the C-type filter has the lowest loss among these filters. The overall loss of the 3rd HP filter is

still a little bit high although it already saves a large portion in filter loss.

Table 3.22 Comparison results of filter loss

Topology	Power loss at different frequencies (kW for each phase)				
	1st	3rd	5th	7th	Total
2nd HP Filter	38.02	7.21	1.04	0.76	47.04
C-type Filter	0.00	9.66	0.99	0.72	11.37
3rd HP Filter	10.94	3.78	1.52	1.39	17.63

The costs of these filters are summarized in the following table. Although the C-type filter has the highest component costs, its low operating cost still makes it the best option for the low-frequency application.

Table 3.23 Comparison results of filter cost

Topology	2nd HP Filter	C-type Filter	3rd HP Filter
Component Cost ($)	103,007	112,356	108,251
Operating Cost ($)	216,325	52,301	81,098
Total Cost ($)	319,332	164,657	189,349

- **Case 2：Medium-frequency Application**

In the second case, the high-pass filters need a three-phase size of 4000 kvar to achieve the required harmonic filtering performance. Similar to the previous analysis, the comparisons are also performed on different aspects of the filter performance, and the results are listed from Table 3.24 to Table 3.27.

Table 3.24 Parameters of designed filters

Topology		2nd HP Filter	C-type Filter	3rd HP Filter
Components	$C_1\,(uF)$	55.7	55.7	55.7
	$C_2\,(uF)$	----	1392.9	48.0
	$L\,(mH)$	5.1	5.1	5.1
	$R\,(\Omega)$	27.3	27.9	14.0
	h_t	5	5	5
	Q	2.87	2.93	1.47

Table 3.25 Harmonic mitigation performance of the high-pass filters

Topology		2nd HP Filter	C-type Filter	3rd HP Filter
Harmonic mitigation performance	5th	78%	78%	62%
	7th	78%	79%	63%
	11th	50%	50%	50%

Table 3.26 Comparison results of filter loss

Topology	Power loss at different frequencies (kW for each phase)				
	1st	5th	7th	11th	Total
2nd HP Filter	3.95	3.48	0.84	0.51	8.77
C-type Filter	0.00	3.60	0.82	0.49	4.92
3rd HP Filter	0.50	2.80	1.32	1.02	5.65

Table 3.27 Comparison results of filter cost

Topology	2nd HP Filter	C-type Filter	3rd HP Filter
Component Cost ($)	65,005	83,591	69,701
Operating Cost ($)	40,343	22,614	25,984
Total Cost ($)	105,348	106,206	95,685

The results show that the 2nd HP filter still has a very high operating cost for the medium-frequency application. The C-type filter has the highest component cost since its C_2 value increases significantly due to the high tuning frequency. In contrast, the 3rd HP filter saves most of the fundamental frequency loss with a reasonable component cost, which makes it an attractive option for the medium-frequency range.

- **Case 3：High-frequency Application**

For the high-frequency application, three filters are designed with a three-phase size of 1800 kvar, as listed below. One can notice that the filter fundamental frequency loss is not a major concern for this case. With such a high tuning frequency, the 2nd HP filter also has a reasonable loss, and its simple topology makes it the preferable solution for the high-frequency application.

Table 3.28 Parameters of designed filters

Topology		2nd HP Filter	C-type Filter	3rd HP Filter
Components	C_1 (uF)	25.1	25.1	25.1
	C_2 (uF)	----	3033.7	21.6
	L	2.3	2.3	2.3
	R (Ω)	32.4	32.7	14.1
	h_t	11	11	11
	Q	3.37	3.40	1.47

Table 3.29 Harmonic mitigation performance of the high-pass filters

Topology		2nd HP Filter	C-type Filter	3rd HP Filter
Harmonic mitigation performance	11th	81%	81%	61%
	13th	85%	86%	69%
	23th	50%	50%	50%

Table 3.30 Comparison results of filter loss

Topology	Power loss at different frequencies (kW for each phase)				
	1st	11th	13th	23th	Total
2nd HP Filter	0.13	0.66	0.33	0.18	1.31
C-type Filter	0.00	0.65	0.33	0.18	1.16
3rd HP Filter	0.00	1.09	0.67	0.40	2.17

Table 3.31 Comparison results of filter cost

Topology	2nd HP Filter	C-type Filter	3rd HP Filter
Component Cost ($)	35,086	70,681	35,843
Operating Cost ($)	6,020	5,341	9,989
Total Cost ($)	40,607	76,022	49,301

- **Guideline for High-pass Filter Selection**

This section will further analyze the previous results, and then a guideline will be provided for determining the most appropriate high-pass filter for a design project. In order to compare the filters with different sizes, all the costs are normalized as the unit price ($/kW) with respect to the filter size. Figure 3.25 compares the filter component and operating prices at different applications.

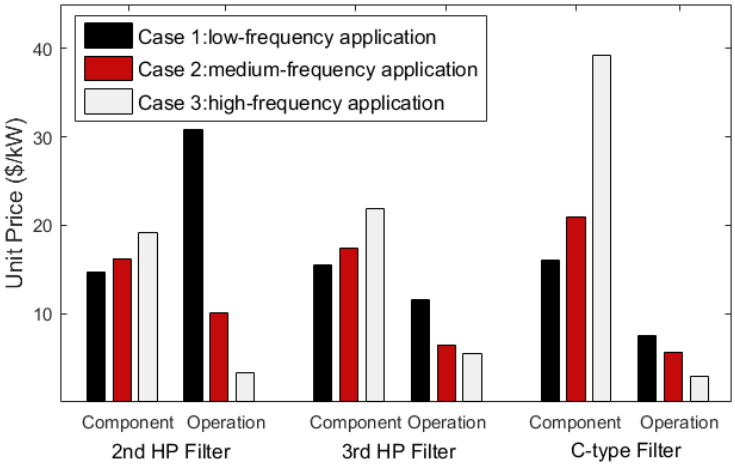

Figure 3.25 Summary of filter component and operating prices

As shown, the 2nd HP filter and 3rd HP filter have a relatively stable component cost. In comparison, the component cost of the C-type filter grows significantly as the frequency increase. In terms of the operating cost, the prices of all filters decrease as the frequency increase, especially for the 2nd HP filter. Its price is the highest for the low-frequency application but becomes comparable to the other two filters for the high-frequency application. Table 3.32 lists the total cost of each high-pass filter.

Table 3.32 Total unit cost of each high-pass filter

Topology	Filter total unit cost (component and operation) ($/kW)		
	Case 1	Case 2	Case 3
2nd HP Filter	45.62	26.34	22.56
C-type Filter	23.52	26.55	42.23
3rd HP Filter	27.05	23.92	27.39

Based on the above analysis, Table 3.33 summarizes the characteristics and suitable applying conditions of the high-pass filters.

Table 3.33 Comparison results of high-pass filters

Topology	Major Characteristics	Application
2nd HP filter	▪ simple filter structure ▪ easy filter design ▪ insensitive to parameter variations ▪ high energy loss	high-frequency (above 11th harmonic)
C-type filter	▪ low energy loss, especially at the fundamental frequency ▪ a large auxiliary capacitor to bypass the resistor branch ▪ complex filter structure and design ▪ insensitive to parameter variations	low-frequency (at or below 3rd harmonic)
3rd HP filter	▪ low energy loss at the fundamental frequency ▪ a smaller auxiliary capacitor value than C-type filter ▪ complex filter structure and design ▪ insensitive to parameter variations ▪ a small filter quality factor than others	medium-frequency (5th to 7th harmonics)

3.6 Summary

This chapter conducted a comprehensive analysis of three common high-pass filters, including the 2nd HP filter, C-type filter, and 3rd HP filter. In order to provide the wide-band filtering performance, a parallel resistor is used to configure these high-pass filters. This resistor will cause filter losses at both the fundamental and harmonic frequencies, resulting in a considerable operating cost. In view of this fact, significant efforts were devoted to select the Q factor for an economical design. The main findings and contributions of this chapter can be summarized as follows:

- Two design issues of the 2nd HP filter were clarified. The first issue is related to the selection of the filter tuning frequency. The analysis revealed that there is no need to concern the effects of the parameter variations for selecting the tuning frequency. For achieving the performance balance in the harmonic range, it is preferred to select the filter tuning frequency directly at the lowest harmonic of concern. The second issue is related to the third design equation

that has not been specified. Under the constraints of fulfilling the harmonic filtering requirements, it was proposed to establish this equation to minimize the filter loss for an economical design. The mathematical analysis showed that a large Q factor leads to a reduced filter loss. Within the normal Q range, the design process can be simplified by selecting the largest Q factor that provides the required filtering performance.

- Similar studies were also conducted to clarify the design issues for the C-type filter and 3rd HP filter. Although research efforts have already been spent on them, There is still no consensus on how to design these two filters. Improved design methods were proposed, and case studies were performed to evaluate the performance of the proposed methods. The results verified that, compared with the previous studies, the proposed design provides a more economical filter option.

- A further study was also conducted on selecting the most appropriate high-pass filter for a given application. According to the analysis, the C-type filter is the best option for low frequencies such as 3rd harmonic or below. It is recommended to apply the 3rd HP filter in the medium-frequency range (5th or 7th harmonic) since this filter saves a large amount of the operating cost with a moderate increase on component cost. The 2nd HP filter is the choice for the high-frequency application like the 11th harmonic or above.

Chapter 4

Damped High-Pass Harmonic Filter

Several harmonic filters are normally grouped as a package to reduce the harmonic emissions entering the supply system. These filters provide bypass circuits at their tuning frequencies such as the 5th, 7th, 11th and 13th harmonics. However, a passive filter normally introduces a parallel resonance point below its tuning frequency [60]. If this point coincides with one of the harmonics, significant harmonic amplification will occur. This concern makes the filter package for multi-pulse industrial drives (such as 12- and 18-pulse) a lot more complex and costly. For example, a 12-pulse variable frequency drive generates only a small amount of non-characteristic harmonics like the 5th and 7th harmonics. Its filtering objective should be the 11th, 13th and high-order characteristic harmonics. However, a filter at the 11th harmonic may create a parallel resonance around the 7th harmonic. Thus, a filter is needed at the 7th harmonic, which in turn requires a 5th non-characteristic filter as well. The main advantage of the 12-pulse configuration, the reduced generation of the 5th and 7th harmonics, is therefore not fully utilized. If the system generates interharmonics, the multiple resonance points created by filters can easily amplify these components, leading to problems such as voltage flicker or interference with the power line carrier systems [61].

In view of the above issues, this chapter proposes a new filtering scheme that eliminates the non-characteristic filters in multi-pulse industrial systems. It is achieved by using a novel characteristic filter that can provide sufficient damping at the non-characteristic harmonics. This chapter is organized as follows: Section 4.1 reviews the existing filtering schemes used for multi-pulse industrial systems. The damping of the common passive filters is investigated in Section 4.2. Section 4.3 introduces a novel characteristic filter and its associated filtering scheme. In Section 4.4, comparative case studies are presented to demonstrate the effectiveness of the new filtering scheme. Section 4.5 provides two other applications of the

proposed filter.

4.1 Existing Filtering Schemes

Multi-pulse converters have been widely employed in industrial systems [90]-[91]. A main advantage of such configurations is the reduced generation of the low order harmonics. Under ideal operating conditions, the AC side current of a *p*-pulse converter only contains $kp\pm1$ order harmonics, where k is an integer. These are the characteristic harmonics of the *p*-pulse system. All the other harmonics are described as the non-characteristic harmonics.

Both the characteristic and non-characteristic harmonics will present under the practical operating condition, but the contents of the non-characteristic harmonics are small [92]. For example, the 5th and 7th characteristic harmonics of a 6-pulse system are 17% and 11%. They become the non-characteristic harmonics in a 12-pulse system, and their magnitudes are normally less than 3%. In comparison, the characteristic 11th and 13th harmonics of the 12-pulse system are about 5~8%. Therefore, the characteristic harmonics are the primary concern.

The primary goal of a filter package is to reduce the characteristic harmonics. For a 12-pulse system, a high pass filter tuned to the 11th harmonic is commonly used to mitigate the 11th, 13th, and high-order characteristic harmonics. Unfortunately, the filter is capacitive below its tuning frequency. This capacitance interacts with the supply system impedance (which is normally inductive) and can lead to a parallel resonance below its tuning frequency, such as at the 7th harmonic frequency. Hence, a small non-characteristic 7th filter is needed to mitigate the resonance. This in turn requires the installation of a small 5th non-characteristic filter as well. A common filter package of the 12-pulse system, therefore, takes the form shown in Figure 4.1 [93]. This arrangement has the following disadvantages.

The advantage of the reduced low-order harmonic generation of the multi-pulse configuration is not fully utilized since the non-characteristic filters are still needed.

Trigging Condition	Interlock Control
5th filter failure	7th filter and 11th filter off
5th filter and 7th filter failure	11th filter off
7th filter failure	5th filter on and 11th filter off

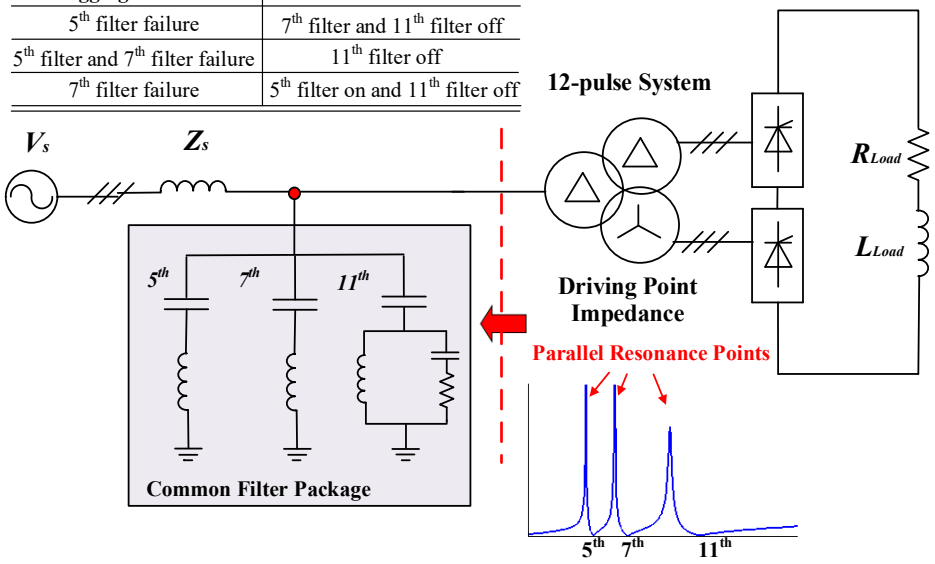

Figure 4.1 Example of existing filtering scheme for 12-pulse system.

In addition to increasing the component costs of the filter package, the non-characteristic filters also increase the space requirement. This can be a significant issue for variable frequency drive applications.

The reliability of the system is reduced since a malfunction of the 5th or 7th filter can lead to the shutdown of the entire system through an interlock mechanism [94]. This is to prevent parallel resonance occurring at the non-characteristic harmonic frequencies.

There are parallel resonance points between the harmonic frequencies, which will amplify the interharmonics if their frequencies coincide with the resonance point. In fact, how to mitigate the interharmonic amplification for such a filter package is still an open question [77].

The filter package is capacitive at low frequencies. It can form a series resonance with the system impedance. If the resonance frequency is close to that of the frequencies of the automatic meter reader (AMR), the AMR signal could be sunk by the filter, causing the communication difficulties for the downstream meters [95].

In summary, the existing filtering schemes for multi-pulse systems have several significant disadvantages. Therefore, it is desirable to have a better alternative solution.

4.2 Damping Performance Analysis

The root cause of the disadvantages summarized above is the resonance caused by the characteristic filter. If one can adopt a different characteristic filter that does not cause resonance below its turning frequencies, all of the disadvantages could be overcome. Motivated by this consideration, a new filter topology and its associated filtering scheme are proposed. The main characteristic of the new filter is its increased damping performance at frequencies below the tuning frequency. In order to understand this unique characteristic, it is useful to analyze the damping performance of the existing filtering schemes.

4.2.1 Damping Performance of Common Passive Filters

According to the previous chapters, several filters are already available to serve as the characteristic harmonic filters for multi-pulse systems. Their topologies are summarized in Figure 4.2.

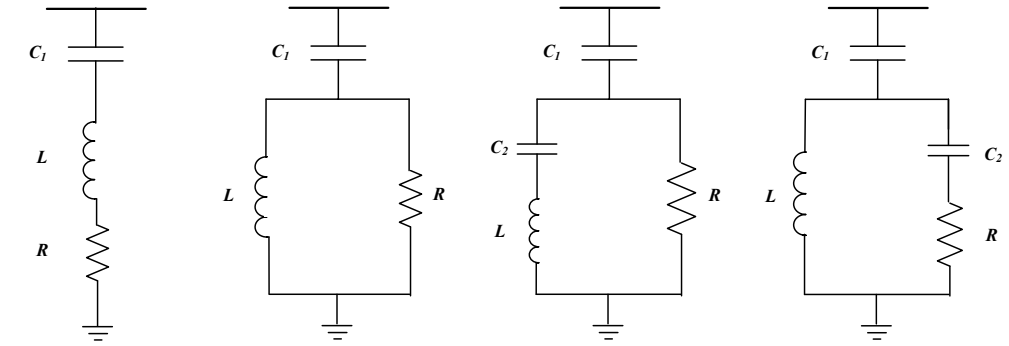

(a) Single-tuned filter (b) 2nd HP Filter (c) C type Filter (d) 3rd HP Filter

Figure 4.2 Common passive filter topologies.

Figure 4.3 presents the frequency responses of the above filters under the same reactive power requirement. Here we are interested in the damping performance

(i.e., the value of the equivalent resistance) below the filter tuning frequency.

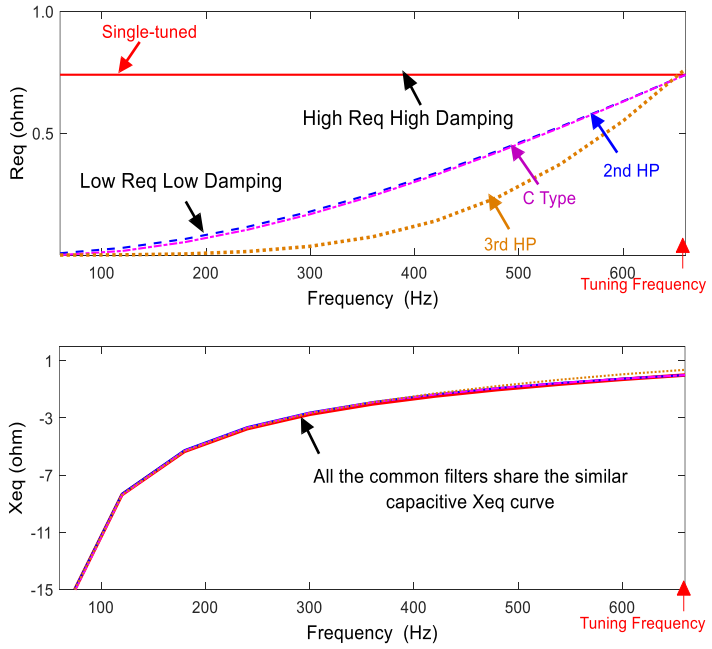

Figure 4.3 Filter equivalent resistance and reactance of common passive filters.

It can be seen that the single-tuned filter with a series resistor provides a constant high resistance at all frequencies. A high resistance implies a good damping performance. However, this represents a high resistance at the fundamental frequency, which is not desirable since it will result in a large power frequency loss.

The three high-pass filters (b), (c), (d) present a low resistance at the fundamental frequency, so the corresponding power frequency loss is small. However, the resistance stays at a low value until the frequency reaches the filter tuning frequency. Consequently, the damping performances of these filters are poor.

This analysis shows that there is a conflict between the power frequency loss requirement and the high damping performance requirement. The former requires a smaller resistance, and the later requires a large resistance. The current filtering practice focuses on meeting the first requirement, which naturally leads to a poor damping performance. This in turn requires the addition of the non-characteristic filters.

4.2.2 Resonance Damping Evaluation

There are various ways to quantify the damping effect of a resistance. Since the focus of this research is to eliminate the amplification of the non-characteristic harmonics, an index is introduced to quantify damping level in terms of its effectiveness to reduce harmonic amplification. This index will be used later to explain the characteristics of the proposed filter. Figure 4.4 presents a general circuit for the analysis of harmonic resonance caused by passive filters.

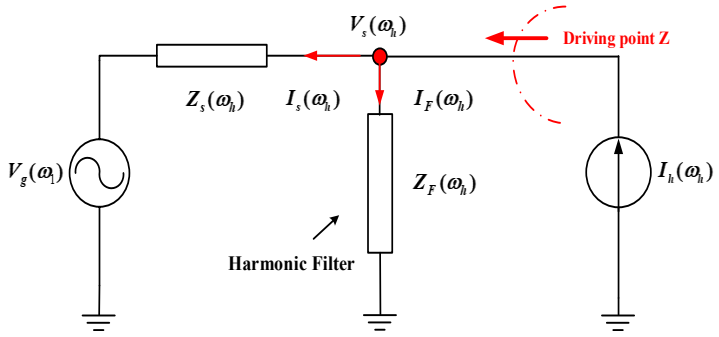

Figure 4.4 General circuit for harmonic amplification analysis.

Prior to the filter connection, the harmonic voltage at the PCC point is $V_{s.pre}(\omega_h)$, where ω_h is the angular frequency. After connecting the filters, the harmonic voltage becomes $V_{s.post}(\omega_h)$. The ratio of these two voltages is defined as the harmonic amplification ratio (HAR) caused by filters; i.e.,

$$HAR(\omega_h) = \left| \frac{V_{s.post}(\omega_h)}{V_{s.pre}(\omega_h)} \right| . \tag{4.1}$$

According to Figure 4.4, the PCC harmonic voltages before and after the filter connection can be derived as (4.2) and (4.3):

$$V_{s.pre}(\omega_h) = Z_s(\omega_h) \times I_h(\omega_h) \tag{4.2}$$

$$V_{s.post}(\omega) = \frac{Z_s(\omega_h) \cdot Z_F(\omega_h)}{Z_F(\omega_h) + Z_s(\omega_h)} \times I_h(\omega_h) . \tag{4.3}$$

Substituting (4.2) and (4.3) into (4.1) yields

$$HAR(\omega_h) = \sqrt{\frac{R_F^2(\omega_h) + X_F^2(\omega_h)}{(R_s(\omega_h) + R_F(\omega_h))^2 + (X_s(\omega_h) + X_F(\omega_h))^2}}, \tag{4.4}$$

where $R_S(\omega_h)$ and $X_S(\omega_h)$ are the system resistance and reactance, and $R_F(\omega_h)$ and $X_F(\omega_h)$ are the filter resistance and reactance.

As can be seen, the worst amplification condition happens when the system is purely reactive and equals to the negative filter reactance; i.e.,

$$R_s(\omega_h) = 0, \quad X_s(\omega_h) = -X_F(\omega_h). \tag{4.5}$$

Under these conditions, the denominator in (4.4) is minimum, which indicates the worst-case harmonic amplification ($HAR_{worst}(\omega_h)$), as specified by (4.6):

$$HAR_{worst}(\omega_h) = \sqrt{1 + \frac{X_F^2(\omega_h)}{R_F^2(\omega_h)}}. \tag{4.6}$$

The above worst-case harmonic amplification can quantify the filter damping effect easily. For example, $HAR_{worst}(\omega_h)$=5 means that the maximum possible harmonic voltage after the filter connection is 5 times larger than the voltage prior to the filter connection. Figure 4.5 shows the $HAR_{worst}(\omega_h)$ index of the common filter topologies.

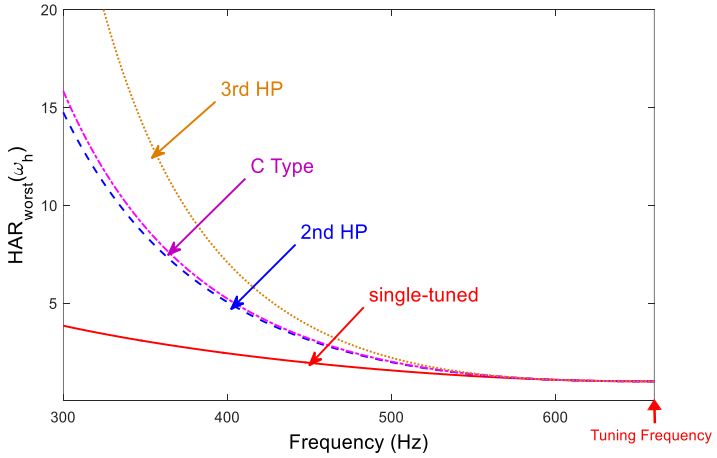

Figure 4.5 $HAR_{worst}(\omega_h)$ index of common passive filters

In order to avoid the resonance at the non-characteristic harmonics, $HAR_{worst}(\omega_h)$ in the frequency range of the non-characteristic harmonics below the filter tuning frequency should be minimized.

4.3 Proposed Filtering Scheme

Based on the above analysis, a novel filtering scheme is presented in this section. This scheme can meet both the requirements of a low power loss at the fundamental frequency and a high damping performance at the non-characteristic harmonic frequencies simultaneously.

4.3.1 Overall Scheme

The proposed filtering scheme is shown in Figure 4.6. The entire scheme consists of only one characteristic filter. This filter is tuned at the lowest characteristic harmonic (such as 11th for the 12-pulse system and 17th for the 18-pulse system). As will be explained later, this filter can provide sufficient damping at low-order non-characteristic harmonics, so the low-order non-characteristic filters are no longer needed.

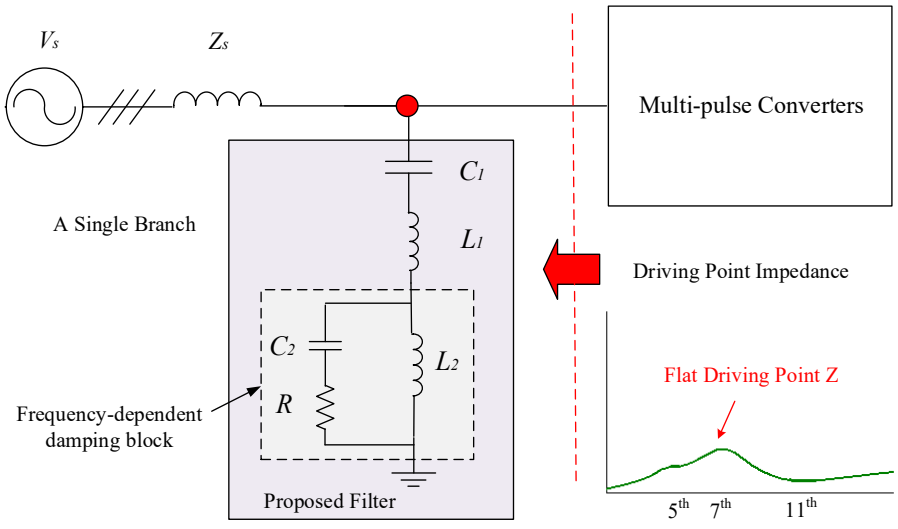

Figure 4.6 New filtering scheme for multi-pulse industrial system.

4.3.2 Filter Topology and Principle

The topology of the proposed characteristic filter has been shown in Figure 4.6. The proposed filter can be seen as a single tuned filter in series with a frequency-dependent damping block, and this block presents a high resistance at the concerned non-characteristic harmonics. The high resistance is achieved by creating a parallel resonance between the C_2-R and L_2 branch. The resonance forces the resistance of the damping block to increase rapidly. A high damping performance is obtained consequently.

At the fundamental frequency, the impedance of the L_2 branch is much smaller than that of the C_2-R branch, which means only a small amount of the filter currents passing through R and, therefore, the power frequency loss is reduced. For the frequency equaling to or higher than the characteristic harmonic frequencies, the L_2 impedance is higher than that of the C_2-R branch. Thus, L_1-C_1 branch and C_2-R branch form a damped single-turned filter. The tuning frequency corresponds to the lowest order characteristic harmonic.

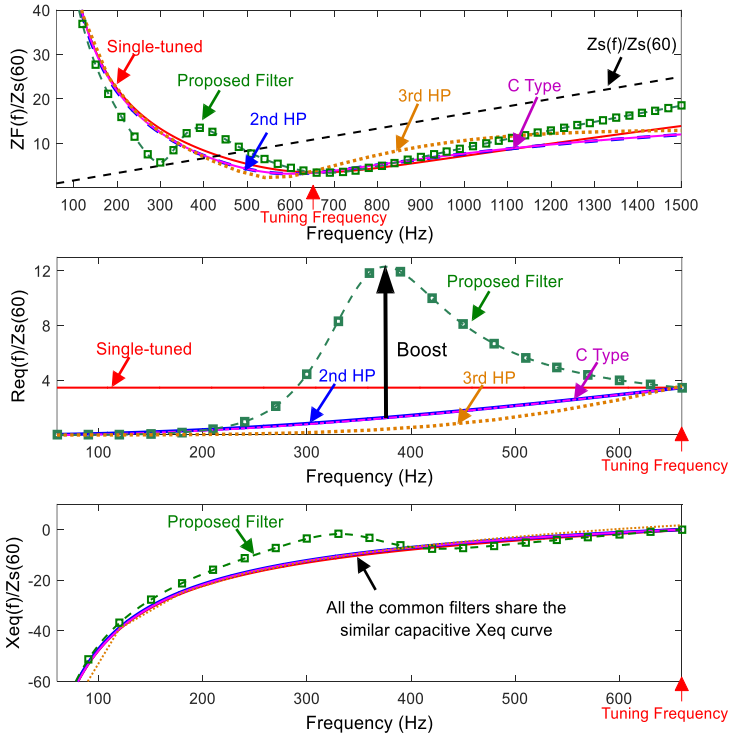

Figure 4.7 Comparison results of filters frequency response.

The nominalized frequency responses of the proposed filter are illustrated in Figure 4.7 and are compared with those of other filters. It can be seen that the equivalent resistance of the proposed filter is boosted significantly higher at low frequencies. However, the filter resistance at power frequency is still low, which indicates a low power frequency loss.

The $HAR_{worst}(\omega_h)$ index is compared with the previous common passive filters, as shown in Figure 4.8. It can be seen that the proposed filter has a much smaller $HAR_{worst}(\omega_h)$, which indicates a higher damping performance.

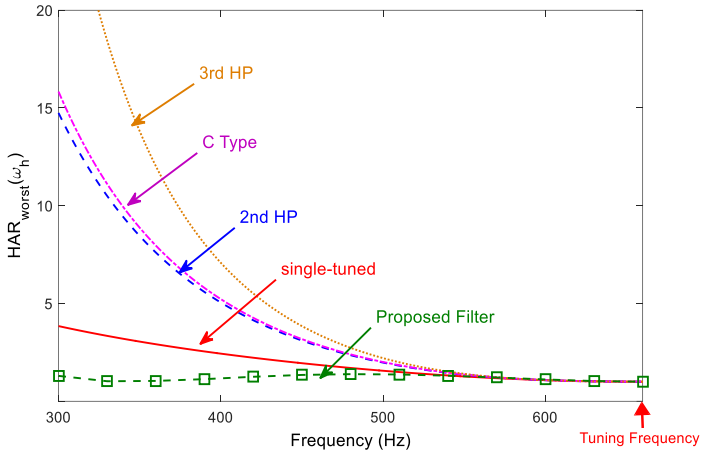

Figure 4.8 Comparison of HAR_{worst} index

Note that the proposed filter shares the same topology with that of a double-tuned filter in [64]. However, the working principles, design considerations, and frequency responses of these two filters are completely different. The double-tuned filter is designed, as their name implies, to trap two characteristic harmonics. The proposed filter has one tuning frequency and is designed to create high resistance below the tuning frequency. In view of its unique damping characteristic, the proposed filter is called the Damped High-Pass (DHP) filter.

4.3.3 Design Methods

According to Figure 4.6, the impedance of the proposed filter can be expressed as:

$$Z_F(\omega) = \frac{j\omega L(j\omega C_2 R + 1)}{(1 - \omega^2 C_2 R) + j\omega C_2 R} - j\frac{1}{\omega C_1} + j\omega L_1 = R_F(\omega) + jX_F(\omega)\,. \qquad (4.7)$$

where

$$R_F(\omega) = \frac{\omega^4 R L_2{}^2 C_2{}^2}{(\omega R C_2)^2 + (\omega^2 L_2 C_2 - 1)^2}\ , \qquad (4.8)$$

$$X_F(\omega) = \frac{\omega L_2(1 - \omega^2 L_2 C_2) + \omega^3 R^2 L_2 C_2{}^2}{(\omega R C_2)^2 + (1 - \omega^2 L_2 C_2)^2} - \frac{1}{\omega C_1} + \omega L_1\ . \qquad (4.9)$$

The DHP filter is composed of five components (main capacitor C_1, auxiliary capacitor C_2, series reactor L_1, parallel reactor L_2 and damping resistor R). Hence, five design equations are required to determine all the component parameters. These equations are explained below.

- **Design Equation 1: Reactive Power Requirement**

Similar to common passive filters, the filter reactive power output is determined based on the system reactive power requirement Q_F. This can be used to determine the main capacitor C_1 as shown below:

$$C_1 = \frac{Q_F}{\omega_1 V_s^2(\omega_1)}, \qquad (4.10)$$

where $V_s(\omega_1)$ is the system nominal voltage.

- **Design Equation 2: Selection of Filter Tuning Frequency**

The filter tuning frequency ω_t is selected at the lowest characteristic harmonic frequency. For example, it is the 11th harmonic for a 12-pulse system or the 17th harmonic for a 18-pulse system. The filter tuning frequency ω_t is defined as the frequency where the reactive component of the filter impedance equals to zero; i.e.,

$$X_F(\omega_t) = 0\,, \qquad (4.11)$$

By substituting (4.9) into (4.11), the series reactor L_1 can be derived as

$$L_1 = \frac{L_2(\omega_t^2 / \omega_p^2 - 1) - \omega_t^2 R^2 / L_2 \omega_p^4}{(\omega_t R C_2)^2 + (1 - \omega_t^2 / \omega_p^2)^2} + \frac{1}{\omega_t^2 C_1}, \tag{4.12}$$

where ω_p is the parallel resonance frequency between C_2 and L_2.

- **Design Equation 3: Harmonic Reduction Capability**

The filter should be able to filter the characteristic harmonic it is tuned to. The degree of the harmonic reduction is defined as a user input parameter α%; i.e.,

$$I_{s.post}(\omega_t) = (1 - \alpha\%)\, I_{s.pre}(\omega_t), \tag{4.13}$$

where $I_{s.pre}(\omega_t)$ and $I_{s.post}(\omega_t)$ are the harmonics flowing into the system before and after the filter connection.

Assuming a purely inductive supply impedance which is a common case for the industrial systems, the filter parallel reactor L_2 can be derived as

$$L_2 = R\omega_t \sqrt{\frac{K}{R\omega_t^4 + 2K\omega_t^2\omega_p^2 - K(\omega_t^4 + \omega_p^4)}}, \tag{4.14}$$

where

$$K = \frac{\alpha\%}{\sqrt{1 - \alpha\%^2}} Z_s(\omega_t).$$

- **Design Equation 4: Parallel Resonance Frequency**

The parallel resonance between R-C_2 and L_2 is intended to boost the total filter resistance for the concerned non-characteristic harmonics. Therefore, the resonance frequency ω_p can be selected to be between the two lowest order non-characteristic harmonics (i.e. 5th and 7th). The proposed frequency is the 6th harmonic frequency. This will create a large $R_F(\omega_h)$ for both the 5th and 7th non-characteristic harmonics. The C_2 and L_2 relationship can be derived as:

$$C_2 = \frac{1}{\omega_p^2 L_2}. \tag{4.15}$$

- **Design Equation 5: Damping Performance**

The filter must limit the amplification of the concerned non-characteristic harmonics. This is achieved by minimizing the worst-case harmonic amplification factor as follows:

$$min\ \{HAR_{worst}(\omega) = \sqrt{1 + \frac{X_{eq}^2(\omega)}{R_{eq}^2(\omega)}} \quad (\omega_{5th} \le \omega \le \omega_t)\}. \tag{4.16}$$

4.3.4 Design Procedure

Among the five design equations, C_1 can be determined based on (4.10). L_1, L_2, and C_2 can be determined from (4.12), (4.14) and (4.15) respectively once R is known. Therefore, the problem is a single variable optimization problem with R as the variable to minimize $HAR_{worst}(\omega_h)$. There are many methods to solve a single variable optimization problem. The simplest method is to scan all feasible values of R to find the global minimal of $HAR_{worst}(\omega_h)$. This is the method adopted here and it is shown in Figure 4.9. The computation effort is quite small since the equations are very simple.

It is useful to note that the design equations (4.12) and (4.14) can be used to establish the search range of the optimal R as specified in (4.17). The principle behind the above range is that the resistor must reside in a range that ensures L_1 and L_2 to have positive values.

$$\frac{K(\omega_t^2 - \omega_p^2)^2}{\omega_t^4} < R \le \frac{\omega_t(1+P_R) + \sqrt{\omega_t^2 + 2P_R\omega_p^2}}{2C_1^2 K\omega_t^3} \tag{4.17}$$

where $P_R = 2C_1^2K^2(\omega_t^2 - \omega_p^2)$.

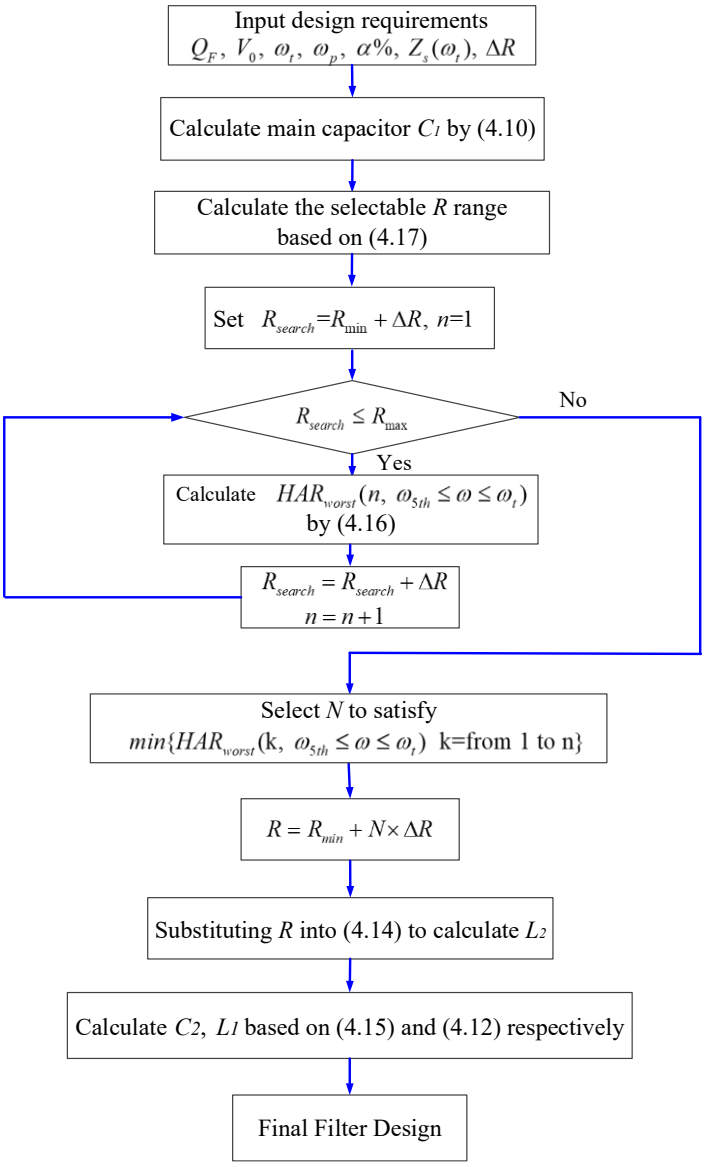

Figure 4.9 Flow chart for DHP filter design

Note that the above design method just uses one system impedance versus frequency curve. It works for many industry cases since the supply system and customer is connected through a transformer. The transformer impedance dominates the equivalent system impedance. For systems that experience significantly different frequency-dependent impedances (such as a HVDC terminal), an optimization method may be needed, which will be discussed in the next Chapter.

4.4 Comparative Case Study

In this section, a case study is presented for evaluating the effectiveness of the proposed filtering scheme. The performance of the proposed scheme is compared with that of the existing schemes.

4.4.1 System Description

The case study involves a natural gas plant at Southwest of Alberta, Canada. Its configuration is shown in Figure 4.10. A 5 MVA transformer is used to connect the facility to a 25 kV supply. The transformer short-circuit impedance (*Zs%*) is 6.18%. The non-linear load represents a variable frequency drive (VFD) with 12-pulse front-end, and it is represented by a harmonic current source for analysis. The harmonic spectrum of a typical 12-pulse LCC VFD system is adopted [92], as illustrated in Figure 4.10.

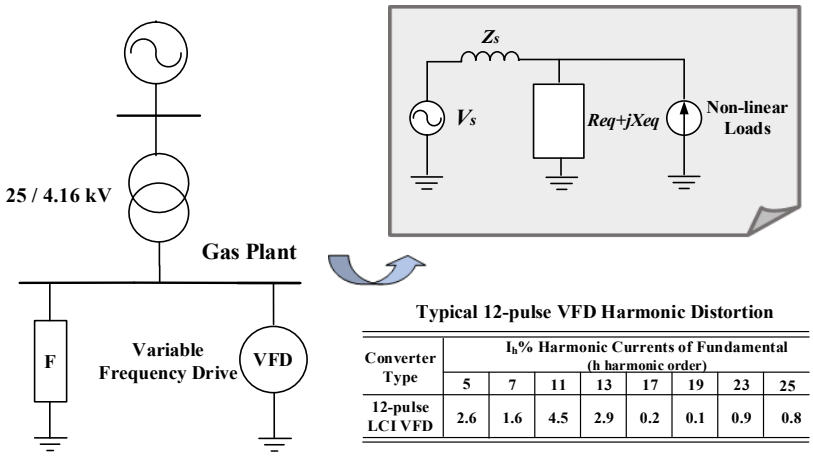

Typical 12-pulse VFD Harmonic Distortion

Converter Type	I_h% Harmonic Currents of Fundamental (h harmonic order)							
	5	7	11	13	17	19	23	25
12-pulse LCI VFD	2.6	1.6	4.5	2.9	0.2	0.1	0.9	0.8

Figure 4.10 Configuration of a practical industrial facility

4.4.2 Performance Evaluation

Four filter options are evaluated. They are:

1. One 11th 3rd HP (1Mvar),
2. 11th 3rd HP(1Mvar) + 7th ST(0.25Mvar),

3. 11th 3rd HP(1Mvar) + 5th ST(0.25Mvar) + 7th ST(0.25Mvar),

4. One proposed DHP filter turned to 11th (1Mvar).

The design input data for the DHP filter are Q_F=1 Mvar, ω_r=1320π *rad/s*, ω_p=720π *rad/s*, α%=70%. The resulting filter parameters are given in Table 4.1. Table 4.2 presents the harmonic emissions into the supply system.

Table 4.1 Parameter of designed filters

Topology		3rd HP Filter	Proposed Filter
Components	C_1 (uF)	153.28	153.28
	C_2 (uF)	85.03	440.53
	L_1 (mH)	---	0.51
	L/L_2 (mH)	0.38	0.44
	R (Ω)	2.63	0.40

Table 4.2 Harmonic current flowing into system

Option	I_h% Harmonic Currents of Fundamental (h harmonic order)								
	5	7	11	13	17	19	23	25	TDD
No Filter	2.6	1.6	4.5	2.9	0.2	0.1	0.9	0.8	6.3
1	4.3	8.2	1.4	1.1	0.1	0.0	0.4	0.3	9.5
2	6.0	0.7	1.3	1.1	0.1	0.0	0.4	0.3	6.3
3	1.9	0.6	1.3	1.0	0.1	0.0	0.4	0.3	2.7
4	3.2	2.0	1.4	0.8	0.1	0.0	0.4	0.3	4.1
IEEE-519[34]	4.0	4.0	2.0	2.0	1.5	1.5	0.6	0.6	5.0

It can be seen that the 5th and 7th non-characteristic harmonics of the typical 12-pulse system can meet the limits specified by IEEE-519. Only the high-order characteristic harmonics (the 11th, 13th, 23th and 25th harmonic) should be attenuated. This is consistent with the analysis in Section 4.2. In Options 1 and 2, the low-order non-characteristic harmonics are amplified considerably, which actually cause more harmonics injection into the system. This makes the two small non-characteristic filters in Option 3 necessary. In comparison, Option 4 with the proposed filter can effectively attenuate the non-characteristic harmonic amplification. Both the individual and total harmonic distortions meet the IEEE limits.

Figure 4.11 presents the comparison results of the driving point impedance seen from the harmonic source. It can be seen that Option 3 has managed to reduce the impedances at the non-characteristic harmonics. However, the resonance points still exist, and they can amplify interharmonics. In comparison, the DHP filter presents a flat, low driving point impedance for the whole frequency range. Hence, no harmonic amplification problems at filter bus need to be concerned.

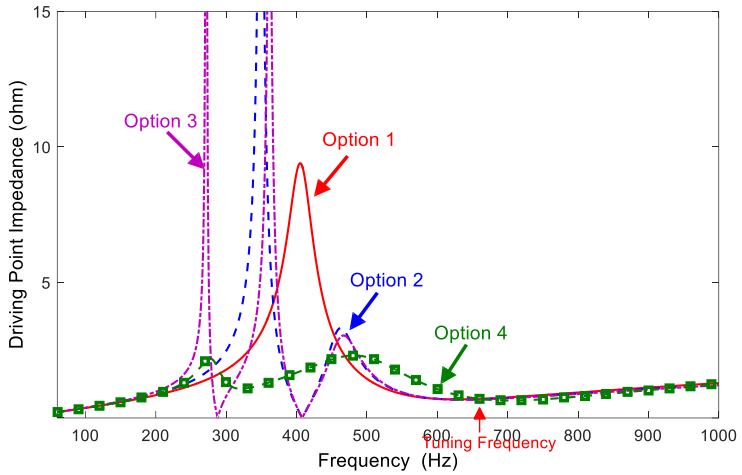

Figure 4.11 Driving point impedance comparison

The comparison of the non-characteristic $HAR(\omega_h)$ is illustrated in Table 4.3. It can be noticed that the options with the non-characteristic filters have a larger maximum $HAR(\omega_h)$ than the options with only the characteristic filter. This is due to the resonance introduced by the non-characteristic filters. Among all the options, only Option 4 achieves an acceptable $HAR(\omega_h)$.

Table 4.3 Harmonic amplification of different options

Option	Harmonic Amplification Ratio ($HAR(\omega_h)$)		
	5th	7th	Max from (5th to 11th)
1	1.7	5.1	5.1 (7th)
2	2.3	0.4	5.6 (6th)
3	0.7	0.4	29.1 (6th)
4	1.2	1.3	1.4 (8th)

In practice, the system impedance may change which can lead to different harmonic amplification ratios. The $HAR_{worst}(\omega_h)$ value for the 3rd HP (Option 1) is 74.3 at the 5th harmonic and 9.3 at 7th harmonic. In comparison, these values are only 1.3 and 1.3 for the DHP filter. These results demonstrate that the proposed DHP filter has an excellent damping performance.

The performances of the characteristic harmonic reduction are shown in Table 4.4, which shows that Options 3 and 4 are comparable. The DHP filter has slightly less reduction of the harmonics. This is due to the fact that it is closer to a single-tuned filter than to a 3rd HP filter at high frequencies.

Table 4.4 Filtering performance for characteristic harmonics

Option	Ratio of Characteristic Harmonics Reduction				
	13th	23th	25th	35th	37th
1	61%	55%	57%	66%	68%
2	63%	57%	59%	67%	68%
3	64%	58%	59%	67%	69%
4	73%	58%	57%	55%	55%

Table 4.5 presents a numerical loss analysis of the proposed filter. It assumes that the system operates at full load, i.e. 5 MVA. The filter power loss for each harmonic frequency is expressed as a percentage (%) of the filter size, i.e., the reactive power support.

Table 4.5 Numerical power loss analysis

Filter	Power loss percentage in % with respect to the filter size									
	1st	5th	7th	11th	13th	17th	19th	23th	25th	Total
DHP	0.002	0.108	0.039	0.197	0.045	0.000	0.000	0.002	0.001	0.395

As shown, the overall power loss of the DHP filter is quite small (less than 1%). The losses at different frequencies are highly dependent on the harmonic currents produced by converter system. The maximum loss happens at the 11th harmonic frequency, which is the largest individual harmonic produced by the 12-pulse system (referring to Figure 4.10).

The economic analysis is also conducted, and the results are listed in Table 4.6. The filter loadings are calculated at the full-load condition, and the price of each component is based on the quotations from the industrial manufactures. The details are available in Appendix F.

Table 4.6 Economic analysis of the proposed scheme

	Option 3	Option 4
Component Cost ($)	32,650	23,350
Operating Cost ($)	3,717	6,048
Total Cost ($)	36,367	29,398

It can be seen that the proposed scheme can save about 20% in filter cost, which makes it a more economical and attractive harmonic solution for multi-pulse industrial systems. The proposed scheme presents a little higher operating cost due to the damping required at the non-characteristic harmonics. Since the proposed filtering scheme has only one filter branch, it can save more money in practice if one takes the other factors, such as the switchgear, CTs and the labor cost, into consideration.

The space requirement of the two options are also analyzed in Appendix F. The results show that the proposed scheme can save at least 30% of the space required by the current scheme.

4.4.3 Additional Cases

The performance of the proposed filter has also been investigated for the cases involving the 18-pulse and 24-pulse systems. The filter frequency response in comparison with that of the 3rd HP filter is shown in Figure 4.12. Both are designed with a α% value of 90%. One can notice that both filters have comparable performance in providing a low impedance for the characteristic harmonics.

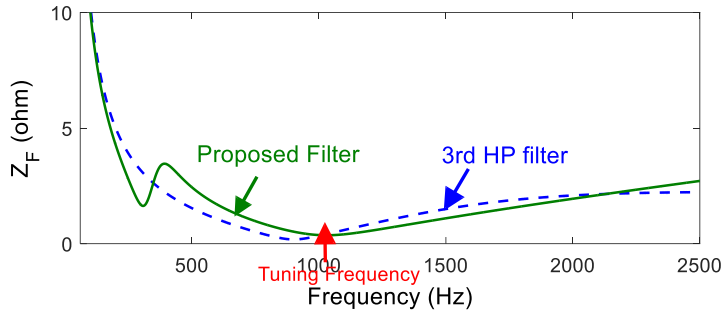

(a) 18-pulse system

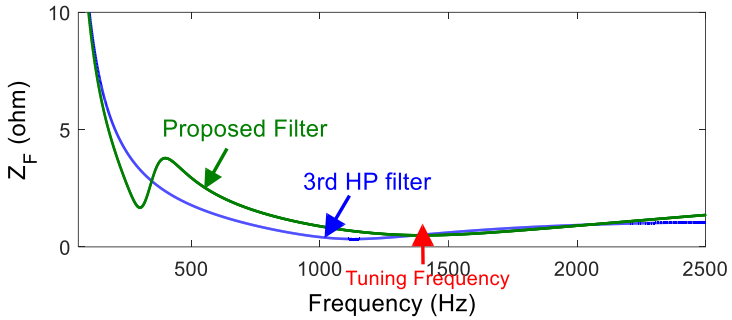

(b) 24-pulse system

Figure 4.12 Filter frequency response for 18 & 24 -pulse systems

In term of the performance at the non-characteristic harmonics, the $HAR(\omega_h)$ indices are compared as shown in Figure 4.13. This figure also shows the DHP filter with α%=70%. It can be seen that the DHP filter does not amplify the harmonics. On the other hand, the 3rd HP filter results in significant amplification at low-order non-characteristic harmonics, and thereby it requires the non-characteristic filters.

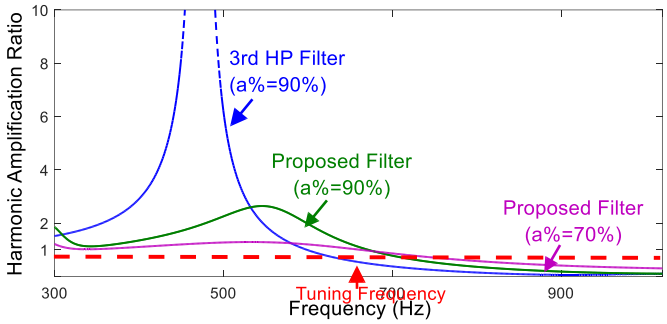

(a) 18-pulse system

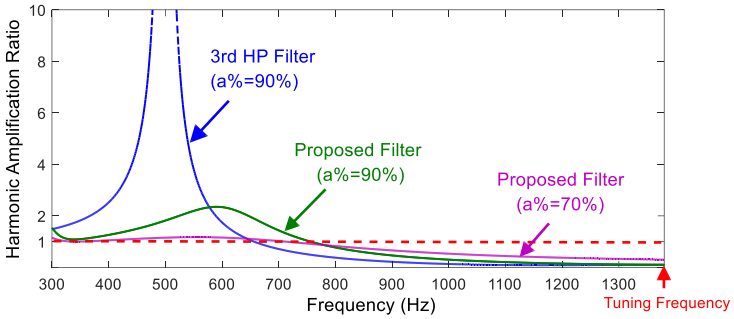

(b) 24-pulse system

Figure 4.13 Harmonic amplification ratio for 18 & 24 -pulse systems.

In conclusion, the proposed filter presents a very attractive option to filter harmonics for multi-pulse industrial systems. The filter has a performance similar to that of the 3rd HP filter at the characteristic harmonic frequencies but does not have its problems at the non-characteristic harmonic frequencies.

4.5 Interharmonic Mitigation

Another potential application of the proposed filter is interharmonic mitigation. Variable frequency drives (VFD) are well-known interharmonic sources in power systems [96]-[97]. In recent years, several interharmonic problems have been reported. Further analysis reveals that these problems are due to the harmonic resonance caused by the filter package [61],[98]. Since the frequencies of the interharmonics vary with the operating speed of the drive, common passive filters are not valid for them. The high damping performance of the DHP filter makes it a promising solution for these problems. To illustrate this, the following presents two examples of applying DHP filters to solve interharmonic problems.

4.5.1 Voltage Flickers

The first example involves a realistic case where interharmonics produced by VFD causes voltage flicker [61]. This case involves a 12-pulse VFD in a pipeline compressor station, as shown in Figure 4.14.

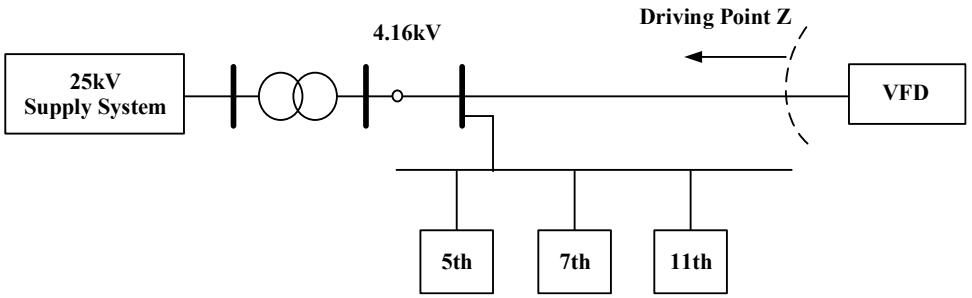

Figure 4.14 Full arrangement of the VFD facility

Three passive filters (5th, 7th and 11th) are installed in this facility. One 11th 2nd HP filter is to attenuate the characteristic harmonics produced by the 12-pulse drive (such as the 11th, 13th, 23th and 25th harmonics, etc.). Two small 5th and 7th single-tuned filters are also used to avoid the potential resonance at these harmonic frequencies. Table 4.7 lists the filter parameters.

Table 4.7 Filter parameters of the drive system

Harmonic	Topology	C (Mvar)	L (mH)	R (ohm)
5th	single-tuned	0.19	12.2	---
7th	single-tuned	0.15	6.2	---
11th	2nd HP	0.60	6.3	10

Since the installation of this facility, voltage flicker problems have been reported. The field tests found two dominant interharmonic components (117 & 237Hz). Further study shows that the interharmonic currents generated by the drive are actually small, but the resonance between the filter package and supply system results in the excessive interharmonic voltages.

According to the operating speed, the drive will produce interharmonics within the frequency range from 120Hz to 390Hz. Figure 4.15 shows the driving point impedance seen from the drive. It can be noticed that, after connecting the filters (5th, 7th and 11th), the driving point impedance has sharp resonance peaks in this frequency range. Once coinciding with interharmonics produced by the drive, these impedance peaks can significantly amplify the interharmonics, which results in severe flicker problems.

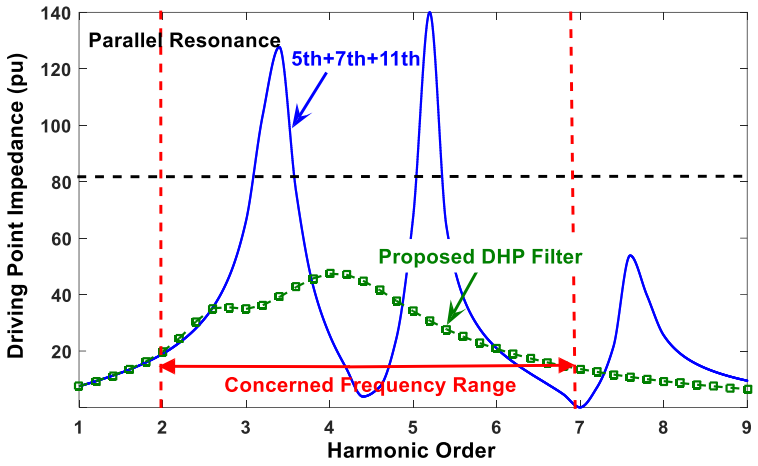

Figure 4.15 Comparison of the driving point impedances

To solve this problem, one DHP filter tuning at 11th harmonic is used to replace the 5th, 7th and 11th filter branches. The parallel resonance point of the frequency-dependent damping block is selected at the 3rd harmonic because the concerned frequency range is 120~390Hz. The driving point impedance with DHP filter is also illustrated in Figure 4.15. As can be observed, the DHP filter presents a lower driving point impedance than the original filter arrangement. This is because it can provide high damping in the concerned frequency range. Table 4.8 lists the harmonic amplification ratios at the non-characteristic harmonic and interharmonic frequencies.

Table 4.8 Non-characteristic harmonics & interharmonics amplification

Filter	Non-characteristic & Inter- harmonic Amplification		
	5th harmonic	7th harmonic	Interharmonic
Original	0.02	0.03	5.48
Updated	1.13	0.30	1.93

The results reveal that the DHP filter can effectively reduce the interharmonic amplification. The maximum amplification is reduced from 5.48 to 1.93. As a result, there is no need to worry about the voltage flickers caused by the interharmonics. Another benefit of the high damping performance is that the DHP filter can damp the harmonic amplification at the non-characteristic harmonics. This offers a more economic filter solution by saving the 5th and 7th non-characteristic filters.

The harmonic mitigation performance of the updated filter arrangement is also studied, and the results are summarized in Table 4.9. It indicates that the harmonic performance of the two arrangements are comparable.

Table 4.9 Harmonic mitigation performance at characteristic harmonics

Filter	Characteristic Harmonics Reduction			
	11th	13th	23th	25th
Original	95%	95%	57%	64%
Updated	95%	95%	57%	65%

4.5.2 Powerline Communication Interference

The second example involves a powerline communication (PLC) interference problem. Figure 4.16 presents the system configuration.

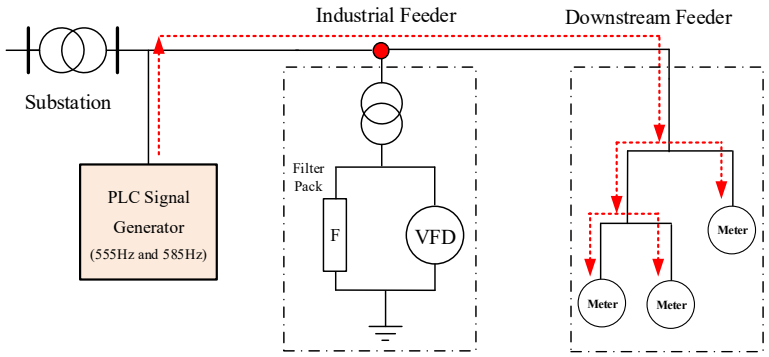

Figure 4.16 Configuration of powerline communication system

This distribution system has two feeders. One feeder connects to an industrial customer, and the other one connects to the local residential loads. There is an 18-pulse drive in the industrial customer. For harmonic mitigation, several single-tuned filters are installed in this facility, and their parameters are given in Table 4.10.

Table 4.10 Filter arrangement and parameters in drive system

Harmonic	Capacitor (Mvar)	Reactor (mH)
5th	0.16	12.53
7th	0.16	6.06
17th	0.16	1.00
19th	0.16	0.81
33th	0.56	0.07

For communication purpose, the supply utility injects currents at 555Hz and 585Hz interharmonic currents at the substation side [99]. These interharmonics interact with the impedance of lines and loads at downstream side, and then produce the voltage signals. The customer billing meters will send the billing information back after picking up the voltage signals.

However, upon the commissioning of this system, a large number of meters on downstream feeder are unable to respond to the command issued by the substation. Several field measurements show that the problem is caused by the drive filters. The drive filters resonate with the customer branch, resulting in a low impedance path for the PLC signals, as indicated in Figure 4.17. Since the signals cannot reach the downstream endpoints, the downstream meters cannot respond to the reading requests.

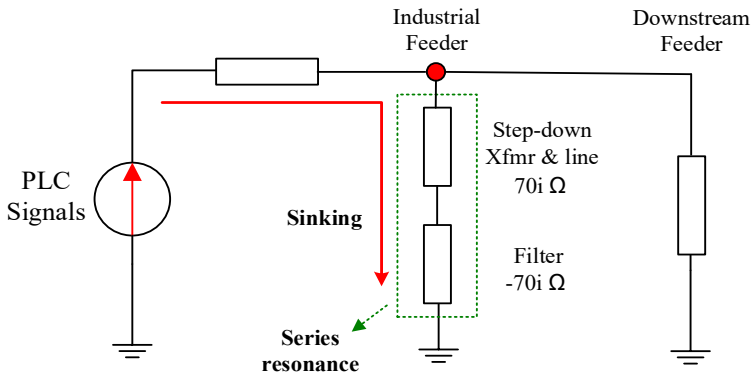

Figure 4.17 Simplified circuit for analysis of PLC signal sinking

The DHP filter is adopted to update the filter package by replacing the 5th, 7th, 17th and 19th filters. It is tuned at 17th harmonic with the same reactive power compensation. Its response is compared with the old filter package in Figure 4.18. As shown, the proposed filter leads to a higher impedance at customer branch than the old filter package. The high customer impedance strengths the PLC signal received by the downstream meters, so the interference problem can be solved accordingly.

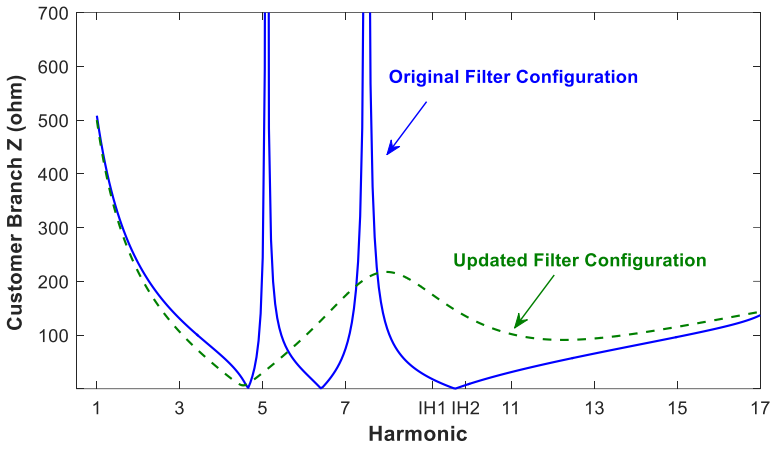

Figure 4.18 Frequency response comparison of the customer branch

Table 4.11 presents the downstream PLC signal level for the two filter packages. The operation without the industrial customer branch is selected as the base case; i.e., all the signals (100%) will reach the downstream. As can be seen, less than 30% PLC signals can be received by the downstream when the old filter package is connected. In comparison, the DHP filter can guarantee over 75% of the PLC signal reach the downstream branch. Based on operating experience, such a signal level is workable for the communication system.

Table 4.11 PLC signal received by downstream branch

PLC Signal	Old Package	Updated Package
9.25th	21%	89%
9.75th	4%	79%

4.6 Summary

This chapter presented a new and effective filtering scheme for multi-pulse industrial systems. This is achieved by a novel filter topology that can perform harmonic mitigation at the characteristic harmonics and prevent harmonic resonance at the non-characteristic harmonics. The main contributions of this chapter are summarized as follows.

- A new filtering concept for multi-pulse industrial systems. This concept avoids the use of the non-characteristic filters, thus eliminating various

problems and extra costs of the existing filter schemes;

- A novel filter topology called DHP filter that makes the above concept feasible. The core idea of this topology is a frequency-dependent damping block that can provide a high resistance at the non-characteristic harmonic frequencies;

- Demonstration of two potential applications of the filter concept and scheme. They are a low-cost filter package for multipulse industrial systems and a scheme to mitigate interharmonic problems caused by the use of non-characteristic filters. The proposed scheme can also be used for HVDC links and Static Var Compensators (SVC).

Chapter 5

Application of Damped High-Pass Filter at HVDC Terminals

In recent years, high voltage direct current (HVDC) has become the dominating technology for the large capacity and long-distance power transmission. Despite its effectiveness, the power-electronic-devices-based HVDC converters are natural harmonic sources for the power grid. This is especially true for the line-commutated converter (LCC) HVDC terminals [100]-[101]. The injected harmonics are associated with the converter configuration. It is common to use the 12-pulse configuration at LCC HVDC terminals. The major harmonics produced by the converters are the 11th, 13th, 23rd, 25th, etc. However, it has been reported that the system still suffer severe harmonic distortions at the low-order non-characteristic harmonics such as the 5th and 7th, due to the parallel resonance between the HVDC filters and supply system [102]-[104]. To address this issue, the current practice is to add extra filters at these non-characteristic harmonic frequencies. As a result, the advantage of the multi-pulse configuration—very low non-characteristic harmonic emission—is, therefore, not fully utilized.

The intention of this chapter is to apply the previously proposed damped high-pass (DHP) filter to offer an alternative filtering scheme for the multi-pulse LCC HVDC terminals. To make this idea feasible, a new design method is developed to address two unique issues faced by the design of HVDC filters: a wide range of system impedances seen by an HVDC terminal and a variable reactive compensation configuration at the terminal. Both are challenging filter design problems even for traditional filter banks. Using realistic industry case and sensitivity studies, it has shown that the proposed filtering scheme and design method can result in saving in filter costs and space without sacrificing performance in comparison with the current filtering scheme. The proposed design concepts are

also applicable to the design of other filters facing the same issues.

This chapter is organized as follows. Section 5.1 reviews the current filter arrangement for HVDC terminals. Section 5.2 proposes an alternate filtering scheme based on the previously developed DHP filter in Chapter 4. Two practical design issues, the variable network impedance and flexible reactive power requirement, are discussed in Section 5.3 and 5.4, respectively. An improved design method is then developed in Section 5.5. Section 5.6 evaluates the performance and effectiveness of the proposed design through a real-life case study. Finally, an assessment of the filter sensitivity to the parameter variations is conducted in Section 5.7.

5.1 Review on HVDC Filtering Scheme

A typical filtering arrangement of a 12-pulse LCC HVDC terminal is shown in Figure 5.1. As explained, the system primary harmonics of concern are the 12k±1 characteristic harmonic produced by the converters.

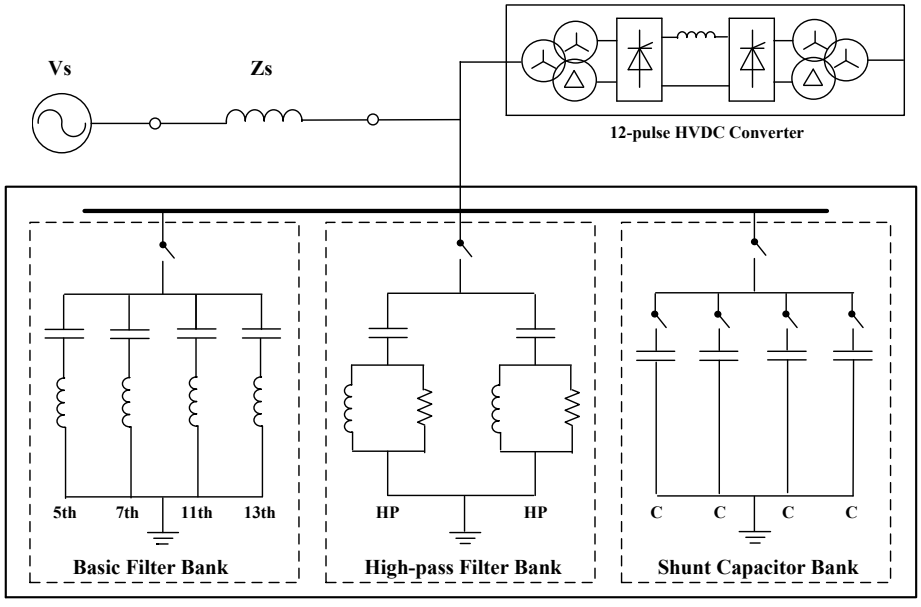

Figure 5.1 Example filter arrangement at HVDC terminals

To mitigate these harmonic components, the current filtering scheme includes the 11th, 13th and high-pass filters. Since passive filters are capacitive below their tuning frequency, they may resonate with the inductive network impedance, resulting in serious harmonic amplifications at the non-characteristic harmonics [60],[105]. To avoid this, two extra non-characteristic harmonic filters with the tuning frequency at the 5th and 7th harmonic are installed, even though the harmonic contents at these frequencies are quite limited.

In practice, HVDC terminals are quite susceptible to the resonance at these low-order non-characteristic harmonics for the following reasons:

- The power transmitted by HVDC is continuously growing over the recent years. It decreases the system short-circuit level and leads to a low system resonance frequency.
- A high reactive power compensation is normally required at HVDC terminals. The amount sometimes can be 60% of the total transmitted power, which also increases the possibility of the low frequency resonance.
- The HVDC filters may experience a large variation of network impedance since they are directly connected to the supply system without any isolation transformers. This makes it hard to avoid the resonance even at the designing stage.
- The capacitances of the long-distance overhead lines or cables also contribute to the harmonic resonance at the low frequencies.

All these facts necessitate the low-order non-characteristic filters in the current filtering scheme. It should be noted that, besides the increased cost and space requirement, these extra filters may bring additional troubles for system operation. For example, the total reactive power support of the basic filter bank is increased. Under the light-load condition, shunt reactors may be needed to prevent too much reactive power flowing back into the supply system [105].

5.2 Proposed Filtering Scheme

Figure 5.2 illustrates the proposed filtering scheme based on the DHP filter. As can be seen, the DHP filter is used as one characteristic filter in the basic filter bank. Here the DHP filter has two main functions: 1) it replaces one characteristic filter to achieve the required harmonic mitigation performance at this frequency; 2) it provides high damping to suppress the resonance at the non-characteristic harmonics.

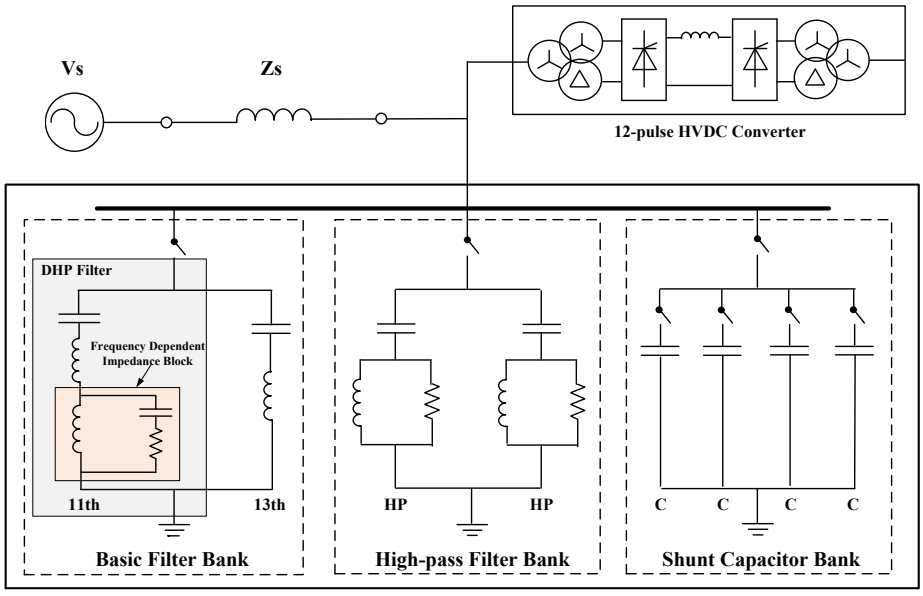

Figure 5.2 Proposed filtering scheme at HVDC terminals

It is suggested to use the DHP filter as the lowest characteristic filter to ensure the DHP filter stay connected for all the operating conditions, such as the 11th harmonic for a 12-pulse HVDC terminal. As will be shown later, a properly designed DHP filter can provide sufficient damping at the non-characteristic harmonics. As a result, there is no need to add the non-characteristic filters in this new filtering scheme.

Unlike the industrial case, the DHP filter design at HVDC terminals is more challenging due to the complex system operations. To make the above idea feasible, a new design method of the DHP filter is required. This is because it is essential to consider (1) the various operating modes of the reactive power compensators at the

HVDC terminal, and (2) the wide range of network impedances seen by the terminal and its compensators. The impact of these issues should be fully considered and addressed at the designing stage.

5.3 Network Impedance Variation

As shown in Figure 5.2, HVDC filters are connected to the supply system directly without any isolation transformer. This makes them quite vulnerable to the variation of the network impedance. This section will discuss about the design of the DHP filter under this circumstance.

An accurate representation of the network impedance is essential for filter design. It is common to define network impedance in a range that covers all the possible impedance values [105]. Figure 5.3 shows three typical envelopes for impedance representation.

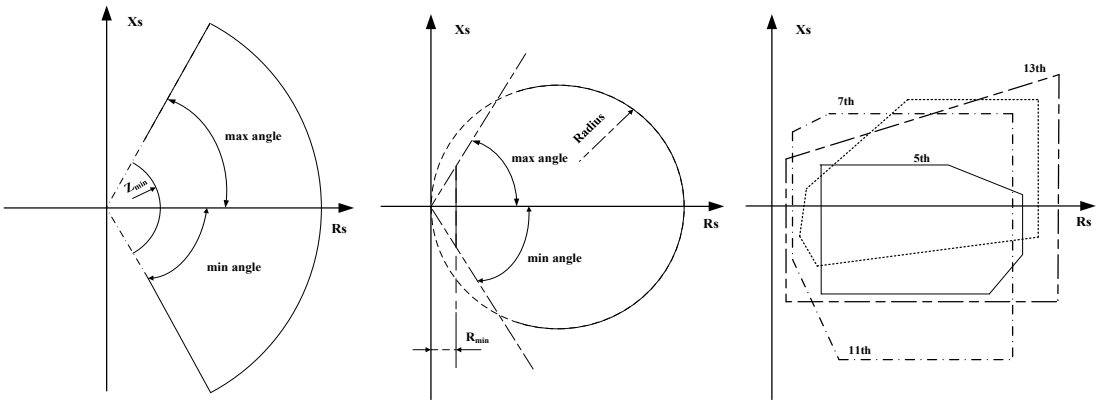

(a) sector (b) circle (c) polygon

Figure 5.3 Typical network impedance representation

The sector impedance is obtained based on the minimum and maximum impedance values and angles, as shown in Figure 5.3(a). One sector is used to describe the possible impedance values for all the frequencies. However, the maximum and minimum impedance values normally refer to the resonance condition where the impedance angle is supposed to be small. Thus, this

representation has a high possibility to include a large non-applicable impedance area.

The circle impedance uses an impedance circle to cover the network impedance variation, as shown in Figure 5.3(b). This method has a small impedance angle for the maximum impedance values, which reduces the non-applicable area caused by the resonance. Similar to the sector impedance, one circle is used to describe the impedances for all the harmonic frequencies. This simplification, however, limits the accuracy of the circle impedance.

The polygon impedance uses several discrete polygons to represent the network impedance, as shown in Figure 5.3(c). These polygons can be obtained based on simulations or measurements of the supply system at different operating conditions. Each polygon is used to cover the possible impedance values at every harmonic frequency. This representation can describe the frequency-dependent characteristic of the network impedance, and therefore has a relatively high accuracy.

Due to its high accuracy, the polygon impedance is adopted for filter design in the following study. Although the polygon represents the variation of the network impedance sufficiently, how to design a harmonic filter for a range of impedances with a guaranteed performance is still an unsolved problem, even for the design of the traditional filters. Since there are infinity impedance values within each polygon, it is practically impossible to traverse the entire polygon in filter design.

In this work, we propose to identify the potential impedance values that lead to the worst-case conditions first. The filter is then designed for these impedance values. A general equation for this analysis is shown in (5.1).

$$\frac{V_{s.post}(\omega_h)}{V_{s.pre}(\omega_h)} = \sqrt{\frac{R_F^2(\omega_h) + X_F^2(\omega_h)}{(R_s(\omega_h) + R_F(\omega_h))^2 + (X_s(\omega_h) + X_F(\omega_h))^2}} \tag{5.1}$$

where $V_{s.pre}(\omega)$ and $V_{s.post}(\omega)$ are the harmonic voltages at the interconnection point prior and after filter bank connection, $Z_s(\omega)=R_s(\omega)+jX_s(\omega)$ and $Z_F(\omega)=R_F(\omega)+jX_F(\omega)$ are the supply system impedance and filter bank impedance.

As can be seen from (5.1), regardless of the filter impedance, a larger system resistance $R_s(\omega)$ always leads to a better harmonic performance, i.e. a small $V_{post}(\omega)/V_{pre}(\omega)$, for the system impedances with the same reactance $X_s(\omega)$. Hence, the worst-case condition occurs at the impedance with the smallest $R_s(\omega)$. This finding significantly narrows the impedance values that need to be considered for filter design. To illustrate this finding, a polygon impedance is shown in Figure 5.4. If one draws an auxiliary line in parallel with the x-axis, all the impedances on this line have the same reactance value. The impedance with the smallest resistance can be identified as the one on the left boundary of the polygon, e.g., point A. If the filter fulfills the required harmonic performance at this point, then there is no need to worry about the other impedances on this line.

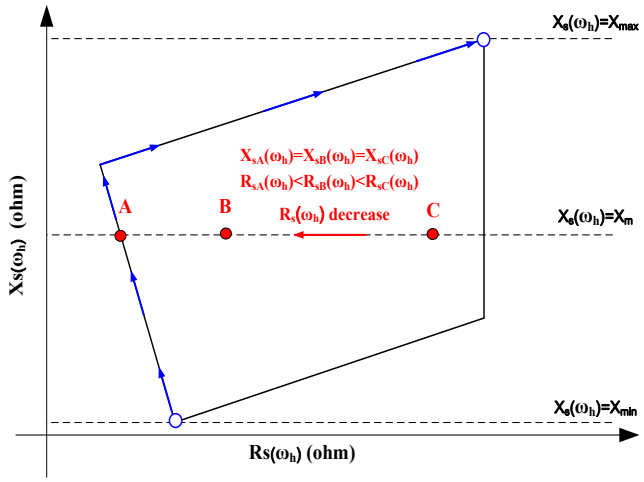

Figure 5.4 Analysis of polygon network impedance

In summary, the filter design only needs to focus on the left boundary of the polygon. Practically, it may start from the impedance point with the smallest reactance, and then scan the left-side boundary until reaching the one with the largest reactance. A proper design should fulfill the harmonic requirements for all these impedances. It should be emphasized that the above approach is applicable to all the impedance diagrams.

5.4 Switchable Reactive Power Support

A variable reactive power support is necessary for voltage support at HVDC terminals. It is achieved by switching filters and capacitors on and off at different operating conditions. Thus, the DHP filter needs to operate with various filter configurations. This fact puts a stringent requirement on the DHP filter performance, especially at the non-characteristic harmonics.

Figure 5.5 presents a typical reactive power management of HVDC terminals [105]. In this figure, the solid line represents the reactive power consumed by the HVDC converters, and the dashed line is the switching point of filters and capacitors.

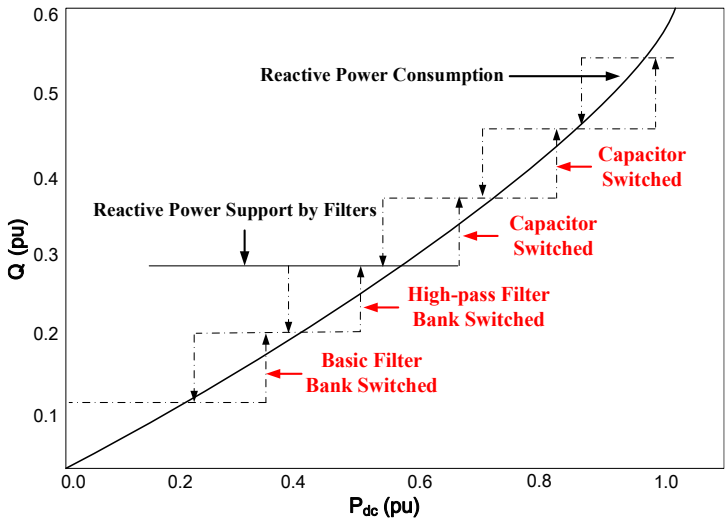

Figure 5.5 Typical reactive power management at HVDC terminals

The switching sequence of filter bank is determined by two main factors, i.e., the permitted reactive power interchange and harmonic mitigation requirement. The harmonic mitigation is the major constraint under the light-load condition. To satisfy the minimum harmonic filtering requirements, the basic filter bank, including all dominant characteristic filters, should be switched on as the first group. In normal operation, this bank should stay connected for all the conditions. The growth of the transmitted power will increase the high-order characteristic harmonics produced by the converters. Thus, the second group further switches on

the high-pass filter bank. Under the full-load condition, the permitted reactive power interchange turns into the major constraint. Thus, it is common to have one or more shunt capacitors to compensate the remaining reactive power. Note that the capacitors should only be switched on after all filters are connected.

The switchable reactive power support requires the DHP filter to operate in parallel with various filters and capacitors, as shown in Figure 5.6. The design in Chapter 4 only considers the resonance caused by the DHP filter itself, which may not be effective in solving the problems caused by the other filters or capacitors. Therefore, a new design method should be developed to take this new situation into consideration.

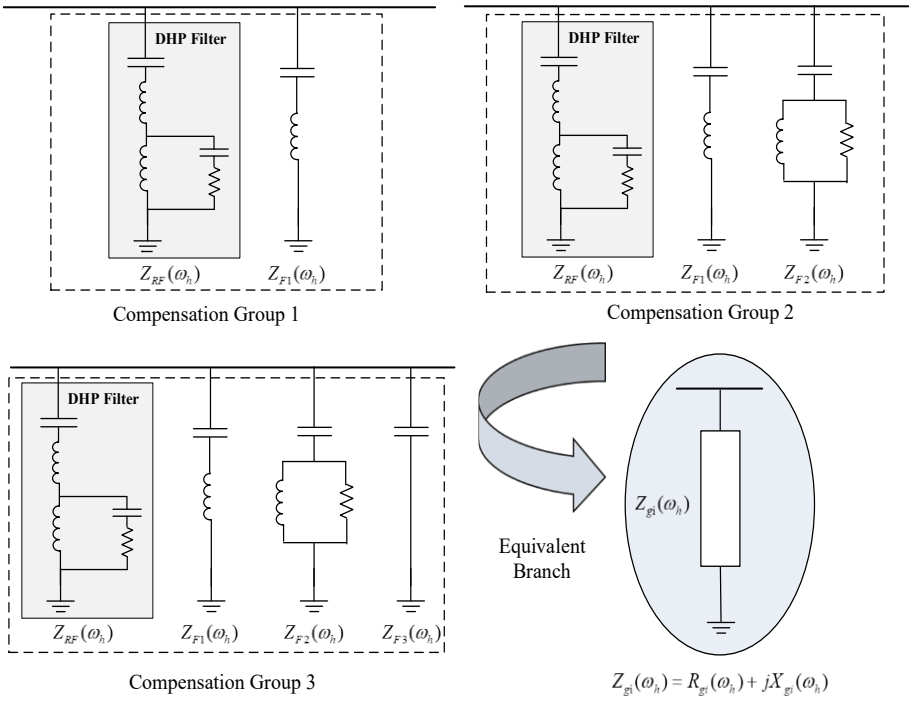

Figure 5.6 Analysis of each compensation group

In the design process, each compensator group should be treated as an equivalent branch, as indicated in Figure 5.6. The impedance of the equivalent branch can then be derived as a function of DHP filter; i.e.,

$$Z_{gi}(\omega_h) = R_{gi}(\omega_h) + X_{gi}(\omega_h) = f(Z_{DHP}(\omega_h)), \tag{5.2}$$

where $R_{gi}(\omega_h)$ and $X_{gi}(\omega_h)$ is the resistance and reactance of equivalent branch, $Z_{DHP}(\omega_h)$ is the DHP filter impedance.

For each group, the worst-case amplification ratio is defined in (5.3) to evaluate the damping performance of the DHP filter. A large $HAR_{gi.worst}(\omega_h)$ indicates that the HVDC terminal may experience a severe harmonic amplification when it operates with the compensator group i. It is worthwhile to point out that the previous design for industrial cases uses a relatively pessimistic assumption; i.e., the resonance happens at all the non-characteristic harmonics, and the network has no damping. This is because it is hard to get an accurate network information for customers. However, there is no need to use such an assumption since the polygon network impedance is already available.

$$HAR_{gi.worst}(\omega_h) = max\left\{\sqrt{\frac{R_{gi}^2(\omega_h)+X_{gi}^2(\omega_h)}{(R_s(\omega_h)+R_{gi}(\omega_h))^2+(X_s(\omega_h)+X_{gi}(\omega_h))^2}}\right\} \quad (5.3)$$

In the above equation, $R_s(\omega_h)$ and $X_s(\omega_h)$ are the resistance and the reactance of network impedance defined in the polygon. It has been explained that the worst-case only occurs on the left boundaries of the polygon, i.e., the impedance value with the smallest $R_s(\omega_h)$. Therefore, one can scan all these impedance values to obtain $HAR_{gi.worst}(\omega_h)$.

The overall damping performance of the DHP filter can be further quantified by the maximum amplification ratio of all the groups, as shown in (5.4). To eliminate the resonance concern, the design objective should try to minimize this value in the frequency range of concern.

$$HAR_{worst}(\omega_h) = max(HAR_{gi.worst}(\omega_h) \quad gi=1,2,\ldots,N) \quad (5.4)$$

5.5 Damped High-pass Filter Design

The previous sections discussed two main design issues and their solutions. A complete design method is developed for the DHP filter in this section.

5.5.1 Design Equations

Since the DHP filter is composed of five components, five design equations are required to determine all the component parameters. The first three equations are the same as the previous design in Chapter 4: the reactive power support, filter tuning frequency and the parallel resonance frequency of the damping block. These equations are listed below.

- **Design Equation 1: Reactive Power Requirement**

The filter main capacitor is determined based on the reactive power requirement Q_F, as shown below,

$$C_1 = \frac{Q_F}{\omega_1 V_s^2(\omega_1)}. \tag{5.5}$$

- **Design Equation 2: Selection of Filter Tuning Frequency**

The DHP filter should be tuned at the lowest characteristic harmonic, such as the 11th harmonic for a 12-pulse HVDC terminal. Here the filter tuning frequency ω_t is defined as the frequency where the filter reactance equals to zero; i.e.,

$$X_{eq}(\omega_t) = 0. \tag{5.6}$$

Accordingly, the reactor L_1 can be derived as

$$L_1 = \frac{L_2(\omega_t^2/\omega_p^2 - 1) - \omega_t^2 R^2 / L_2 \omega_p^4}{(\omega_t R C_2)^2 + (1 - \omega_t^2/\omega_p^2)^2} + \frac{1}{\omega_t^2 C_1}. \tag{5.7}$$

- **Design Equation 3: Parallel Resonance Frequency**

The frequency-dependent damping block intends to create a parallel resonance to boost the filter resistance. The resonance frequency ω_p is selected between the concerned non-characteristic harmonics, such as the 6th between the 5th and 7th harmonics. The capacitor C_2 can then be derived as:

$$C_2 = \frac{1}{\omega_p^2 L_2}. \tag{5.8}$$

The last two design equations are related to the filter harmonic performance. As explained, the network impedance variation and switchable reactive power support affects the DHP filter performance at both the characteristic and non-characteristic harmonics. In view of this fact, the design equations should take their impacts into consideration. The details are discussed below.

- **Design Equation 4: Harmonic Mitigation Performance**

The filter should meet the required harmonic mitigation performance at its tuning frequency, as specified in (5.9). Note that (5.9) should be satisfied for all the impedances on the polygon left boundary.

$$\frac{V_{s.post}(\omega_t)}{V_{s.pre}(\omega_t)} \le 1-\alpha\% \tag{5.9}$$

For a specific system impedance $R_s(\omega_t)$ and $X_s(\omega_t)$, the reactor L_2 can be obtained by (5.10):

$$L_2 = \sqrt{\frac{R^2\omega_t^{\,2}[R\omega_t^{\,4}(\sqrt{A(B-AX_s^2(\omega_t))}+AR_s(\omega_t))+ABC^2)}{(1-A)R^2\omega_t^{\,8}-ABC^4-2AC^2R_s(\omega_t)R\omega_t^{\,4}}}\,, \tag{5.10}$$

where $A=(1-\alpha\%)^2$, $B=R_s^2(\omega_1)+X_s^2(\omega_1)$ and $C=\omega_t^2-\omega_p^2$.

It should mention that this design ignores the impact of other filters and capacitors at this frequency. The reason is that their harmonic impedances are normally much larger when compared with the DHP filter.

- **Design Equation 5: Damping Performance**

The last design equation is to maximize the overall system damping performance, i.e., to minimize the $HAR_{worst}(\omega_h)$ in (5.11). Here ω_{low} and ω_{high} are the frequencies of the lowest and highest concerned non-characteristic harmonic.

$$min\ \{HAR_{worst}(\omega_h)\quad (\omega_{low} \le \omega_h \le \omega_{high})\} \tag{5.11}$$

5.5.2 Design Process

Among the five filter components, C_1 can be determined by (5.5). L_1 and C_2 can be determined from (5.7)-(5.8) once L_2 and R is known. Therefore, the problem is a two-variable (i.e. L_2 and R) optimization problem to minimize $HAR_{worst}(\omega)$. To achieve the global minimal value, the simplest way is to scan all the feasible values, as illustrated in Figure 5.7.

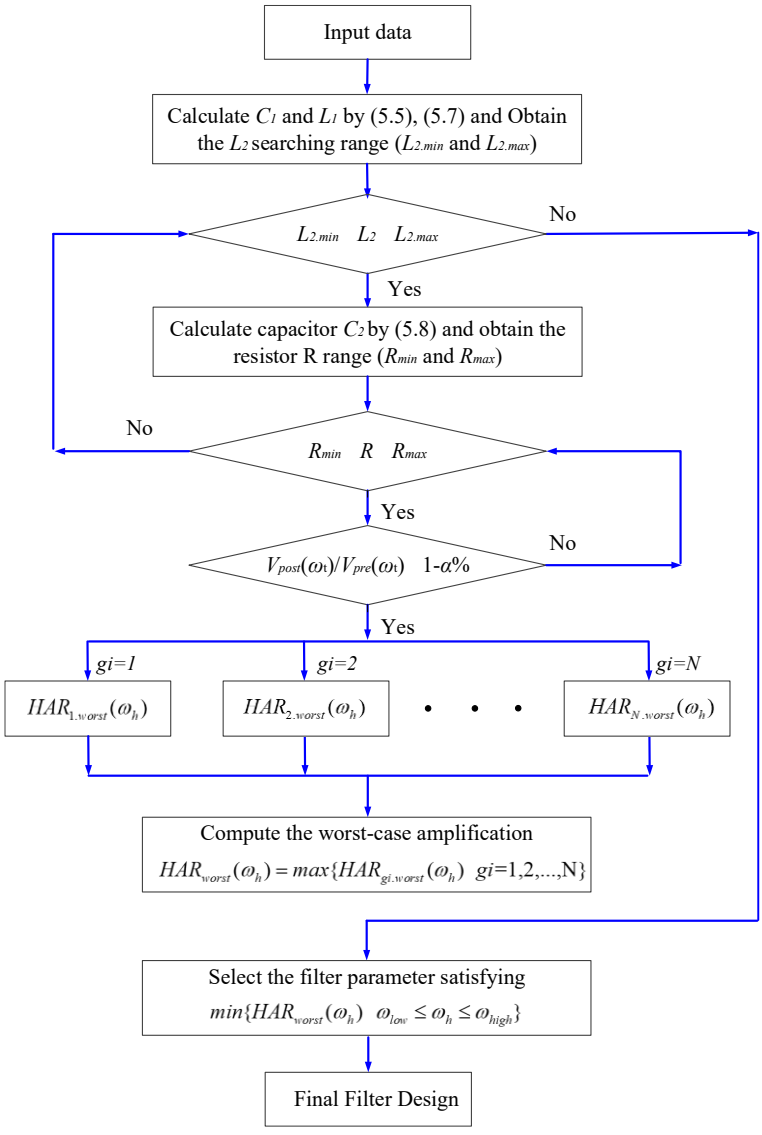

Figure 5.7 Flow chart of DHP filter design at HVDC terminals

To improve the searching efficiency, the search range of the L_2 and R can be established. The range of the L_2 can be obtained from (5.9) based on the polygon impedance at the tuning frequency. Once L_2 is obtained, the range of the R can be decided for the purpose of ensuring a positive L_1 and L_2 values.

5.6 Comparative Case Study

A case study has been conducted on a real-life HVDC project to verify the effectiveness of the proposed filtering scheme. All the system data adopted is based on the measurements in [106].

5.6.1 System Description

This study involves a classic 12-pulse HVDC terminal with a total transmitted capacity of 1440 MW. A simplified system configuration is illustrated in Figure 5.8.

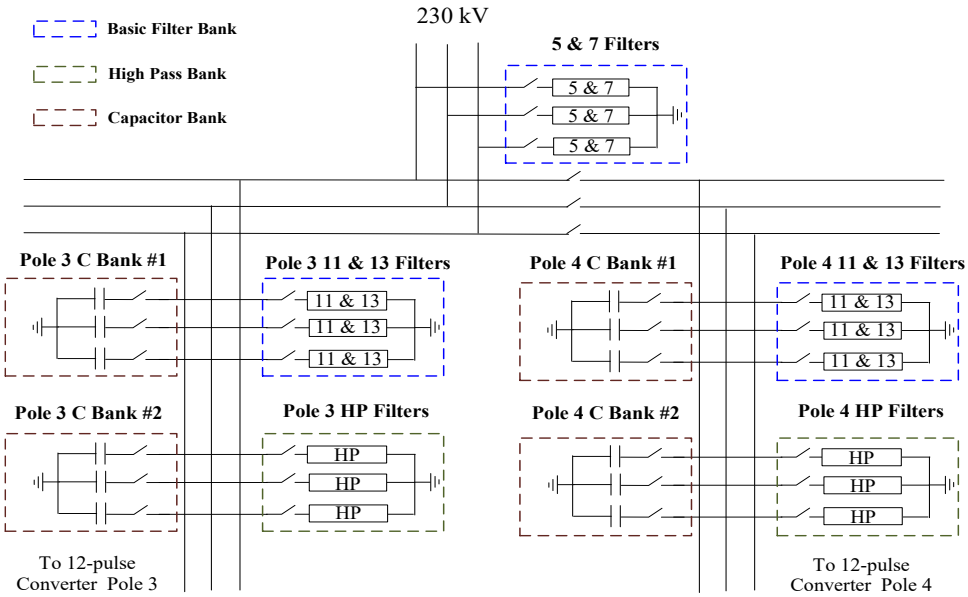

Figure 5.8 A real-life HVDC substation configuration

In this system, there are three types of filter banks, including the basic filter bank (5th, 7th, 11th and 13th filters), high-pass filter bank and capacitor bank. When the system operates under the light-load condition, the measured harmonic voltage

without filters or capacitors are shown in Figure 5.9.

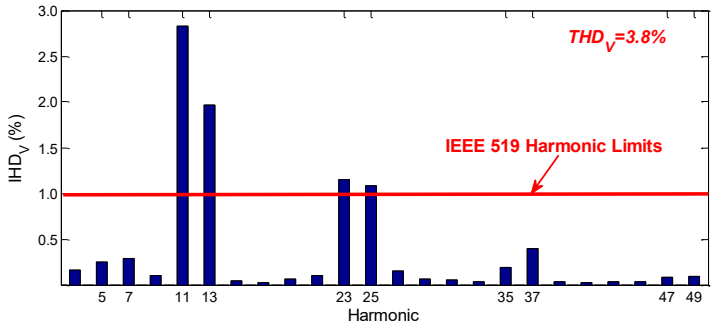

Figure 5.9 Harmonic voltage spectrum at low power level

In this system, the primary harmonic concerns are the 11th, 13th, 23th and 25th characteristic harmonics. Hence, two pairs of the characteristic filters (i.e., 11th, 13th and HP) are used in the current scheme. In comparison, the non-characteristic harmonics (5th and 7th) are within the specified harmonic limits [34], and thereby only one pair of the non-characteristic filters is added to address the resonance concern. The detailed parameters can be found in Table 5.1.

Table 5.1 Parameters of original filters and capacitors

Branch	5th	7th	11th	13th	HP	C
Topology	ST	ST	ST	ST	2nd HP	Shunt C
C_1 (uF)	2.46	1.28	1.33	0.95	3.9	3.9
L_1 (mH)	114	114	44	44	5.5	---
R (Ω)	0.86	1.18	0.82	0.93	40	---

Since there is no data available for the system operating at the other load conditions, the harmonics produced by converters are assumed to increase linearly with the system load level. A correction factor is used for the medium- and high-load conditions (1.5 for the medium-load and 2.0 for the high-load).

5.6.2 Performance Evaluation

Four filtering schemes are studied for comparison, and the basic filter bank is the only difference among them, as shown in Table 5.2.

Table 5.2 Basic filter bank of each filter scheme

Scheme	Basic Filter Bank
1 (original)	5th single-tuned filter×1 7th single-tuned filter×1 11th single-tuned filter×2 13th single-tuned filter×2
2 (comparative)	11th single-tuned filter×2 13th single-tuned filter×2
3 (chapter4)	11th DHP filter×2 (design method in Chapter 4) 13th single-tuned filter×2
4 (proposed)	11th DHP filter×2 (new proposed design) 13th single-tuned filter×2

The first scheme is the current filtering scheme for this system. The second one is used for comparison by eliminating the non-characteristic filters. The last two schemes include the DHP filter, where Scheme 3 uses the design method in Chapter 4, and Scheme 4 uses the proposed design method. To provide the same reactive power support, the sizes of the 11th filters are adjusted in the last three schemes. Table 5.3 lists the filter parameters.

Table 5.3 Parameters of the 11th filter branch for each scheme

Scheme		1	2	3	4
Topology		single-tuned	single-tuned	DHP filter	DHP filter
Components	C_1 (uF)	1.33	3.20	3.20	3.20
	C_2 (uF)	----	----	17.18	12.43
	L_1 (mH)	----	----	22.7	24.40
	L/L_2 (mH)	44.00	18.30	11.40	15.70
	R (Ω)	0.82	----	4.77	6.35

Three operating conditions are studied, which include the light-, medium- and high-load conditions. The status of filters and capacitors for each condition are listed below:

- Light-load: basic filter bank
- Medium-load: basic filter bank + HP filter bank
- High-load: basic filter bank + HP filter bank + capacitors

For each condition, the harmonic analysis is conducted for the above four filtering schemes. Both the total and individual harmonic distortion indexes are calculated, and the results are shown in Figure 5.10-Figure 5.12.

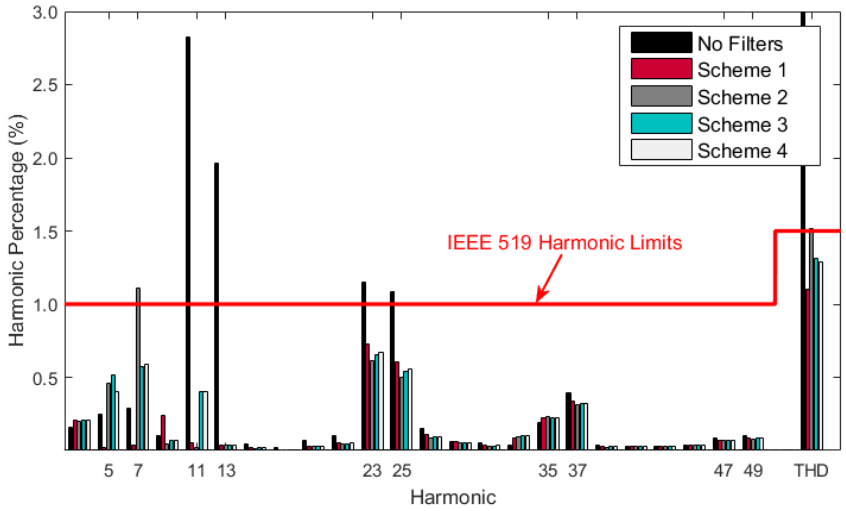

Figure 5.10 Harmonic voltage spectrum under light-load condition

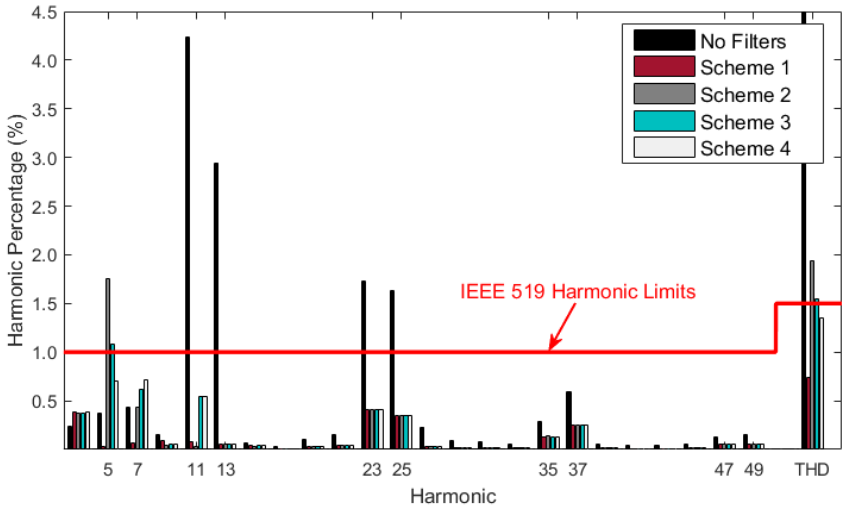

Figure 5.11 Harmonic voltage spectrum under medium-load condition

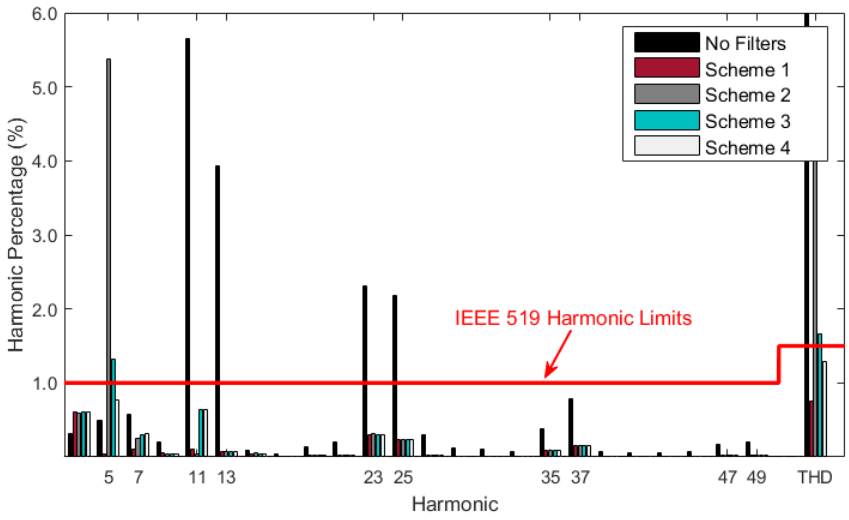

Figure 5.12 Harmonic voltage spectrum under high-load condition

As can be seen, Scheme 1 can meet the specified limits for both the total and individual harmonic indexes. The non-characteristic filters are proved to be essential, as Scheme 2 experiences severe amplifications at the 5th and 7th harmonics. Scheme 3 meets the harmonic limits under the light-load condition. However, the non-characteristic harmonics still exceed the limits when the high-pass filters and capacitors are switched on. This is because the design in Chapter 4 does not consider the resonance caused by the other branches. In comparison, the DHP filter designed by the proposed method successfully solves the non-characteristic harmonic problems. It can meet the harmonic limits at both the non-characteristic and characteristic harmonics.

Table 5.4 lists the amplification ratios at the non-characteristic harmonics. As can be expected, Scheme 2 has the largest amplification where the 5th harmonic is amplified over 10 times. In Scheme 3, the DHP filter helps relieve the amplification problem but the 5th harmonic is still amplified about 3 times. In contrast, Scheme 4 with the new designed DHP filter effectively solves the harmonic amplification problems at the non-characteristic harmonics. The largest amplification ratio is limited within 2, which is only 1/5 compared to that of Scheme 2.

Table 5.4 Non-characteristic harmonic amplification

Scheme	Harmonic Amplification Ratio					
	Light-load		Medium-load		High-load	
	5th	7th	5th	7th	5th	7th
1	0.1	0.1	0.1	0.2	0.1	0.2
2	1.87	3.84	4.7	1.0	10.94	0.42
3	2.09	1.98	2.95	1.44	2.68	0.52
4	1.62	2.04	1.92	1.65	1.58	0.54

A further study is conducted to analyze the power losses of the DHP filters, as shown in Table 5.6. The results show that the DHP filters present a low power loss in both the scheme 3 and scheme 4. The overall power losses are only about 1% of the filter size. The maximum loss occurs at the frequency where the filter is tuned, i.e., the 11th harmonic.

Table 5.5 Power loss analysis of DHP filter

Arrangement		Power loss percentage in % of filter reactive power output							
		1st	5th	7th	11th	13th	23th	25th	Total
Light	3	0.002	0.043	0.036	0.352	0.001	0.003	0.002	0.438
	4	0.002	0.059	0.030	0.352	0.001	0.003	0.002	0.448
Medium	3	0.002	0.019	0.043	0.654	0.001	0.001	0.001	0.894
	4	0.002	0.019	0.045	0.654	0.001	0.001	0.001	0.889
High	3	0.002	0.283	0.010	0.893	0.001	0.001	0.001	1.190
	4	0.002	0.224	0.009	0.893	0.001	0.001	0.001	1.130

In summary, the above real-life case study verifies the effectiveness of the proposed design method for the application of DHP filter at HVDC terminals. It is able to simultaneously mitigate the characteristic harmonic and provide a sufficient damping at the non-characteristic harmonics for all the operating conditions. In consequence, there is no need to add the non-characteristic filters.

5.7 Sensitivity Study

In practice, the parameter variations, such as manufacturing tolerance and frequency deviation, may affect the filter performance at the harmonic frequencies. To evaluate such impacts, a Monte-Carlo simulation has been conducted for the

previous study case under the light-load condition. The results of the medium- and high-load conditions are similar, thus omitted for space limitation. The typical variation range in Table 2.3 are adopted for this analysis.

The impacts of the parameter variations are analyzed from two perspectives - performance indexes and loading indexes. The performance indexes include reactive power support, power loss and filter harmonic performances, and the loading indexes cover the major loading indexes of filter components. The results are illustrated in Table 5.6 and Table 5.7. All the indexes are presented in percent of the standard value without parameter variations.

Table 5.6 Performance sensitivity to parameter variations

		average	worst-case	95% confidence interval	
				lower	upper
Reactive power support		2.0%	5.6%	0.5%	3.6%
Non-characteristic harmonic amplification	5th	-13.8%	24.4%	-29.1%	1.6%
	7th	1.9%	11.3%	-2.3%	6.2%
11th harmonic mitigation		-2.9%	26.7%	-13.3%	6.7%
Filter power loss		1.1%	12.2%	-3.0%	5.2%

Table 5.7 Loading sensitivity to parameter variations

		average	worst-case	95% confidence interval	
				lower	upper
Main Capacitor	Voltage	2.0%	5.6%	0.5%	3.6%
	Capacity	4.1%	11.6%	0.9%	7.3%
Auxiliary Capacitor	Voltage	0.6%	5.1%	-1.3%	2.5%
	Capacity	0.4%	15.6%	-4.8%	5.5%
Main Reactor	Current	2.0%	5.5%	0.5%	3.5%
	Capacity	3.7%	11.2%	0.8%	6.6%
Auxiliary Reactor	Current	1.7%	8.0%	-0.8%	4.2%
	Capacity	0.9%	8.1%	-2.3%	4.2%
Resistor	Voltage	0.6%	5.1%	-1.3%	2.5%
	Current	0.6%	5.1%	-1.3%	2.5%

As shown, both the filter's loading and performance indexes are not sensitive to the parameter variations. The reason is that the DHP filter has part of the high-pass filtering characteristics. This result demonstrates that the DHP filter is a robust filter topology that is suitable for HVDC applications.

5.8 Summary

This chapter presented a new filtering scheme for HVDC terminals. This filtering scheme uses the developed DHP filter as a characteristic harmonic filter which can damp the non-characteristics harmonic resonance. The contributions are summarized as follows.

- A novel filtering scheme based on the DHP filter idea was proposed for the LCC HVDC terminals. This scheme can result in savings in terms of cost of filter banks and space requirements.
- A design method was developed for the filter. The method considered two unique issues faced by the HVDC filter designs: the variable system impedance and flexible reactive power support. Both are very challenging design issues not solved in the past even for the design of traditional filters. Therefore, the proposed design concepts can be applied to other filtering schemes.
- The effectiveness of the proposed scheme was demonstrated by a real-life case study. The results revealed that the proposed design can provide a very good performance. A sensitivity assessment was also performed to verify the robustness of the DHP filter.

Chapter 6

Conclusions and Future Work

This chapter summarizes the findings of the thesis and provides suggestions for future work.

6.1 Thesis Conclusions and Contributions

This thesis attempts to clarify the issues and address the challenges involved in passive harmonic filtering. The main conclusions and contributions are summarized as follows.

- This thesis introduced an equivalent circuit model to define the harmonic filtering problem in industrial systems. Based on this circuit model, the filter design problem is simplified to focus on the relationship between the voltage and current at the PCC bus with those at the filter bus. The rest of the system can be replaced by their equivalent circuit. This approach provides a general tool for filter design in any complex network.

- A clarification was conducted to clear up the two issues about the single-tuned filter design. Firstly, a mathematical study was conducted to evaluate the Q factor impact on single-tuned filter performance. The results revealed that, within the normal manufacturing range, the Q factor selection is not helpful for the optimization the filter harmonic performance. As a result, a large Q factor should be preferred in filter design since it leads to a low filter loss. Secondly, a discussion was conducted on how to select the filter tuning frequency with the consideration of the parameter variations. A technically sound approach was proposed to compensate for the parameter variations. This approach can provide a guaranteed filtering performance without attracting too many unnecessary harmonics, which leads to a more economical design than the existing one.

- Three common high-pass filters were studied, which includes the 2nd HP filter, C-type filter and 3rd HP filter. This research mainly focused on two problems related to the high-pass filter application. The first one is to clarify the issues in the design of these high-pass filters. Improved design methods were proposed, and their effectiveness was verified through comparative case studies. The second one is to discuss the suitable applying conditions for these high-pass filters. Three conditions are evaluated, including the low-, medium- and high-frequency applications. The results provided valuable guidance for the selection of high-pass filters in the future.

- A new filtering scheme was proposed for multi-pulse industrial systems. It is based on a novel passive filter topology named the DHP filter, which does not cause resonance at the non-characteristic harmonics. As a result, the traditional non-characteristic 5th and 7th harmonic filters are no longer needed, resulting in cost and space savings. The core idea is a frequency-dependent damping block that can provide a high resistance at the non-characteristic harmonics of concern. The design method was developed for the proposed DHP filter, and its effectiveness was demonstrated through case studies. The DHP filter is also useful to solve the problems caused by interharmonics.

- The DHP filter was applied to provide an alternative filter arrangement for HVDC terminals since they are also susceptible to the problems caused by the non-characteristic harmonics. To accommodate for this application, the design of the DHP filter needs to face two challenges, i.e., the variation of the network impedance and switched reactive power compensation. A new design method was developed by considering these challenging issues, and its performance was verified through the study of a real-life HVDC project. A sensitivity study was also performed to verify the robustness of the DHP filter.

6.2 Suggestions for Future Work

As for the future work in this field, several extensions and modifications of this thesis can be explored as below:

- The main focus in Chapter 2 and 3 was to clarify the issues for the single passive filter design. As an extension of this work, future research can be conducted on how to properly design a filter package for a given system. For this research, significant efforts should be spent to provide a scientific method for the determination of the branch number, reactive power allocation and topology selection. This research would be very helpful to guide the filter design in practice.

- In this thesis, a new passive filter named DHP filter was proposed. The study can further focus on the issues associated with this filter application. For example, in some cases, it may require an oversize auxiliary capacitor for meeting the BIL requirements. The 1.2 kV capacitor unit is used to construct the auxiliary capacitor even though its actual operating voltage is below 1 kV (as discussed in Appendix F). A proper solution to this oversize problem can help further improve the economic advantage of the DHP filter.

- Another extension is to investigate the assembly of the DHP filter. The purpose is to build a compact and economical filter by properly arranging each filter component. One promising direction is to use a single two-coil coupling reactor to replace the two separate reactors for the DHP filter. To achieve this, the key is to find a proper way to control the mutual coupling between the two coils. There are already some studies discussing the mutual coupling reactor, and they could provide valuable references for this study.

- The primary objective of this work still focuses on the large centralized harmonic sources. As explained before, the dramatic proliferation of the power-electronic based home appliances is continuously increasing the harmonic distortions in residential systems. How to mitigate the harmonics caused by these massively distributed harmonic sources would be another trend for the harmonic filtering in the future.

References

[1] J. Arrillaga, D. A. Bradley, and P. S. Bodger, *Power System Harmonics*: John Wiley & Sons, 1985.

[2] V. E. Wagner, J. C. Balda, D. C. Griffith, A. McEachern, T. M. Barnes, D. P. Hartmann, et al., "Effects of harmonics on equipment," *IEEE Transactions on Power Delivery*, vol. 8, pp. 672-680, Apr. 1993.

[3] IEEE Task Force on Harmonics Modeling and Simulation, "Modeling and simulation of the propagation of harmonics in electric power networks, Part I: concepts, models, and simulation techniques", *IEEE Transactions on Power Delivery*, vol. 11, no. 1, pp. 452-465, Jan. 1996.

[4] E. F. Fuchs, D. J. Roesler, F. S. Alashhab, "Sensitivity of electrical appliances to harmonics and fractional harmonics of the power system voltage. Part I: transformers and induction machines", *IEEE Transactions on Power Delivery*, vol. 2, no. 2, pp. 437-444, Apr. 1987,

[5] E. F. Fuchs, D. J. Roesler, K. P. Kovacs, "Sensitivity of electrical appliances to harmonics and fractional harmonics of the power system voltage. Part II: television sets, induction watthour meters and universal machines", *IEEE Transactions on Power Delivery*, vol 2, no. 2, pp. 445-453, Apr. 1987.

[6] IEEE Working Group on Nonsinusoidal Situations: Effects on meter performance and definitions of power, "practical definitions for powers in systems with nonsinusoidal waveforms and unbalanced loads: a discussion", *IEEE Transactions on Power Delivery*, vol. 11, no. 1, pp. 79-101, Jan. 1996.

[7] G. C. Montanari and D. Fabiani, "The effect of nonsinusoidal voltage on intrinsic aging of cable and capacitor insulating materials," *IEEE Transactions on Dielectrics and Electrical Insulation*, vol. 6, pp. 798-802, Dec. 1999.

[8] IEEE Task Force on Harmonics Modeling and Simulation, "Modeling devices with nonlinear voltage-current characteristics for harmonic studies", *IEEE Transactions on Power Delivery*, vol. 19, no. 4, pp. 1802-1811, Oct. 2004.

[9] M. F. McGranaghan, and D. R. Mueller, "Designing harmonic filters for adjustable speed drives to comply with IEEE-519 harmonic limits," *IEEE Transactions on Industrial Applications*, vol. 35, no.2, pp. 312-318, Mar. 1999.

[10] M. Grotzbach, R. Redmann, "Line current harmonics of VSI-fed adjustable-speed drives", *IEEE Transactions on Industry Application*, vol. 36, no. 2, pp. 683-690, Mar.

2000.

[11] L. Hu, R.E. Morrison, "The use of modulation theory to calculate the harmonic distortion in HVDC system operating on an unbalanced supply", *IEEE Transactions on Power System*, vol. 12, no. 2, pp. 973-980, May 1997.

[12] A. Nassif, "Modeling, measurement and mitigation of power system harmonics," PhD thesis, Dept. Elect. Comput. Eng., Univ. Alberta, Edmonton, AB, Canada, 2009.

[13] Q. Shi, "Power quality impact of photovoltaic systems on residential distribution networks," M. Sc. dissertation, Dept. Elect. Comput. Eng., Univ. Alberta, Edmonton, AB, Canada, 2014.

[14] W. Xu, J. E. Drakos, Y. Mansour, and A. Chang, "A three-phase converter model for harmonic analysis of HVDC systems," *IEEE Transactions on Power Delivery*, vol. 9, no. 3, pp. 1724–1731, Jul. 1994.

[15] C. Liang, J. Zhu, L. Luo, Y. Li and Q. Qi et al., "Harmonic elimination using parallel delta-connected filtering windings for converter transformers in HVDC systems," *IEEE Transactions on Power Delivery*, vol. 32, no. 2, pp. 933–941, Apr. 2017.

[16] G. C. Montanari, M. Loggini, A. Cavallini, L. Pitti, D. Zanielli, "Arc furnace model for the study of flicker compensation in electrical networks", *IEEE Transactions on Power Delivery*, vol. 9, no. 4, pp. 2026-2036, Oct. 1994.

[17] M. Anxo Prieto el al. "An improved time domain arc furnace model for harmonic analysis". *IEEE Transactions on Power Delivery*, vol. 19, no. 1, pp. 367-373, Jan. 2004.

[18] M. Ermis, A. Acik, B. Gultekin and A. Terciyanli etc., "Power quality solutions for 12-pulse smelter converters in ETI aluminum works", *IEEE Transactions on Industry Application*, vol. 40, no. 6, pp. 1644-1655, Nov. 2004.

[19] R. Ellis, B. Guidry, "Power quality concerns/solutions on a 2500hp pipeline booster station adjustable frequency drive", *50th Annual Petroleum and Chemical Industry Conference*, 2003.

[20] V. Kazakbaev, V. Prakht, V. Dmitrievskii, "Interpolation error estimation of synchronous reluctance electric drive efficiency at various load points of booster heat pump profile", *AC Electric Drives 2018 International Ural Conference*, pp. 1-6, Apr. 2018.

[21] B. Turkay, "Harmonic filter design and power factor correction in a cement factory", *IEEE Porto Power Tech Conference*, Sep. 2001.

[22] R. K. Varma, S. A. Rahman, T. Vanderheide, M. Dang, "Harmonic impact of a 20-

mw PV solar farm on a utility distribution network", *IEEE Journal on Power and Energy Technology Systems*, vol. 3, no. 3, pp. 89-98, Apr. 2016.

[23] N. K. Roy, H. R. Pota, "Current status and issues of concern for the integration of distributed generation into electricity networks", *IEEE Journal on Systems*, vol. 9, no. 3, pp. 933-944, Feb. 2014.

[24] S. A. Papathanassiou, M. P. Papadopoulos, "Harmonic analysis in a power system with wind generation", *IEEE Transactions on Power Delivery*, vol. 21, no. 4, pp. 2006-2016, Oct. 2006.

[25] S. Liang, Q. Hu, W. Lee, "A survey of harmonic emissions of a commercially operated wind farm," *IEEE Transactions on Industrial Application*, vol. 48, no. 3, pp. 1115-1123, May. 2012

[26] R. I. Bojoi, L. R. Limongi, D. Roiu, A. Tenconi, "Enhanced Power Quality Control Strategy for Single-Phase Inverters in Distributed Generation Systems", *IEEE Transactions on Power Electronics*, vol. 26, no. 3, pp. 798-806, Mar. 2011.

[27] M. Prodanovic, K. De Brabandere and J. Van etc. "Harmonic and reactive power compensation as ancillary services in inverter-based distributed generation", *IET Generation Transmission & Distribution*, vol. 1, no. 3, pp. 432-438, May 2007.

[28] D. Salles, C. Jiang, W. Xu, W. Freitas, and H. E. Mazin, "Assessing the collective harmonic impact of modern residential loads -- Part I: Methodology," *IEEE Transactions on Power Delivery*, vol. 27, pp. 1937-1946, Oct. 2012.

[29] C. Jiang, D. Salles, W. Xu, and W. Freitas, "Assessing the collective harmonic impact of modern residential loads--Part II: Applications," *IEEE Transactions on Power Delivery*, vol. 27, pp. 1947-1955, Oct. 2012.

[30] A. Mau Teng and J. V. Milanovic, "Establishing harmonic distortion level of distribution network based on stochastic aggregate harmonic load models," *IEEE Transactions on Power Delivery*, vol. 22, no.2, pp. 1086-1092, Apr. 2007.

[31] A. Mansoor, W. M. Grady and P. T. Staats etc., "Predicting the net harmonic currents produced by large numbers of distributed single-phase computer loads," *IEEE Transactions on Power Delivery*, vol. 10, pp. 2001-2006, Oct. 1995.

[32] Q. Shi, H. Liang, T. Hou, L. Bai, W. Xu, and F. Li, "Passive filter installation for harmonic mitigation of residential distribution systems," *2017 IEEE Power Engineering Society General Meeting*, Chicago, pp. 1-5, Jul. 2017.

[33] T. Ding, H, Liang, W. Xu, “An Analytical Method for Probabilistic Modeling of the Steady-State Behavior of Secondary Residential System”, *IEEE Transactions on*

Power Delivery, vol. 8, no.6, pp. 2575-2584, Nov. 2017.

[34] IEEE Recommended Practices and Requirements for Harmonic Control in Electrical Power Systems, IEEE Std. 519-2014 (Revision of IEEE Std 519-1992), Jun. 2014.

[35] IEC/TR 61000-3-6, "Electromagnetic compatibility (EMC) – part 3-6: limits – assessment of emission limits for the connection of distorting installations to MV, HV and EHV power systems", IEC, Ed 2.0, 2008.

[36] J. C. Das, "Passive filters—Potentialities and limitations", *IEEE Transactions on Industry Application*, vol. 40, no. 1, pp. 232-241, Feb. 2004.

[37] B. Badrzadeh, K. S. Smith, and R. C. Wilson, "Designing passive harmonic filters for an aluminum smelting plant," *IEEE Transactions on Industry Applications*, vol. 47, no. 2, pp. 973–983, Apr. 2011.

[38] A. Dekka, A. R. Beig, S. Kanukollu and M. S. Al Rahis, "Retrofitting of harmonic power filters in onshore oil drilling rigs: challenges and solutions," *IEEE Transactions on Industry Applications*, vol. 50, no. 1, pp. 142-154, Jan.-Feb. 2014.

[39] G. W. Chang, H. L. Wang, S. Y. Chu, "A probabilistic approach for optimal passive harmonic filter planning", *IEEE Transactions on Power Delivery*, vol. 22, no. 3, pp. 1790-1798, Jul. 2007.

[40] G. W. Chang, H. L. Wang, G.S. Chuang, S.Y. Chu, "Passive harmonic filter planning in a power system with considering probabilistic constraints", *IEEE Transactions on Power Delivery*, vol. 24, no. 1, pp. 208-218, 2009.

[41] A. B. Nassif, W. Xu, W. Freitas, "An investigation on the selection of filter topologies for passive filter applications", *IEEE Transactions on Power Delivery*, vol. 24, no. 3, pp. 1710-1718, 2009.

[42] C. Su, C. Hong, "Design of passive harmonic filters to enhance power quality and energy efficiency in ship power systems", *IEEE Industrial Communication and Power System Technology Conference*, pp. 1-8, Apr. 2013.

[43] D. Pan, X. Ruan, X. Wang, H. Yu, Z. Xing, "Analysis and design of current control schemes for LCL-Type grid-connected inverter based on a general mathematical model", *IEEE Transactions on Power Electronics*, vol. 32, no. 6, pp. 4395-4410, Aug. 2017.

[44] J. Fang, X. Li, X. Yang, Y. Tang, "An integrated trap-LCL filter with reduced current harmonics for grid-connected converters under weak grid conditions", *IEEE Transactions on Power Electronics*, vol. 32, no. 11, pp. 8446-8457, Nov. 2017.

[45] H. Hu, Q. Shi, Z. He, J. He, S. Gao, "Potential harmonic resonance impacts of PV

inverter filters on distribution systems", *IEEE Transactions on Sustainable Energy*, vol. 6, no. 1, pp. 151-161, Jan. 2015.

[46] T. Ding, W. Xu, "A filtering scheme to reduce the penetration of harmonics into transmission systems", *IEEE Transactions on Power Delivery*, vol. 31, no. 1, pp. 59-66, Feb. 2016.

[47] H. Akagi, Y. Kanazawa, A. Nabae, "Instantaneous reactive power compensators comprising switching devices without energy storage components", *IEEE Transactions on Industrial Application*, vol. IA-20, no.3, pp. 625-630, May 1984.

[48] H. Akagi, A. Nabae, S. Atoh, "Control strategy of active power filters using multiple voltage-source PWM converters", *IEEE Transactions on Industrial Application*, vol. IA-22, no.3, pp. 460-465, Jun. 1986.

[49] F. Z. Peng, H. Akagi, A. Nabae, "A study of active power filters using quad-series voltage-source PWM converters for harmonic compensation", *IEEE Transactions on Power Electronics,* vol. 5, no.1, pp. 9-15, Jan. 1990.

[50] H. Akagi, "Trends in active power line conditioners", *IEEE Transactions on Power Electronics*, vol. 9, no.3, pp. 263-268, May 1994.

[51] B. Singh, K. Al-Haddad, A. Chandra, "A review of active filters for power quality improvement", *IEEE Transactions on Industrial Electronics*, vol. 46, no. 5, pp. 960-971, 1999.

[52] W. Lenwari, N. Okaeme, "A novel heuristic optimization algorithm for automated design of resonant compensators for shunt active filters", *Power Electronics IET*, vol. 6, no. 9, pp. 1842-1850, Nov. 2013.

[53] M. Badoni, A. Singh, B. Singh, "Adaptive recursive inverse-based control algorithm for shunt active power filter", *Power Electronics IET*, vol. 9, no. 5, pp. 1053-1064, Apr. 2016.

[54] H. Fujita, H. Akagi, "A practical approach to harmonic compensation in power systems-series connection of passive and active filters", *IEEE Transactions on Industrial Application*, vol. 27, no. 6, pp. 1020-1025, Nov/Dec. 1991.

[55] J. C. Salmon, "Reliable 3-phase PWM boost rectifiers employing a stacked dual boost converter subtopology", *IEEE Transactions on Industry Applications*, vol. 32, no. 3, pp. 542-551, May/Jun. 1996.

[56] C. S. Lam, W. H. Choi, M. C. Wong, Y. D. Han, "Adaptive dc-link voltage-controlled hybrid active power filters for reactive power compensation", *IEEE Transactions on Power Electronics,* vol. 27, no. 4, pp. 1758-1772, Apr. 2012.

[57] A. Bhattacharya, C. Chakraborty, S. Bhattacharya, "Parallel-connected shunt hybrid active power filters operating at different switching frequencies for improved performance", *IEEE Transactions on Industrial Electronics*, vol. 59, no. 11, pp. 4007-4019, Nov. 2012.

[58] T. L. Lee , Y. C. Wang, J. C. Li, and J. M. Guerrero, "Hybrid active filter with variable conductance for harmonic resonance suppression in industrial power systems," *IEEE Transactions on Industrial Electronics*, vol. 62, no. 2 , pp. 746–756, Feb. 2015.

[59] Haofeng Bai, Xiongfei Wang, Frede Blaabjerg, "A grid-voltage-sensorless resistive-active power filter with series LC-Filter", *IEEE Transactions on Power Electronics*, vol. 33, no. 5, pp. 4429-4440, May 2018.

[60] IEEE Guide for Application and Specification of Harmonic Filters, IEEE Standard 1531-2003, Nov. 2003.

[61] W. Xu, T. Tayjasanant, G. Zhang and R. Bahry, "Mitigation of interharmonics using a switched filter scheme," *Eur. Trans. Electr. Power*, vol. 20, no. 1, pp. 83–95, Jan. 2010.

[62] IEEE Task Force on Harmonics Modeling and Simulation., "Test systems for harmonics modeling and simulation", *IEEE Transactions on Power Delivery*, vol. 14, no. 2, pp. 579-585, Apr. 1999.

[63] H. W. Wahlquist, "Power System and Shunt for reducing harmonic therein," US Patent 2,241,831, May 13, 1941.

[64] E. W. Kimbark, Direct Current Transmission, USA: John Wiley & Sons, Inc., 1971.

[65] D.J. Melvold, "Pacific HVDC/Intertie System, AC Side Harmonics Studies," *IEEE Transactions on Power Apparatus and Systems*, vol. PAS-92, no. 2, pp. 690-701, March/April 1973.

[66] Vithayathil, "Experience with harmonic problems at Celilo HVDC Station," *IEE Conf. on high voltage DC and/or AC power transmission*, no.107, pp. 6-10, 1973.

[67] CIGRE WG 14.03, "AC Harmonic Filter and Reactive Compensation for HVDC, A General Survey, Electra No. 63, pp 65-102, 1979.

[68] D. E. Steeper, R. P. Stratford, "Reactive Compensation and Harmonic Suppression for Industrial Power Systems Using Thyristor Converters", *IEEE Transactions on Industry Applications*, vol. IA-12, no. 3, pp. 232-254, 1976.

[69] D. A. Gonzalez, J. C. McCall, "Design of filters to reduce harmonic distortion in industrial power systems", *IEEE Transactions on Industry Applications*, vol. IA-23,

no. 3, pp. 504-511, May/June 1987.

[70] J. C. Das, "Shunt capacitor filters for motor starting load voltage and harmonic distortion control", *Conf. Rec. 1991 IEEE Ind. Appl. Soc. Pulp and Paper industry conf.,* Jun. 1991.

[71] J.C. Das, Power System Analysis: Short-circuit Load flow and Harmonics: Boca Raton, CRC Press, 2012.

[72] H. W. Wahlquist, "Power System and Shunt for reducing harmonic therein," US Patent 2,241,831, May 13, 1941.

[73] Ainsworth, J.D., 1965, Filters, damping circuits, and reactive volt-amps in HVDC converters, in High Voltage Direct Converters and Systems, Cory, B.J., Ed., Macdonald, London, pp. 137–174.

[74] C. H. Stanley, J. J. Price and G. L. Brewer, "Design and performance of ac filters for 12-pulse HVDC schemes, " *IEE Conf. Publ.*, vol.154, pp.1558-161, 1977.

[75] M. A. Zamani et al., “C-type filter design based on power-factor correction for 12-pulse HVDC converters,” *in Proc. IEEE 34th Annu. Conf. Ind. Electron.*, pp. 3039–3044 Nov. 2008.

[76] H. Hu, Z. He, and S. Gao, “Passive filter design for china high-speed railway with considering harmonic resonance and characteristic harmonics,” *IEEE Transactions on Power Delivery*, vol. 30, no. 1, pp. 505–514, Feb. 2015.

[77] W. Xu, T. Ding, X. Li and H. Liang, "Resonance-free shunt capacitors—configurations, design methods and comparative analysis," *IEEE Transactions on Power Delivery*, vol. 31, no. 5, pp. 2287-2295, Oct. 2016.

[78] Y. Wang and W. Xu, ``A shared resonance damping scheme for multiple switchable capacitors," *IEEE Transactions on Power Delivery*, vol. 33, no. 4, pp. 1973_1980, Aug. 2018.

[79] J.C. Das, “Design and Application of a Second-Order High-Pass Damped Filter for 8000-hp ID Fan Drives—A Case Study,” *IEEE Transaction on Industry Applications*, Vol. 51, No. 2, pp. 1417-1426, Mar./Apr. 2015.

[80] C. J. Wu, J. C. Chiang, S. S. Yen, C. J. Liao, J. S. Yang, and T. Y. Guo, “Investigation and mitigation of harmonic amplification problems caused by single-tunes filters,” *IEEE Transactions on Power Delivery*, vol. 13, no. 3, pp. 800–806, Jul. 1998.

[81] L. Morán, C. A. Albistur, R. Burgos, "Multimega var passive filters for mining applications: Practical limitations and technical considerations", *IEEE Transaction on Industry Applications*, vol. 52, no. 6, pp. 5310-5317, Nov./Dec. 2016.

[82] Wakileh, G. J., Power Systems Harmonics, Fundamentals, Analysis and Filter Design, 2001, Springer.

[83] Y. Xiao, J. Zhao and S. Mao, "Theory for the design of C-type filter," *2004 11th International Conference on Harmonics and Quality of Power*, pp. 11-15, 2004

[84] R. Klempka, A. Górniczo-Hutnicza and W. Elektrotechniki, etc. “A New Method for the C-Type Passive Filter Design”. *Przeglad Elektrotechniczny*, vol. 88, no. 7 A, pp. 277-281, 2012.

[85] S. H. E. Abdel Aleem, A. F. Zobaa, M. Mamdouh Abdel Aziz, "Optimal C-type passive filter based on minimization of the voltage harmonic distortion for nonlinear loads", *IEEE Transactions on Industrial Electronics*, vol. 59, no. 1, pp. 281-289, Jan. 2012.

[86] C. Stéphane, A. Mboving, Z. Hanzelka, “Application of C-type Filter to DC Adjustable Speed Drive” *2015 Modern Electric Power Systems (MEPS)*, Jul. 2015.

[87] A. Lamlom, A. Ibrahim and M. E. Balci etc. “Optimal design and analysis of anti-resonance C-type high-pass filters,” *2017 EEEIC / I&CPS Europe*, Jun. 2017.

[88] T, Ding, W. Xu, and H. Liang "Design method for 3rd order high-pass filter," *IEEE Transactions on Power Delivery*, vol. 31, no. 1, pp. 402-403, Jul. 2015.

[89] S.H.E. Abdel, A.F. Zobaa, M.E. Balci, "Optimal resonance-free third-order high-pass filters based on minimization of the total cost of the filters using Crow Search Algorithm", *Electr Pow Syst Res*, vol. 151, pp. 381-394, 2017.

[90] B. Wu, High-Power Converters and AC Drives. Wiley-IEEE Press, 2006.

[91] B. Singh, S. Gairola, B. N. Singh, A. Chandra and K. Al-Haddad, "Multipulse ac–dc converters for improving power quality: a review, " *IEEE Transactions on Power Electronics*, vol. 23, no. 1, pp. 260–281, Jan. 2008.

[92] IEEE Guide for Harmonic Control and Reactive Compensation of Static Power Converters, IEEE Standard 519. 1981.

[93] Wakileh, G. J., Power Systems Harmonics, Fundamentals, Analysis and Filter Design, 2001, Springer.

[94] X. Liang , O. Ilocbonwu. "Passive harmonic filter design scheme for subsea cable applications with six-pulse variable frequency drives, " *IEEE energy conversion congress and exposition*, pp. 597–603, 2009.

[95] X. Li, W. Xu, "A novel filter to mitigate interharmonic problems caused by variable frequency drives," *2017 IEEE International Conference on Power Electronics and Drive System*, pp. 887-892, Dec. 2017.

[96] G. Chang, S. Chen, "An analytical approach for characterizing harmonic and interharmonic currents generated by VSI-fed adjustable speed drives", *IEEE Transactions on Power Delivery*, vol. 20, no. 4, pp. 2585-2593, Oct. 2005.

[97] G. Chang, S. Chen, H. Su, P. Wang, "Accurate assessment of harmonic and interharmonic currents generated by VSI-fed drives under unbalanced supply voltages", *IEEE Transactions on Power Delivery*, vol. 26, no. 2, pp. 1083-1091, Apr. 2011.

[98] L. Tang, D. Mueller, D. Hall, M. Samotyj, J. Randolph. "Analysis of DC Arc Furnace Operation and Flicker Caused by 187Hz Voltage Distortion, " *IEEE Transactions on Power Delivery*. vol. 9, no. 2, pp:1098-1107, Apr. 1994.

[99] Rolf J. Flen, Stuart L.Haug, "Endpoint Transmitter and Power Generation System," U.S. Patent 7,102,490 B2, Sep. 5, 2006.

[100] W. Xu, J. E. Drakos, Y. Mansour, and A. Chang, "A three-phase converter model for harmonic analysis of HVDC systems," *IEEE Transactions on Power Delivery*, vol. 9, no. 3, pp. 1724–1731, Jul. 1994.

[101] F. Marvasti, A. Mirzaei, "A Novel Method of Combined DC and Harmonic Overcurrent Protection for Rectifier Converters of Monopolar HVDC Systems" *IEEE Transactions on Power Delivery*, vol. 33, no. 2, pp. 892–900, Apr. 2018.

[102] CIGRÉ WG 14.03, "AC harmonic filters and reactive compensation for HVDC with particular reference to non-characteristic harmonics." Jun. 1990.

[103] N. Kaul and R.M. Mathur, "Solution to the Problem of Low Order Harmonic Resonance from HVDC Converters", *IEEE Transactions on Power Delivery*, vol. 5, no. 4, pp 1160-1167, Nov. 1990.

[104] P. S. Wright, A. Bergman, A. P. Elg, M. Flood, P. Clarkson, K. Hertzberg, "Onsite measurements for power-quality estimation at the Sweden-Poland HVDC Link", *IEEE Transactions on Power Delivery*, vol. 29, no. 1, pp. 472-479, Feb. 2014.

[105] CIGRÉ WG 14.03, "Guide to the Specification and Design Evaluation of AC Filters for HVDC Systems." Apr. 1999.

[106] Electric Power Research Institute, "HVDC-AC System Interaction from AC Harmonics Volume 1: Harmonic Impedance Calculations." Sep. 1982.

Appendix A
Equivalent Circuit Model for Filter Design

The intention of this section is to provide a further explanation of the equivalent circuit model introduced in Section 2.1. To illustrate this, the harmonic power flow based approach for filter design is introduced first. Then, the simplified equivalent circuit model is developed, including the details about how to construct the circuit and how to use it for filter design.

A.1 Harmonic Power Flow based Approach for Filter Design

The harmonic flow throughout an industrial system with various harmonic loads is normally analyzed by nodal analysis. As explained in Section 2.1.1, the harmonic loads can either be modeled as harmonic current sources (CSC-type harmonic loads) or harmonic voltage sources (VSC-type harmonic loads). For modelling these harmonic loads, the load flow study should be performed first to determine the system operating condition. The harmonic source model can then be established based on the load flow results and harmonic spectrum.

For each harmonic frequency, the nodal voltage equation can be derived as shown in (A.1).

$$\begin{bmatrix} I_s(\omega_h) \\ I_f(\omega_h) \\ . \\ . \\ I_{c1}(\omega_h) \\ . \\ . \\ I_{cn}(\omega_h) \\ I_{v1}(\omega_h) \\ . \\ . \\ I_{vm}(\omega_h) \end{bmatrix} = \begin{bmatrix} Y_{s,s}(\omega_h) & Y_{s,f}(\omega_h) & . & Y_{s,cn}(\omega_h) & . & Y_{s,vm}(\omega_h) \\ Y_{f,s}(\omega_h) & Y_{f,f}(\omega_h) & . & Y_{f,cn}(\omega_h) & . & Y_{f,vm}(\omega_h) \\ . & . & . & . & . & . \\ . & . & . & . & . & . \\ Y_{c1,s}(\omega_h) & Y_{c1,f}(\omega_h) & . & Y_{c1,cn}(\omega_h) & . & Y_{c1,vm}(\omega_h) \\ . & . & . & . & . & . \\ . & . & . & . & . & . \\ Y_{cn,s}(\omega_h) & Y_{cn,f}(\omega_h) & . & Y_{cn,cn}(\omega_h) & . & Y_{cn,vm}(\omega_h) \\ Y_{v1,s}(\omega_h) & Y_{v1,f}(\omega_h) & . & Y_{v1,cn}(\omega_h) & . & Y_{v1,vm}(\omega_h) \\ . & . & . & . & . & . \\ . & . & . & . & . & . \\ Y_{vm,s}(\omega_h) & Y_{vm,f}(\omega_h) & . & Y_{vm,cn}(\omega_h) & . & Y_{vm,vm}(\omega_h) \end{bmatrix} \begin{bmatrix} V_s(\omega_h) \\ V_f(\omega_h) \\ . \\ . \\ V_{c1}(\omega_h) \\ . \\ . \\ V_{cn}(\omega_h) \\ V_{v1}(\omega_h) \\ . \\ . \\ V_{vm}(\omega_h) \end{bmatrix} \quad \text{(A.1)}$$

where *s* represents the PCC bus, *f* represents the bus for filter connection, *c1*, …, *cn* are the buses with CSC-type harmonic loads, and *v1*, …, *vm* are the buses with VSC-type harmonic loads.

In the above equation, the Y matrix can be obtained through the network configuration. The currents of buses with CSC-type harmonic load are determined by the harmonic current sources, the voltages of buses with VSC-type harmonic load are determined by the harmonic voltage sources. The bus currents are zero for all the other buses without harmonic loads, including the PCC bus and filter bus.

The PCC bus voltage can be obtained by solving Equation (A.1). Then, the harmonic current entering the system can be computed by the following equation. In this equation, the first term represents the effects of harmonic current sources, and the second term represents the effects of harmonic voltage sources.

$$I_s(\omega_h) = \frac{1}{Z_s(\omega_h)}[\sum_{k=c1}^{cn} Z_{s,k}(\omega_h) I_k(\omega_h) + \sum_{i=s}^{cn} Z'_{s,i}(\omega_h) \sum_{j=v1}^{vm} Y_{i,j}(\omega_h) V_j(\omega_h)] \quad \text{(A.2)}$$

where $Z_s(\omega_h)$ is the supply system impedance, $Z_{i,j}(\omega_h)$ is the transfer impedance from bus *i* to *j*, $Z'_{i,j}(\omega_h)$ is the transfer impedance obtained from the partitioned Z matrix excluding the buses with harmonic voltage sources.

The filter installation will change the impedance and admittance values in (A.2), resulting in a reduced harmonic current. However, although the filter only modifies the self-admittance of its own bus, the inverse of the Y matrix makes it affect the self- and transfer- impedance at all the buses. It is therefore hard to obtain an analytical model for filter design based on the harmonic power flow study. As a result, the filter parameters need to be first pre-determined and substituted into the Y matrix for computing the self- and transfer- impedance at each bus. Then, the harmonic currents entering the system can be evaluated through Equation (A.2). The filter parameters need to be adjusted accordingly until the harmonic filtering requirements are met.

The above analysis reveals that the harmonic power flow based approach needs a trial-and-error process to complete the filter design. This fact not only complicates the design process but also make it difficult to obtain an analytical design model. Thus, it is still preferred to have a better alternative approach for filter design.

A.2 Equivalent Circuit Model based Approach for Filter Design

An equivalent circuit model has been developed in Section 2.1.2 Compared to the harmonic power flow based approach, this circuit model provides a genetic tool to design filters analytically in any complex network. This section describes how to obtain the parameters of the circuit model. For the purpose of explanation, the circuit model is re-drawn in Figure A.1.

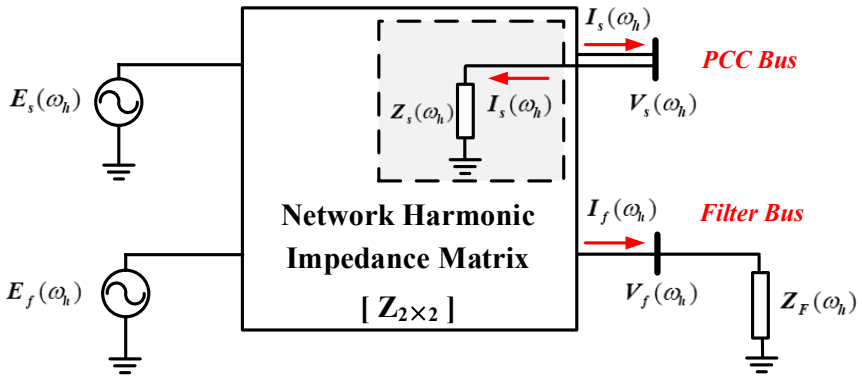

Figure A.1 Simplified equivalent circuit model

The above circuit model can be expressed by the following equations.

$$\begin{bmatrix} V_s(\omega_h) \\ V_f(\omega_h) \end{bmatrix} = \begin{bmatrix} E_s(\omega_h) \\ E_f(\omega_h) \end{bmatrix} - \begin{bmatrix} Z_{ss}(\omega_h) & Z_{sf}(\omega_h) \\ Z_{fs}(\omega_h) & Z_{ff}(\omega_h) \end{bmatrix} \begin{bmatrix} I_s(\omega_h) \\ I_f(\omega_h) \end{bmatrix} \tag{A.3}$$

$$I_f(\omega_h) = \frac{V_f(\omega_h)}{Z_F(\omega_h)}. \tag{A.4}$$

To construct this circuit, $Z_{ss}(\omega_h)$, $Z_{sf}(\omega_h)$, $Z_{fs}(\omega_h)$ and $Z_{ff}(\omega_h)$ can be obtained by using frequency scan analysis. To get $Z_{ss}(\omega_h)$ and $Z_{fs}(\omega_h)$, 1pu harmonic current is injected at terminal *s*, and then the resulting voltage values at terminal *s* and *f* are equal to $Z_{ss}(\omega_h)$ and $Z_{fs}(\omega_h)$ respectively. Similarly, we can repeat the above process

at terminal f to obtain $Z_{ff}(\omega_h)$ and $Z_{sf}(\omega_h)$.

The equivalent harmonic sources $E_s(\omega_h)$ and $E_f(\omega_h)$ can be determined using the harmonic power flow study per the following steps: (1) obtain the bus voltages with the harmonic loads by using load flow study, (2) establish the harmonic source models based on the load flow results and harmonic spectrum, and (3) use nodal analysis to solve the equivalent voltages at the two buses.

The above parameters are not affected by the filter design. They represent the system equivalent circuit before filter connection. Therefore, there is no need to update these parameters in the filter design process. This feature allows the equivalent circuit model based approach to design the filter in an analytical way, which simplifies the filter analysis in industrial systems. The relationship between the filter and the PCC bus can be easily obtained based on (A.3) and (A.4).

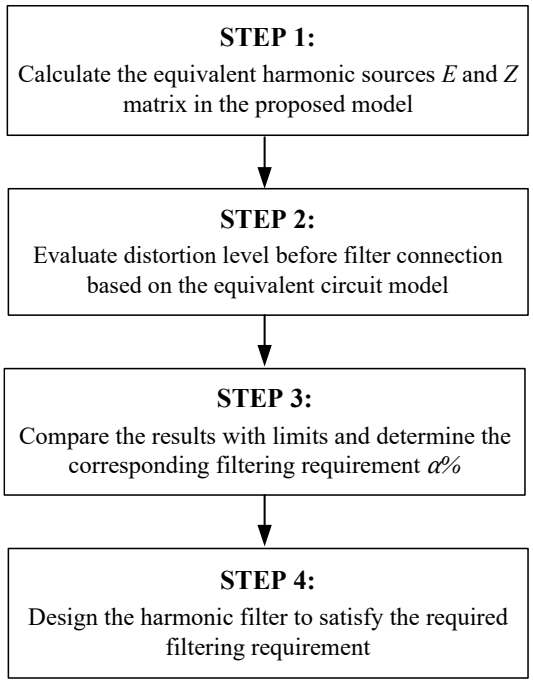

Figure A.2 Flow chart for harmonic filter design

Figure A.2 provides a flow-chart explaining how to use the circuit model for filter design. The first step is to calculate the harmonic sources and Z matrix based on the above methods. Then, the distortion level at the PCC bus is evaluated before

filter connection. The third step computes the harmonic filtering requirements based on the method explained in Section 2.1.4. In the final step, the filter is designed to achieve the required filtering performance.

Appendix B
Data about the study system for filter design

A study system has been introduced in Section 2.2 for verifying the proposed design methods. It is based on the IEEE 13-bus industrial system. The data for this study is summarized as follows:

- system impedance: the supply system equivalent impedance is 0.0015+j0.045 per unit which is based on 10,000 kvar.
- local generator impedance: the local generator has an internal impedance of X=0.03 per-unit based on the generator rated kVA which is 2,000 kVA.

Table B.1 and

Table B.2 list the impedance data of the transformer and the line. The base capacity and voltage are selected as 10,000 kVA and 13.8 kV for this study.

Table B.1 Transformer data for the study system

From	To	Voltage	kVA	R (%)	X (%)
69-1	MILL-1	69:13.8	15000	0.4698	7.9862
GEN1	AUX	13.8:0.48	1500	0.9593	5.6694
FDR F	RECT	13.8:0.48	3000	0.7398	4.4388
FDR F	T3 SEC	13.8:4.16	1725	0.7442	5.9537
FDR G	T11 SEC	13.8:0.48	1500	0.8743	5.6831
FDR H	T4 SEC	13.8:0.48	1500	0.8363	5.4360
FDR H	T7 SEC	13.8:2.4	7000	0.4568	5.4810

Table B.2 Line and cable impedance data

From	To	R	X
UTIL-69	69-1	0.00139	0.00296
MILL-1	GEN-1	0.00122	0.00243
MILL-1	FDR F	0.00075	0.00063
MILL-1	FDR G	0.00157	0.00131
MILL-1	FDR H	0.00109	0.00091

Accordingly, the load flow analysis has been conducted to calculate the voltage profile at each bus, as shown in Table B.3.

Table B.3 Load flow study results

Bus	Vmag (p.u.)	θ(deg)	Pload (kW)	Qload (kvar)
UTIL-69	1.000	0.000	----	----
69-1	0.998	-0.157	----	----
MILL-1	0.993	-3.090	----	----
GEN1	0.995	-3.123	----	----
Aux	0.970	-4.268	600	530
FDR F	0.993	-3.092		
RECT	0.931	-7.740	2300	1150
T3 SEC	0.944	-5.559	1310	1130
FDR G	0.993	-3.089	----	----
T11 SEC	0.956	-4.660	810	800
T4 SEC	0.978	-3.782	370	330
FDR H	0.992	-3.098	----	----
T7 SEC	0.933	-8.308	6000	3000

The following simplifications are also required to model the system at harmonic frequencies:

- all the loads are modelled as a series *RL* circuit excepting for the harmonic-producing ones.
- the harmonic-producing loads are viewed as a pure harmonic current source, and their spectrums are adjusted for different applications.
- the transformer magnetizing branch are neglected so that each transformer can also be modelled as a series *RL* circuit.
- the analysis assumes that all the resistances are independent on the frequency, i.e. ignoring the frequency dependent characteristics of resistance.

Appendix C

Impact of *Q* factor on single-tuned filter performance

This section discusses the relationship between the *Q* factor and the performance of the single-tuned filter. The intension is to answer two questions: 1). whether a small *Q* factor (i.e. a large filter resistance) can lead to a large $Y_{total}(\omega_h)$, 2). If so, how much improvement can be achieved by the selection of the *Q* factor.

As explained in Section 2.3.2, the total admittance $Y_{total}(\omega_h)$ between the filter and system can be used to assess the *Q* factor impact; i.e., a large $Y_{total}(\omega_h)$ implies a good filtering performance. To facilitate the analysis, the total admittance $Y_{total}(\omega_h)$ in (2.19) is re-written below.

$$Y_{total}(\omega_{\mathrm{h}}) = \frac{Z_s(\omega_{\mathrm{h}}) + Z_f(\omega_{\mathrm{h}})}{Z_s(\omega_{\mathrm{h}}) Z_f(\omega_{\mathrm{h}})} \tag{C.1}$$

According to (C.1), the absolute value of the total admittance $Y_{total}(\omega_h)$ can be derived as:

$$\left|Y_{total}(\omega_{\mathrm{h}})\right|^2 = \left(G_f^2 + B_f^2\right) + \frac{2R_s(\omega_h)\left(G_f - B_f k_s\right)}{R_s^2(\omega_h) + X_s^2(\omega_h)} + \frac{1}{R_s^2(\omega_h) + X_s^2(\omega_h)} \tag{C.2}$$

where

$$G_f = \frac{R_f(\omega_h)}{R_f^2(\omega_h) + X_f^2(\omega_h)}, \quad B_f = -\frac{X_f(\omega_h)}{R_f^2(\omega_h) + X_f^2(\omega_h)}, \quad k_s = \frac{X_s(\omega_h)}{R_s(\omega_h)}.$$

It is worthwhile to mention that the impact of *Q* factor can be quantified by the filter resistance $R_f(\omega_h)$, i.e. a small *Q* factor corresponds to a large $R_f(\omega_h)$. As shown in (B.2), $R_f(\omega_h)$ only exists in the first two terms including G_f and B_f. The first term can be expanded in (C.3). It is clear that the first term decreases with the increase of $R_f(\omega_h)$, i.e. the maximum value happens when $R_f(\omega_h)$=0. Thus, the selection of the *Q* factor cannot reduce the first term.

$$G_f^2 + B_f^2 = \frac{R_f^2(\omega_h)}{[R_f^2(\omega_h) + X_f^2(\omega_h)]^2} + \frac{X_f^2(\omega_h)}{[R_f^2(\omega_h) + X_f^2(\omega_h)]^2} = \frac{1}{R_f^2(\omega_h) + X_f^2(\omega_h)} \quad \text{(C.3)}$$

Similarly, the second term can also be derived as below:

$$G_f - B_f k_s = \frac{R_f(\omega_h)}{R_f^2(\omega_h) + X_f^2(\omega_h)} + \frac{X_f(\omega_h)k_s}{R_f^2(\omega_h) + X_f^2(\omega_h)} = \frac{R_f(\omega_h) + X_f(\omega_h)k_s}{R_f^2(\omega_h) + X_f^2(\omega_h)} \quad \text{(C.4)}$$

The impact of $R_f(\omega_h)$ can be analyzed by differentiating the above equation, as illustrated in (C.5).

$$\frac{d\left(G_f - B_f k_s\right)}{dR_f} = -\frac{(R_f(\omega_h) + k_s X_f(\omega_h))^2 - (k_s^2 + 1)X_f^2(\omega_h)}{[R_f^2(\omega_h) + X_f^2(\omega_h)]^2} \quad \text{(C.5)}$$

Accordingly, the condition that a large $R_f(\omega_h)$ helps increase $Y_{total}(\omega_h)$ can be obtained as:

$$\frac{X_f(\omega_h)}{R_f(\omega_h)} > \frac{1}{\sqrt{k_s^2 + 1} - k_s} = \sqrt{k_s^2 + 1} + k_s \approx 2k_s \quad \text{(C.6)}$$

Since $X_f(\omega_h)/R_f(\omega_h)=2\,\delta Q$ and $k_s=X_s(\omega_h)/R_s(\omega_h)$, the above condition can be further specified as:

$$\delta Q > \frac{X_s(\omega_h)}{R_s(\omega_h)} \quad \text{(C.7)}$$

As explained in Section 2.3.2, the above condition is hard to satisfy in practice, i.e. a large $R_f(\omega_h)$ or a small Q factor normally deteriorates the filter performance instead of improving it. In other words, the best filtering performance occurs when the reactor has no resistance. If assuming (C.7) is satisfied in some special cases, a further assessment is conducted to evaluate the performance improvement achieved by selecting the Q factor. The following equation is used to quantify such effect, where $Y_{total}(\omega_h)$ is the total admittance with $R_f(\omega_h)$, and $Y'_{total}(\omega_h)$ is the total admittance without $R_f(\omega_h)$.

$$\text{KY}=\left|\frac{Y'_{\text{total}}(\omega_{\text{h}})}{Y_{\text{total}}(\omega_{\text{h}})}\right| = \left|1 + Me^{-j\beta}\right| \quad \text{(C.8)}$$

where

$$M = \frac{R_f(\omega_h)}{X_f(\omega_h)} \times \frac{\sqrt{R_s^2(\omega_h) + X_s^2(\omega_h)}}{\sqrt{(X_s(\omega_h) + X_f(\omega_h))^2 + (R_f(\omega_h) + R_s(\omega_h))^2}} \tag{C.9}$$

$$-\beta = -[\frac{\pi}{2} + a\tan(\frac{X_s(\omega_h) + X_f(\omega_h)}{R_s(\omega_h) + R_f(\omega_h)}) - a\tan(\frac{X_s(\omega_h)}{R_s(\omega_h)})] \ . \tag{C.10}$$

In this equation, KY<1 indicates that the selection of the Q factor improves the harmonic filtering performance. As an example, KY=0.8 indicates that the Q factor selection can achieve a 20% performance improvement. Therefore, this analysis is interested in the minimum KY value. Figure C.1 presents the vector diagram of the admittance ratio KY.

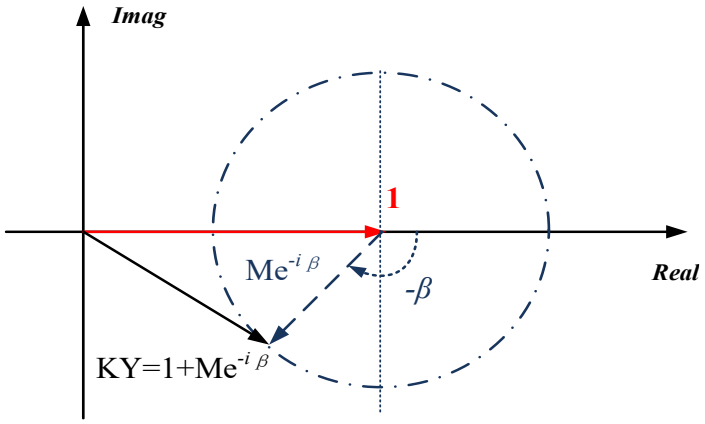

Figure C.1 Vector diagram of the admittance ratio KY

In power systems, the system impedance is dominated by the transformer and line impedances and therefore are usually inductive, i.e. $X_f(\omega_h) \geq 0$. Under this condition, one can simplify (C.9) and (C.10) as below:

$$M = \frac{R_f(\omega_h)}{X_f(\omega_h)} \times \frac{\sqrt{R_s^2(\omega_h) + X_s^2(\omega_h)}}{\sqrt{(X_s(\omega_h) + X_f(\omega_h))^2 + (R_f(\omega_h) + R_s(\omega_h))^2}} < \frac{R_f(\omega_h)}{X_f(\omega_h)} \tag{C.11}$$

$$-\beta > -[\frac{\pi}{2} + a\tan(\frac{X_f(\omega_h)}{R_f(\omega_h)}) - a\tan(\frac{X_s(\omega_h)}{R_s(\omega_h)})] \tag{C.12}$$

The angle $-\beta$ falls into the range from $-\pi$ to $-\pi/2$. Therefore, the vector $Me^{-j\beta}$ is in the third quadrant, as shown in Figure C.1. Under this condition, a large M or a small $-\beta$ will lead to a small KY value. For a conservative assessment, (C.13) can be used to approximately evaluate the minimum KY value:

$$\mathrm{KY}_{\min} = \left| 1 + \frac{R_f(\omega_h)}{X_f(\omega_h)} e^{-j[\frac{\pi}{2} + a\tan(\frac{X_f(\omega_h)}{R_f(\omega_h)}) - a\tan(\frac{X_s(\omega_h)}{R_s(\omega_h)})]} \right| \qquad \text{(C.13)}$$

Based on the above equation, the minimum KY value is analyzed, the results are shown in Figure C.2. In this figure, K_{fs} is defined in (C.14) as the impedance ratio between $X_f(\omega_h)/R_f(\omega_h)$ and $X_f(\omega_h)/R_f(\omega_h)$. Note that a small K_{fs} indicates a large $R_f(\omega_h)$.

$$K_{fs} = \frac{X_f(\omega_h)}{R_f(\omega_h)} \times \frac{R_s(\omega_h)}{X_s(\omega_h)} \qquad (K_{fs} \geq 2 \text{ to satisfy (C.7)}) \qquad \text{(C.14)}$$

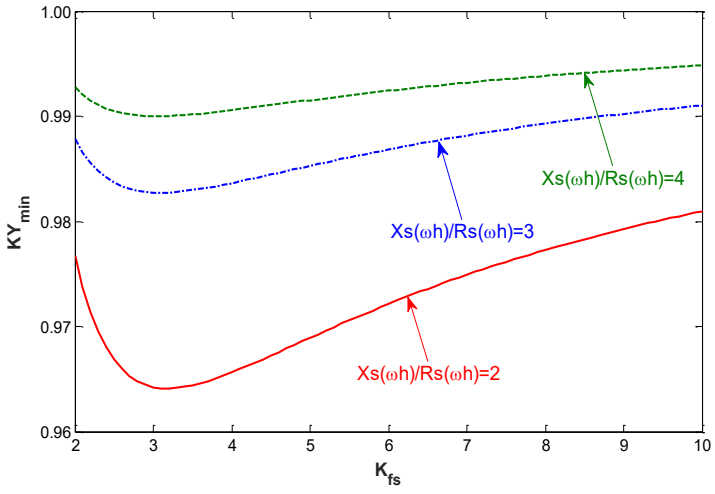

Figure C.2 Relationship between $\mathrm{KY}_{\min}$ and K_{fs}

The above results show that the performance improvement by selecting the Q factor is only about 2%~4%. Such a minor improvement is ignorable in practice. It is known that a small Q factor increases the filter operating loss. It is therefore preferred to choose a large Q factor for the single-tuned filter within the manufacturing range.

Appendix D

Analysis of Relation between $\Delta Z_F(ht)$ and Δht

The study in Section 2.3.3 uses the tuning frequency variation Δh_t to compensate for the parameter variation since it is much easier to be normalized. However, it is based on the assumption that the two variables have a linear relationship. This study uses a numerical method to justify this assumption.

For a given set of $\Delta\omega_1$, ΔL and ΔC, one can obtain $\Delta Z_F(h_t)$ and Δh_t based on the (D.1) and (D.2) respectively. In this way, a number set of $\Delta\omega_1$, ΔL and ΔC can be used to calculate their corresponding $\Delta Z_F(h_t)$ and Δh_t.

$$\Delta Z_F(h_t) = \sqrt{\frac{(1+\Delta\omega_1)^4 M^2\beta^4 + Q^2[(1+\Delta\omega_1)^2 M\beta^2 - 1]^2}{(1+\Delta\omega_1)^2(1+\Delta C)^2[\beta^4 + Q^2(\beta^2-1)^2]}} - 1 \qquad \text{(D.1)}$$

$$\Delta h_t = \frac{1}{(1+\Delta\omega_1)\sqrt{(1+\Delta L)(1+\Delta C)}} - 1 \qquad \text{(D.2)}$$

where $\beta = h_t / h$, $M = (1+\Delta L)(1+\Delta C)$.

Figure D.1 shows the numerical study results. Note that the different h_t/h values are studied since $\Delta Z_F(h_t)$ is also a function of $h_t(\beta=h_t/h)$. The following conclusions can be obtained:

- $\Delta Z_F(h_t)$ has a variation range from -0.5 to 1.5 due to the parameter variation, and the result indicates that the filter harmonic performance is quite sensitive to parameter variations.
- $\Delta Z_F(h_t)$ varies with the different h_t/h values. This fact makes it hard to be normalized. In contrast, Δh_t has a normalized range since it is independent of filter parameters.
- it can be noticed that $\Delta Z_F(h_t)$ and Δh_t share a nearly linear relation. Thus, it is reasonable to use Δh_t to compensate for $\Delta Z_F(h_t)$.

- the relation between $\Delta Z_F(h_t)$ and Δh_t will become more linear for a larger h_t/h ratio, which is the common case for the single-tuned filters.

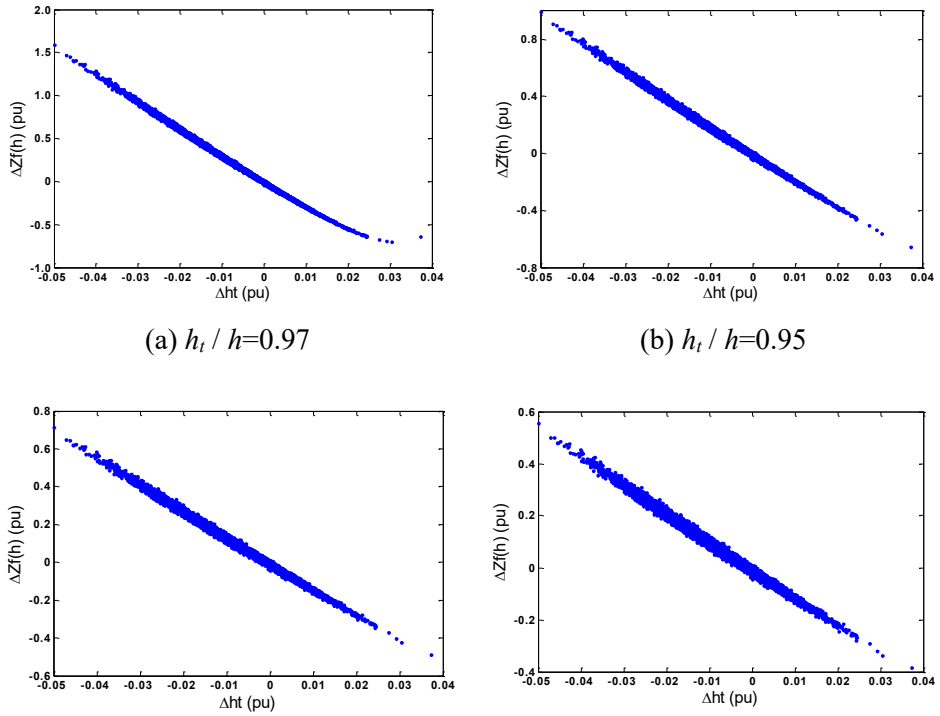

(a) h_t / h=0.97 (b) h_t / h=0.95

(c) h_t / h=0.93 (d) h_t / h=0.91

Figure D.1 Numerical results about the relation between $\Delta Z_F(h_t)$ and Δh_t

In summary, the single-tuned filter is quite sensitive to the impact of parameter variations. Since Δh_t and $\Delta Z_F(h_t)$ share a linear relation, it is reasonable to use Δh_t to compensate for the parameter variation.

Appendix E
Economic Analysis for Passive Filters

This section provides a general process to calculate the filter cost. This process is used to conduct the economic analysis of the common passive filters in Chapter 2 and Chapter 3.

E.1 Component Cost Analysis

- **Capacitor Costs**

The filter capacitor bank is commonly assembled by a number of basic capacitor units. Table E.1 illustrates the basic capacitor units and their corresponding Basic Insulation Levels (BILs).

Table E.1 Basic capacitor unit and their insulation level

Voltage Ratings	Basic Insulation Level (BIL) (kV)
216V, 240V, 480V, 600V	30
1.2kV,1.5kV, 2.4kV, 2.77kV, 4.16kV,4.8kV	75, 95,125,150,200
6.35kV, 6.64kV, 7.20kV, 8.32kV,9.96kV, 11.4kV 12.47kV,13.28kV,14.4kV	95,125,150,200
15.13kV, 15.92kV, 19.92 kV	125,150,200
20.8kV, 21.6kV, 22.8kV, 23.8kV, 24.94kV	150, 200

The basic capacitor unit should be selected by the rated voltage and the basic insulation level (BIL), whereas the rated voltage is determined by the loading condition of the capacitor, and the insulation level is determined based on the requirement of the supply system. For example, the following table lists the capacitor loadings of the C-type filter in Section 3.3.6. The rated voltage of the studied industrial system is 13.8 kV. It is common for such a system to have a 95 kV BIL level.

Table E.2 Capacitor loading of the designed C-type filter

C-Type Filter	Capacitor C_1		Capacitor C_2	
	C (uF)	V_C (kV)	C (uF)	V_C (V)
Value	41.8	8.27	5056.1	68.0

The voltage experienced by the capacitor C_1 is 8.27 kV, so the capacitor unit with rated voltage 8.32 kV is selected for capacitor C_1. Since the available BIL level for the 8.32 kV capacitor unit starts at 95 kV, it can meet the required insulation level for this system. Accordingly, the capacity of the capacitor C_1 for each phase can be calculated by the following equation:

$$Q_{c1} = \omega_1 C_1 V_c^2 = 1091 \ \ kvar \tag{E.1}$$

For the capacitor C_2, the actual voltage experienced by this capacitor is only 68V. However, the 1.2 kV capacitor unit needs to be selected since this is the lowest voltage for a capacitor unit that satisfies the 95kV BIL. Therefore, the capacity of the capacitor C_2 for each phase can be obtained as follows:

$$Q_{c2} = \omega_1 C_2 V_c^2 = 2745 \ \ kvar \tag{E.2}$$

As a result, the capacity of the capacitor C_2 is more than two times of the capacitor C_1. Such a high capacity will lead to an expensive capacitor bank. This explains the reason that it should avoid tuning the C-type filter at high frequency in practice.

Table E.3 illustrates the capacitor unit price from ABB. Since the original data is about ten years ago, a 10% increase rate is considered to obtain an up-to-date estimation. Note that the capacitor unit price depends on the voltage level as well as the capacity of the capacitor unit.

Table E.3 Price lists of the common capacitor units

	All the prices are listed in US dollar ($)		
	V<5kV	5kV<V<15kV	15kV<V<20kV
50 kvar	$1,440	$1,518	$1,794
100 kvar	$1,666	$1,726	$1,850
150 kvar	$1,886	$1,946	$2,098
200 kvar	$2,122	$2,182	$2,320
300 kvar	$2,562	$2,622	$2,802
400 kvar	$3,128	$3,188	$3,354
500 kvar	$3,570	$3,630	$3,768
600 kvar	$3,956	$4,016	$4,168

Based on the unit price, the cost of the previous two capacitors can be calculated, and the results are listed in Table E.4. The similar process can also be used to calculate the costs of the other filter capacitors in the previous studies.

Table E.4 Capacitor costs of the C-type filter

Capacitor	V_C (kV)	Qc (kvar)	Basic Capacitor Unit	Cost ($)
C_1	8.32	1091	600kvar*6	24,096
C_2	1.20	2745	600kvar*15	60,240

- **Reactor and Resistor Costs**

As discussed before, the cost of the filter reactor includes a constant part and a variable part. The constant part is determined by basic insulation level, iron core or air-core, and the enclosure, etc. The variable part is determined by the inductance value and rated current. The following equation is used to estimate the cost of the filter reactor.

$$\text{Reactor Price (\$)} = 1620 + L(mH) \times 105 + I_L(\text{A}) \times 15 \tag{E.3}$$

The filter resistor cost is relatively stable, and its cost can also be estimated by a constant part plus a variable part depending on the resistor current, as shown below.

$$\text{Resistor Price (\$)} = 2000 + I_R(\text{A}) \times 20 \tag{E.4}$$

The C-type filter in Section 3.3.6 is still used as an example, and the costs of the filter reactor and resistor are listed in Table E.5.

Table E.5 Reactor and resistor costs of the C-type filter

Component	unit price for each phase ($)	Quantity	Total Cost ($)
Reactor	1620+1.4mH×105+130 A×15	3	11,151
Resistor	2000+10A×20	3	66,00

E.2 Operating Cost Analysis

The operating cost is related to the filter loss. A 5-year period is used to estimate the operating cost in the long term. Within this period, the filter operating rate is assumed to be 0.7, and the electricity price is 0.05 $/kWh. As a result, the filter will operate 30,660 (5×365×24×0.7) hours. The previous C-type filter has a total power loss of 3.22kW per phase, referring to Table 3.9. Therefore, the operating cost of the C-type filter can be calculated as below.

$$\text{Operating Cost} = 9.66\text{kW} \times 0.05\$/\text{kWh} \times 30,660 \text{ hours} = 14,794 \$ \qquad \text{(E.5)}$$

Appendix F
Loading and Economic Analysis for DHP Filter

A case study is conducted in Section 4.4 to evaluate the effectiveness of the proposed filtering scheme. To compare the costs of the proposed scheme with the existing one, this section performs an economic analysis about the two filtering schemes.

F.1 Filter Loading Analysis

The component loading is necessary for estimating the filter cost. It is assumed that this 12-pulse industrial system is operating at the full-load condition, i.e. S=5MVA. Accordingly, the component loadings are listed in Table F.1.

Table F.1 Loading of filter components

Filter Option		Option 3			Option 4
		5th ST	7th ST	11th 3rd HP	DHP Filter
Main Capacitor	C_1 (uF)	38.32	38.32	153.28	153.28
	Voltage /kV	2.70	2.62	2.52	2.61
	Capacity /kvar	104.95	99.16	366.24	394.96
Auxiliary Capacitor	C_2 (uF)	---	---	85.03	440.53
	Voltage /V	---	---	126.65	109.48
	Capacity /kvar	---	---	0.51	1.99
Main Reactor	L_1 (mH)	7.97	3.97	---	0.51
	Current /A	38.30	37.34	---	147.28
	Capacity /kvar	4.41	2.09	---	4.19
Auxiliary Reactor	L_2 (mH)	---	---	0.38	0.44
	Current /A	---	---	145.74	154.29
	Capacity /kvar	---	---	3.04	3.95
Resistor	R (ohm)	---	---	2.63	0.40
	Voltage /V	---	---	46.11	22.94
	Current /A	---	---	17.53	57.34

As shown, the component loading of the DHP filter is similar to the 11th 3rd HP filter in option 3. The major difference is that the DHP filter requires a relatively large capacitor C_2 and a series reactor L_1 for providing the preferred damping

performance at the non-characteristic harmonics.

F.2 Component Cost Analysis

- **Capacitor Costs**

The capacitor cost is calculated based on the process described in Appendix E, and the results are shown in Table F.2. Similar to the C-type filter, the 1.2 kV capacitor unit should be selected for the capacitor C_2 of the 3rd HP filter and DHP filter for satisfying the system BIL level (75 kV for the 4.16 kV industrial system).

Table F.2 Capacitor costs of the two options

	Option 3			Option 4
	5th ST	7th ST	11th 3rd HP	DHP Filter
Costs ($)	$4,998	$4,998	$13,704	$15,750

- **Reactor and Resistor Costs**

In practice, the filter reactors and resistor are made to order. Their prices are mainly determined by the insulation level, rated current and inductance/resistance value. Table F.3 lists the prices quoted by industrial manufacturers.

Table F.3 Reactor and resistor costs of the two options

	Option 3			Option 4
	5th ST	7th ST	11th 3rd HP	DHP Filter
Reactor Costs ($)	$1,850	$1,700	$2,100	$4,200
Resistor Costs ($)	----	----	$3,300	$3,400

Accordingly, the component costs of the two filter options can be summarized in Table F.4. Compared to the current scheme, the proposed filtering scheme can save about 30% in filter cost.

Table F.4 Component cost of the two options

	Option 3	Option 4
Capacitor Costs ($)	$23,700	$15,750
Reactor Costs ($)	$5650	$4,200
Resistor Costs ($)	$3300	$3,400
Total component cost ($)	$32,650	$23,350

F.3 Operating Cost Analysis

The same assumptions as Appendix E are used to calculate the operating costs of the two filter options. The results are shown in the following table. It can be noticed that the proposed scheme has a higher operating cost than the current one. This is due to the high loss of the DHP filter at the non-characteristic harmonic for achieving the desired damping performance.

Table F.5 Operating cost of the two options

	Option 3	Option 4
Operating Costs ($)	$3,717	$6,048

F.4 Discussion about the Filter Physical Size

This section discusses the space requirements for the above two options. The physical sizes of filter components are illustrated in Table F.6. In this table, the capacitor sizes are based on the available capacitor units from ABB. The physical sizes of the reactors and resistors are quoted from the manufacturing companies.

Table F.6 Physical size of each component

Physical Size (mm×mm×mm)		Option 3			Option 4
		5th ST	7th ST	11th 3rd HP	DHP Filter
capacitor	C_1	433×534×240	433×534×240	433×534×525	433×534×525
	C_2	-----	-----	433×534×240	433×534×295
reactor	L_1	830×840×580	830×580×500	-----	830×680×589
	L_2	-----	-----	830×700×580	830×680×589
resistor	R	-----	-----	914×914×914	914×914×914

According to Table F.6, the DHP filter requires more space than the 3rd HP filter since it requires one more reactor to provide the desired high damping performance at the non-characteristic harmonics. However, due to the saving of two small non-characteristic filters, the total physical dimension of the new scheme is only about 70% of the current one. Note that the above analysis only considers the space for the filter component. In practice, the proposed scheme may save more space if considering the other factors, such as the switching device and protection device.